

*ADDIS ABABA UNIVERSITY
SCHOOL OF GRADUATE STUDIES
FACULTY OF TECHNOLOGY
DEPARTMENT OF ELECTRICAL AND COMPUTER
ENGINEERING*

Quantum Detection-
Optimal Quantum Receiver
Performance Analysis
For Free Air Channel

By
Abdulrezak Oumer Jeju

February, 2004

**ADDIS ABABA UNIVERSITY
SCHOOL OF GRADUATE STUDIES
FACULTY OF TECHNOLOGY
DEPARTMENT OF ELECTRICAL AND COMPUTER
ENGINEERING**

Quantum Detection-
Optimal Quantum Receiver and
Performance Analysis
For Free Air Channel

By
Abdulrezak Oumer Jeju

Advisor
Dr.Ing.Mohammed Abdo

A thesis submitted to the School of Graduate Studies of Addis Ababa University in partial fulfilment of the requirements for the Degree of Masters of Science in Communication Engineering

DECLARATION

I, the undersigned, hereby declare that this thesis is my original work carried out under the supervision of Dr. Ing. Mohammed Abdo, has not been presented as a thesis for a degree in any other university and that all sources used for the thesis are duly acknowledged.

Abdulrezak Oumer

Acknowledgments

It is a great pleasure to thank the many people who have contributed to this Thesis. In particular, I would like to give my heartiest thanks to my advisor Dr. Ing. Mohammed Abdo, who has helped me in my research in engineering aspects of quantum operations. My deepest thanks go to my friends and family, especially to my brothers and sisters, for their financial support and encouragement. Warm thanks also to the many other people who have contributed to this Thesis, especially Mesfin Ayalew, who has been a terrific mentor, classmate, and friend; to Taye Abdulkadir, who got me started, in research, and unlimited resource supply in quantum information and Matlab guide; and to Endalkachew Amde, whose boundless enthusiasm and encouragement has provided so much inspiration for my research. Throughout my graduate career I have had the pleasure of many enjoyable and helpful discussions with my instructors Prof. Girma Mulisa, Prof. Woldegiorgis Woldemariam, Dr. Ing Hailu Ayele, Dr. Eneyew Adugna and. Many other friends and scholars have helped me with this Thesis.. My especial thanks also to those creative people without whom the quantum of information would not exist as a field of research; especial influences on my thinking were the writings of Dr. Depak Chopera, V.Vilonlotter and C.W.Lau, Howard N.Barnum, Christopher A. Fuchs, Vincent W. S. Chan.

Addis Ababa University
Department of Electrical & Computer Engineering
Dec 2003

Table of Contents

Acknowledgements	I
List of Abbreviations	II
Abstract	IV
Chapter.1	
Introduction	1
Chapter.2	
Optical Communication & the principle of classical detection	8
2.1. Optical Source for Communication	9
2.1.2. Light Emitting Diodes	11
2.1.3. Laser	11
2.1.4. Light power and Intensity	13
2.2. Common Optical Modulation format	14
2.2.1 Binary ON/OFF Key (BOOK)	14
2.2.2 Binary Phase shift Key (BPSK)	15
2.2.3. Pulse position modulation (PPM)	16
2.3 .Free Air .Optical Channel	18
2.4. Classical and semi-classical Optical receiver	19
2.4.1. Direct and Coherent Detection.	21
2.4.1.1. Demodulation in Direct detection	21
2.4.1.2. Demodulation in Coherent Detection	22
2.5. Optimum Detector	24
2.5.1. Maximum a posteriori probability (PAM)	24
2.5.2. Maximum Likelihood (ML).	25
2.6. Fluctuation in photon statistics & its classical interpretation	25
2.7. Summary of the chapter	34

Chapter.3	
Quantum Communication	35
3.1 Interaction of Light with matter	37
3.2. Quantum states-Space Descriptions	38
3.3. Coherent state Representation.	46
Chapter 4	
Quantum signal processing And Detection Operator	48
4.1. Basics of Quantum Detection Operator	50
4.2. Optimal Quantum Measurement	52
4.2.1 Optimal Detection Operator for Binary pure state Signal	54
4.2.2 Optimal Detection Operator for M-array Optical modulation format	60
4.2.3.Procedure for optimization of higher order detection operator	62
4.3. Summary of the chapter	68
Chapter 5	
Performance Analysis Optimal Quantum Receiver	
5.1 Binary On & Off Key	69
5.1.1. Numerical performance analysis Of Binary On Off Key (BOOK)	73
5.2 Binary Phase Shift Key	75
5.2.1. Numerical performance analysis of Binary Phase Shift Keying OFF Key (BPSK)	78
5.3 M-array Pulse Position Modulation	80
5.3.1. Numerical performance analysis Of M-array Pulse Position Modulation (PPM)	82
5.3.1.1.Pulse Position Modulation (PPM-2)	83
5.3.1.2.Pulse Position Modulation (PPM-4)	83

5.3.1.3.Pulse Position Modulation (PPM-8)	84
5.4. Summary of the chapter	84
Chapter.6	
Realization of Optimal Quantum receiver	85
6.1. Decomposition of Detection Operator.	86
6.2 Decomposition of Unitary Operator	89
6.3. Summary	96
Chapter 7	
Conclusions and Recommendations	97
<i>Appendix</i>	101
<i>References</i>	116

List of Abbreviations

A^+	Hermitian Operator
a^-	Annihilation operator
a^{\dagger}	Creation Operator
DFT	Discrete Fourier Transform
BOOK	Binary ON/OFF Keying Modulation format
BPSK	Binary Phase Shift keying modulation format
g	Coupling Constants of physical system
G	Graham matrix
\hat{H}	Hamiltonian Operator
\hbar	Planck constant
K_B	Boltzmann constant
IM/DD	Intensity modulation with direct detection
ML	Maximum Likelihood
MAP	Maximum a posteriori probability
$N n\rangle = n n\rangle$	Number Operator in Fock Space
PPM	Pulse Position Modulation
POV.	Positive Operator Value
POVM.	Projective Operator Value Measure
PVM	Positive Value Measure
QSP	Quantum Signal Processing
SQRM	Square Root Measurement

σ	Pauli operator
\hat{U}	Unitary Operator
$ \psi\rangle$	The Ket represents a vector in an infinite dimensional Hilbert Space
$\langle\psi $	Bra represents the conjugate transpose of Ket
$\hat{\rho}$	Probability density Operator
$\hat{\Pi}$	Detection Operator
$ \psi\rangle\langle\psi $	Outer product
$\langle\psi \psi\rangle$	Inner product
$ \psi\rangle\langle\psi \phi\rangle$	Projection of a vector $ \phi\rangle$ on $ \psi\rangle$
$\langle\psi, \Pi\psi\rangle$	Expected value of the measurement out comes
$n(n=1,2,3,\dots)$ $n(n=1,2,3,\dots)$	Principal quantum number
$l(l=0,1,2,\dots,n-1)$	Azimutal quantum number
$m_l(m_l = -l,\dots,-1,0,+1,\dots,+l)$	Magnetic spin number
$m_s(m_s = +\frac{1}{2},-\frac{1}{2})$	Spin quantum number

Abstract

The fundamental performance limits of optical communications systems operating over the free-space channel will be examined using quantum detection principle. The performance of the optimum quantum receiver for On/OFF keying and Binary Phase-shift keying Optical modulation format in terms of quantum measurement states whose performance is optimized via generalized rotation in Hilbert space is first examined as a pure-state (no-noise) problem. The performance of quantum receiver for M-array pulse-position modulation (PPM), which requires a product state representation, and (M-1) dimensional rotational Algorithm will be evaluated with the development of an efficient rotational algorithm and a computer programme for carrying out the required numerical optimization is described and applied. Performance comparisons shows substantial improvement when quantum detection principle is employed. As a further application of the quantum detection principle, the Realization of quantum detection Operator For M-array Phase shift optical modulation format is also presented.

Introduction

1.0. Background

The subject of signal detection and information theory, on one way or another, deals with processing of information bearing signals in order to make inferences concerning the information they carry. These fields trace back to the classical works of Bays, Gauss, Fisher, Nyman and Pearson. But it was not until the 1930's and 1940's that Weiner, Shannon and other shaped the disciplines into the form we see today.

Ever since the early dawn of signal detection and information theory, the fields have been actively used in multitude of application ranging from communication to engineering and from physics to economics. This progress in much aspect is due to the access of high performing computers, which opens the possibilities to process, store and collect massive amount of data in order to implement many of computationally demanding methodologies within information theory and signal detection.

Still, several applications remain that can benefit from utilizing the general result that have been presented within the discipline, both when it comes to pushing the envelope of already existing method but also explaining and understanding of new phenomena. In this regard the principles of quantum detection believed to led to the new performance limit in optical communication that is much superior to the one extrapolated by direct application of conventional theory.

1.1 Classical Information Theory and Principle of Detection

Light, main carrier in the present information technology, is an electromagnetic wave, and also an ensemble of energy quanta - photon as well. At present only the fact is used that light propagates as an energy flux, and the wave nature of light is never used any more so far. As Christopher A. Fuchs put it in his paper; People encode "classical" information - like the stories in today's newspaper—into the states of quantum systems for a simple reason: to get it from one place to another. Since the world is quantum mechanical, this, in the last analysis, is exactly what one always does in transmitting information. Strangely enough however, literally almost all of modern information theory (as exhibited in the 44 existent volumes of IEEE Transactions on Information Theory) has ignored this fact in any but the most trivial ways. [10]

Indeed, the preoccupation of classical information theory lies in designing of communication system typically based on the wave nature of light-that electromagnetic wave propagate as energy flux. It is generally believed that performance of communications systems is ultimately limited by additive noise entering the receiver along with the signal. The idea can be illustrated with Shannon's capacity formula for band limited classical channels, according to which error-free communication is possible at rates less than $W \log_2(1+S/N)$, [11] where W is the bandwidth, S is the average signal power, and N is the power of additive thermal noise. The above expression shows that, if there is no thermal noise, then error-free communication should be possible at arbitrarily high rates, even with band limited channels. This conclusion seems intuitively correct at first; however, there is a hidden assumption about the accuracy with which the signal can be measured. The Shannon formulation implicitly assumes that arbitrarily precise measurements are possible since, if this were not the case, there would have to be an effective noise term associated with the noisy signal measurements in the denominator of the capacity expression in addition to the thermal noise, and hence the denominator would never actually approach zero. It turns out that indeed the signal cannot be measured with arbitrary precision even in the absence of thermal noise,

due to inherent limitations imposed by the uncertainty principle; hence, quantum effects that are not included in the classical model ultimately limit channel capacity.

It is not only in view of channel Capacity that the classical approach fails to achieve optimal performance limit in optical communication, but similar draw back can be picked out in its mathematical model of receiver. The classical model of receiver is designed mainly on the assumption that deterministic signals are observed in the presence of additive Gaussian noise. This model of receiver is perfectly adequate for describing communications systems operating at radio frequencies, where quantum effects are not readily detectable. However, at optical frequencies, quantum effects tend to be the dominant source of error, and therefore must be taken into account in the communications system model to achieve optimal performance. Actually it is worth to mention the fact that some attempt has been made in classical communication theory to account the quantum effects in terms of fluctuation in photon statistics. This particular receiver model [currently used for optical reception] uses the same statistics as quantum mechanics did. However due to its bench mark assumption that optically transmitted signal received as totally deterministic quantity the performance of the so-called " quantum Mechanically correct" Optical receiver failed to achieve the optimal value [2]. The preoccupation of the classical information theory is mainly focus in making the correlation between sender and receiver as high as possible. This is what communication is all about. But it is only part of the story in Quantum Information Theory. The quantum world brings with it a new resource that senders and receivers can share: quantum entanglement. This new resource, of all the things mentioned so far, is the most truly "quantum" of quantum information. It has no classical analogy, nor might it have been imagined in a classical world.

1.2 Quantum Information Theory and Detection Principle

It is a well known fact that when a communication system operates in quanta, ultimate performance limit of optical communication eventually

given by the law of quantum mechanics that governs photon dynamics. Quantum mechanical particles may well come in at some stage in such a transmission process, and indeed it is a matter of taste (more precisely of quantum statistical mechanics) whether we describe an electromagnetic signal as a classical wave or as a bunch of photons. In fact, every experiment described by quantum theory is like that. The signal generator produces particles (or more complex systems) on which we act with a measuring device, which in turn yields a perfectly classical output in detection. The object of quantum detection is nothing but to predict the probabilities of these outcomes depending on what has been done at the transmitter. By adopting this terminology, the conversion from classical information to quantum information, back and fourth can happen in virtually every quantum communication. More importantly, controlling the quantum mechanical interference effect inherent to quantum system that appears in transitions among sequences of 0 and 1, optimally led to the new performance limit that is much superior to the one extrapolated by conventional theory.

To realize reliable transmission ensured by quantum theory of the channel capacity, one may need quantum computation for the decoding process. This is, however, far beyond present technologies. However, it is often possible to determine the performance of the "quantum optimum" receiver analytically. Therefore, if these measurements could somehow be made and incorporated into a communications receiver, the performance of the quantum optimum receiver would represent the achievable limit on optical communications system consistent with the principles of quantum mechanics.

1.3. The Thesis

One of the most important problems in quantum communication is considered to be developing Quantum Detection Operator, since distinguishing quantum states is at the root of any information processing tasks. In this thesis, we focus on this problem from the viewpoint of minimizing the average probability of error that plays an essential role in

enhancing performance limit of optical communication. So far the optimum detection operator have been developed and clarified for pure-state single photon systems such as binary state optical modulation format. Therefore in this thesis, an algorithm that enable us to analyse the performance of optimal quantum receiver of higher order optical modulation format for a noise - free air channel and its realization has been developed. Computer simulation program is developed to study the performance of the algorithm for binary on/off keying optical modulation format.

As illustrated in Fig1.1 general detection principle in optical communication has gone through three phases. In classical detection, earliest development of all, receiver design mainly relays on the nature of light propagation as an electromagnetic energy flux, and its performance is assumed to limited by additive thermal noise. However, different experiments on optical signals verified that the dominant cause of error in reception is accounted to quantum interference inherent to optical frequencies. Thus, acknowledging this fact, currently developed receivers are designed in a way to account quantum interference. This semi classical approach, though considers the effect of quantum interference on optical receivers performance, due to it benchmark assumption that optically transmitted signal is received as being totally deterministic, it failed to achieve optimal performance limit of optical communication. Details of classical and semi classical detections are presented in chapter two.

As indicated in section 1.2, a purely quantum approach is being developed to reach the optimal performance limit in optical communication. This new detection technique basis its operation both on the knowledge of quantum state of physical systems and the quantity of resources to perform physical tasks, rather than considering light wave only as being a continuous electromagnetic energy flux. The mathematical models, algorithms, and performance evaluation for this optimal receiver are presented in the third and fourth chapters. And performance improvement of optimal quantum receiver, in comparison with classical receivers, is discussed in the fifth chapter. Chapter six of this thesis also deals with realization of optimal quantum receivers for higher order optical modulation format.

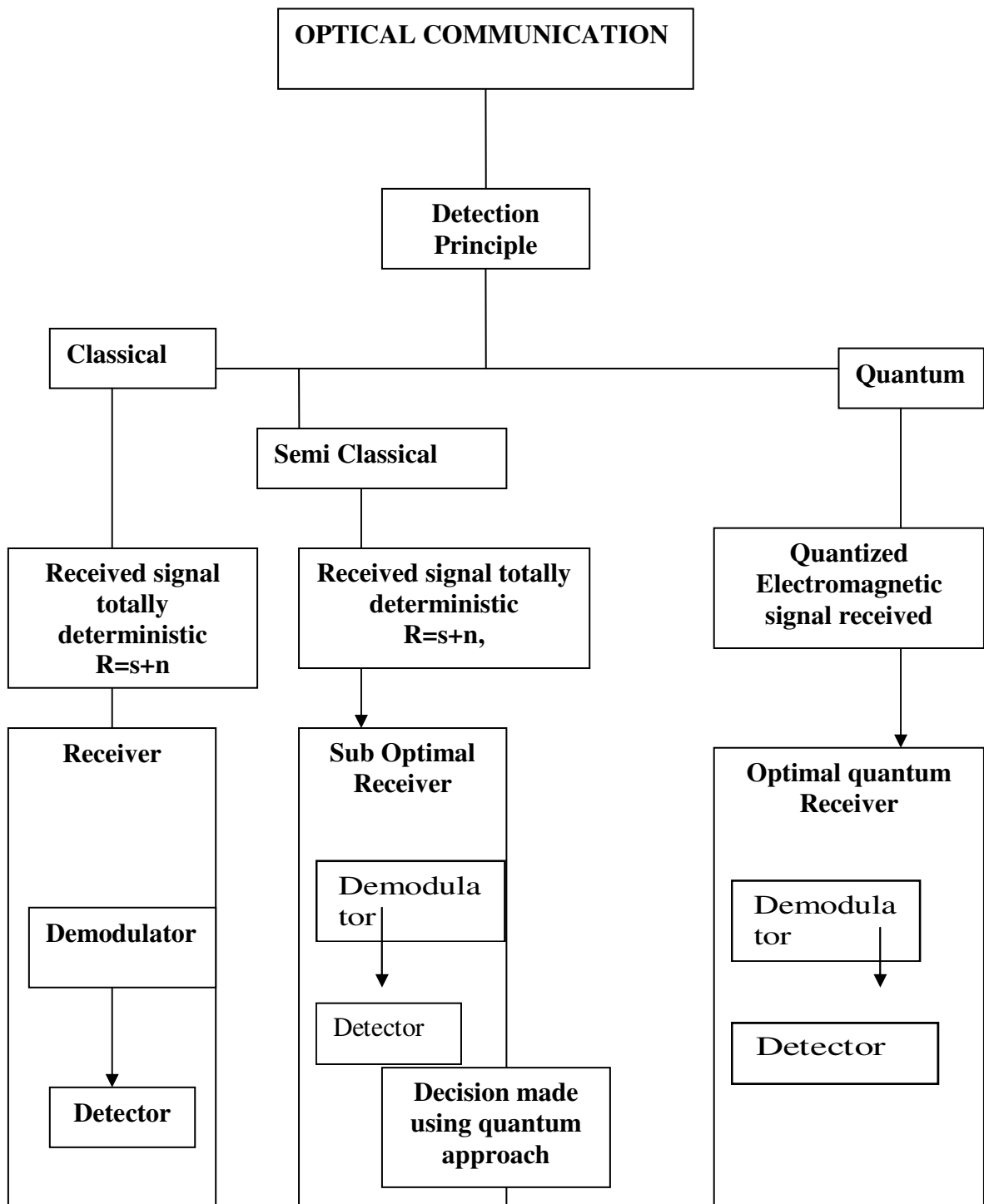


Fig. 1.1. An over view of the procedure

Quantum Information Theory is a fairly young subject, so that a definitive textbook does not exist yet, and probably won't exist for a few years to

come. However, there are some readily available sources of information on the Internet, which provide a good impression of how rapidly this subject is evolving. The study was limited only to the optical communication for free air channel with noise free cases. It was not also possible to include as many optical modulation formats as possible due to the limitations in resources and difficulty in analyzing the findings. Still another major limitation of the study could be observed in the data analysis of the simulation result. In the data analysis there was a compelling pressure to use some quantitative methods in the analysis of the qualitatively collected data from simulation.

Optical Communication & the Principles of Classical Detection

Global communication from any place on Earth is an attractive goal. One method to achieve this aim is to network satellites together to provide global coverage and access. By this method the information is transferred from the ground to the nearest satellite above and relayed among satellites to the satellite above the destination. The last satellite then transmits the information to the destination. Optical inter satellite links have some advantages compared with microwave inter satellite links. The advantages of the optical inter satellites links are smaller size and weight of the terminal, less power consumption, greater immunity to interference, a larger data rate, and acceptability of denser satellite orbit population. In addition to this interesting property space optical communications has power attenuation due to free space diffraction loss, and it is only inversely proportional to the square of the distance traveled. Optical fiber attenuation is exponential in distance and amplifiers/repeaters at regular distances are required to maintain performance. Thus, one can see the possibility that though the start-up cost of optical space communications is higher, eventually for long enough distances, it can be more economical than long distance (especially undersea) fibers systems.

Communications using light is not a new science. Old Roman records indicate that polished metal plates were sometimes used as mirrors to reflect sunlight for long range signaling. The U.S. military used similar sunlight powered devices to send telegraph information from mountaintop to mountaintop in the early 1800s. For centuries the navies of the world have been using and still use-blinking lights to send messages from one ship to another. Back in 1880, Alexander Graham Bell experimented with his "Photo phone" that used sunlight reflected off a vibrating mirror and a selenium photo cell to send telephone like signals over a range of 600 feet. During both world wars some light wave communications experiments were

conducted, but result in no proven system in space. Consequently radio and radar took the spotlight. Moreover the invention of the laser and some new semiconductor devices led to the realization of optical fibers, which makes transmission on optical fibers more significant. Recent new advances in technology, architecture and system understandings and designs, high performance laboratory prototypes and space experiments, will soon establish space optical communications as the key component that sets a new paradigm for future cost-effective space systems. Therefore finding a way that enhances the performance of free space optical communication system is the question of the day.

Optical space communication systems are very complex engineering systems, much more so than terrestrial fiber networks. Proper design approaches are needed for their architectural construction and analysis. One way of doing this is breaking down the complex system into interacting but logically separate subsystems for conceptual design and analysis. Thereof in this chapter the basic principle of optical communication and its receiver structure in relation to detection will be presented. Moreover the drawback of the classical model based on performance will be investigated.

2.1.Optical Source for Communication

Newton demonstrated that color is a quality of light. To understand color, therefore, it is necessary to know something about light. As a form of electromagnetic radiation, light has properties in common with both waves and particles. It can be thought of as a stream of minute energy packets radiated at varying frequencies in a wave motion. Any given beam of light has specific values of frequency, wavelength, and energy associated with it. Frequency, which is the number of waves passing a point in a unit of time, is commonly expressed in units of hertz ($1 \text{ Hz} = 1 \text{ cycle / second}$). Wavelength is the distance between corresponding points of two consecutive waves and is often expressed in units of nanometers ($1 \text{ nm} = 10^{-9} \text{ meters}$). The energy of a light beam can be compared to that possessed by a small particle moving at the velocity of light, except that

no particle having a rest mass could move at such a velocity. The name photon, used for the smallest quantity of light of any given wavelength, is meant to encompass this duality, including both the wave and particle characteristics inherent in wave mechanics and quantum theory. The energy of a photon is often expressed in units of electron volts; it is directly proportional to frequency and inversely proportional to wavelength. Light is not the only type of electromagnetic radiation—it is, in fact, only a small segment of the total electromagnetic spectrum—but it is the one form the eye can perceive. Wavelengths of light range from about 400 nm, the violet end of the spectrum, to 700 nm, red end. (The limits of the visible spectrum are not sharply defined but vary among individuals; there is some extended visibility for high-intensity light. (See Fig 2.1) At shorter wavelengths the electromagnetic spectrum extends to the ultraviolet region and continues through X-rays, gamma rays, and cosmic rays.

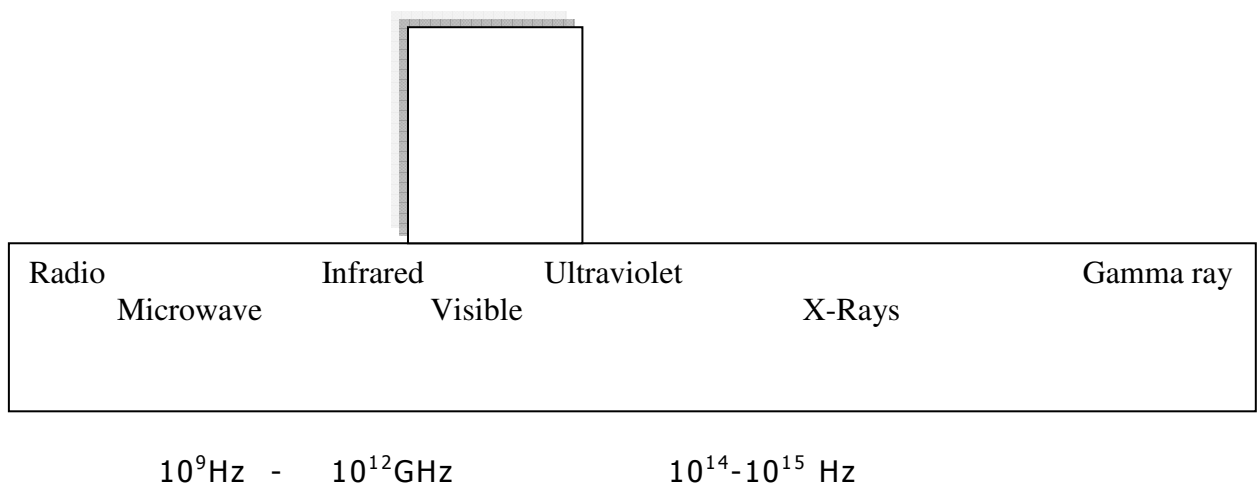


Fig.2.1. Part of Electromagnetic wave spectrum

Unlike the limited number of useable light detectors, there are a wide variety of light emitters that we can use for optical through-the-air communications. Our communications system will depend much more on the type of light source used than on the light detector. We should choose the light source based on the type of information that needs to be

transmitted and the distance we wish to cover to reach the optical receiver.

It commonly occurs that the sources of light for optical communication systems are heated bodies emitting continuous spectra. Most sources of thermal radiation radiate energy in a manner in which can be readily described in terms of a black body emitting through a filter, making it possible to use the black body radiation laws as a starting point for many theoretical Calculations.

2.1.1. Light-Emitting Diodes

Light emitted from Led as a result of the recombining of electron and holes. Electrically, a LED is simply a P-N junction. Under forward bias, minority carriers are injected across the junction. Once they cross, they recombine with majority carriers and give up their energy in the process. The electrons release their energy in the form of radiation in the visible region; that is, a photon of light.

2.1.2. Laser

LASER is an acronym for *Light Amplification by the Stimulated Emission of Radiation*. The concept consists of an excited state atom encountering a photon of the same energy that corresponds to the difference between the excited and ground states of the atom. When such a photon is encountered, it causes the emission of another photon of the same energy. Laser radiation is known for its high monochromaticity, directivity, and power. It is coherent in time and space and also polarized. These properties are characteristics of all Lasers regardless of a specific laser type and its technical data.

The monochromaticity of a laser beam is characterized by its line width, $\Delta\lambda$ measured as the Full Width at Half Maximum Power (FWHM) .For gas laser the FWHM is 10^{-3} to 10^{-4} nm but for semiconductor Laser it is 1-10 nm. This extremely narrow bandwidth of laser beam can be used to

advantage for the spectral selection of useful signals from a noise corrupted environment. The directivity of a laser beam is described in terms of solid angle or corresponding plane divergence angle confining the laser radiation. The radiant power or flux produced by a laser depends on a particular type. The power of continuous gas laser ranges from units to tenth of Mili-watt. For continuous wave laser it is several kilowatts. Observing that the divergence of a laser beam is in the order of a few minutes of arc, even Mili-watts of laser power is capable of producing radiant intensities up to 10^3 Wster^{-1} . Currently a light pulse with short width, high intensity and more spectral range producing devices are available in the market. . As can be seen from Fig.2.2 an operation of short width of 5.6ns and even much lesser time micro pulse is possible. [16]

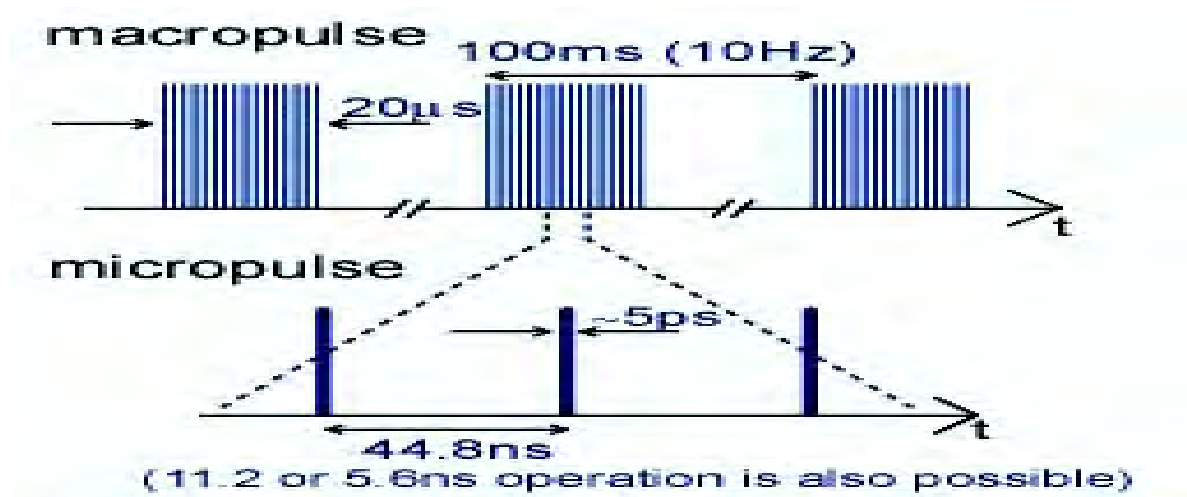


Fig.2.2. Macro and Micro pulses of Laser output

The availability of light sources with the above property has been the key innovation enabling the rapid rise of Optical communication. However due to Doppler-shift, Collision broadening and spontaneous emission the spatial coherence or the temporal coherence from the source can be affected as shown in Fig.2.3. Adjusting the light source producing cavity length to support only required frequencies can minimize these unavoidable phenomena and subsequent spectral filtering leads to the production of coherent light. [26]

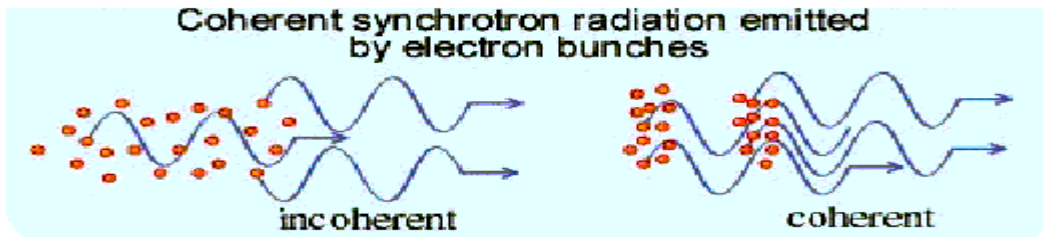


Fig.2.3. *Coherent and Incoherent Radiation*

2.1.3. Light Power and Intensity

The scientific unit for power is the "watt". Since the intensity of a light source can also be described as light power, the watt is perhaps the best unit to use to define light intensity. However, power should not be confused with energy. Energy is defined as power multiplied by time. The longer a light source remains turned on, the more energy it transmits. But all of the light detectors discussed in this thesis are dependent on the strength of energy per unit time at a given instant, power, not on the average energy. They convert light power into electrical power in much the same way as a light source might convert electrical power into light power. The conversion is independent of time. This is a very important concept and is paramount to some of the circuits used for communications. The watt is more convenient to use since light detectors, used to convert the light energy into electrical energy, produce an electrical current proportional to the light power, not its energy. Detectors often have conversion factors listed in the light power to electrical current relationship. This implies that the conversion is independent of the duration of any light pulse. As long as the detector is fast enough, it will produce the same amount of current whether the light pulse lasts one second or one nanosecond. In all cases the light source must be modulated (usually turned on and off or varied in intensity) to transmit information. The modulation rate will determine the maximum rate the information can be transmitted. One may have to make some tradeoffs between the modulations rates needed; the distance to be covered and the amount of money wish to spend.

2.2.Common Optical Modulation Formats

THE MODULATION format in most optical communication transmission systems is limited to intensity modulation with direct detection (IM/DD). In this format, only one bit per symbol is transmitted, leading to poor spectral efficiencies. Recently, Binary phase shift key with coherent detection and pulse position Modulation (PPM) with direct detection has been implemented in the systems. In addition a variety of higher order modulation schemes has been proposed, but most rely on rather complicated receivers structures. Thereof, this thesis introduces here only the most common optical modulation format that used in free air optical channel.

2.2.1. Binary ON/OFF Keying

Binary ON/OFF Key (BOOK) & Binary Phase Shift Key (BPSK) in the optical domain is represented by two signal points on the real axis of a constellation diagram as shown in Fig.2.4.

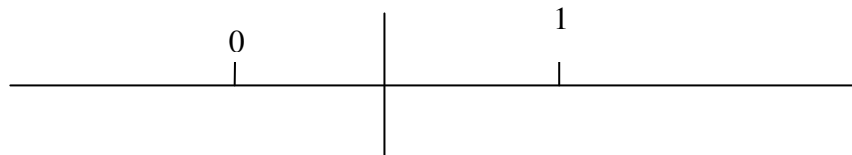


Fig.2.4. Constellation diagram for binary on /off key optical modulation

In the case of BOOK, which has two different magnitudes; (usually represented by 0 and 1), and the signal has a form as follows;

$$\begin{aligned}
 S(t) &= \operatorname{Re}[A_m g(t) \exp(i(2\pi..f_c t))] \\
 S(t) &= A_m g(t) \cos(2\pi..f_c t)
 \end{aligned}
 \tag{2.1.]$$

Where A_m stands for the two possible amplitude variations , $g(t)$ is the pulse shaper. The output of the transmitter, as shown in Fig.2.5, can be expressed by the electric field as follows:

$$E(t) = \sqrt{P} A_n \cos(\omega_c t) \quad [2.2.]$$

Where $\frac{\omega_0}{2\pi}$, is the optical carrier frequency, P is the mean power of laser.

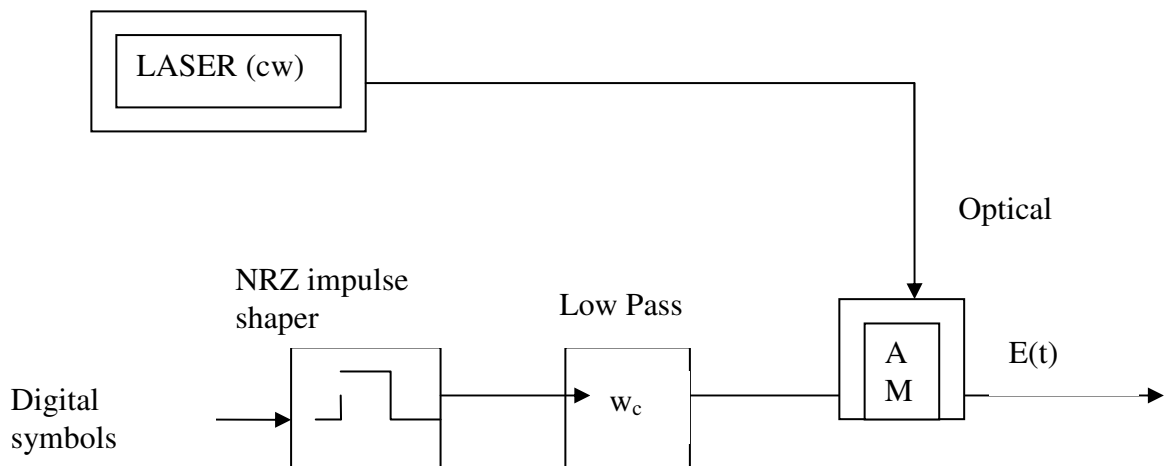


Fig.2.5. Block diagram of binary on /off key optical modulation

The transmitter produces the desired optical signal according to the block diagram in Fig.2.5. In the first stage, the electrical drive signal passed in no return-to-zero (NRZ) pulse shaper, low-pass filtered, and modulates the amplitude of the light from a continuous-wave (CW) laser, representing the bit stream. The amplitude modulator generates the amplitudes (for bit "0") and (for bit "1").

2.2.2. Binary Phase Shift Keying

In the case of BPSK, the amplitude of the two signals is constant. Hence, the two possible variations are the phase angles, usually denoted by 0 and π , represented mathematically as:

$$S(t) = g(t) \cos(2\pi f_c t + \phi_m) \quad [2.3.]$$

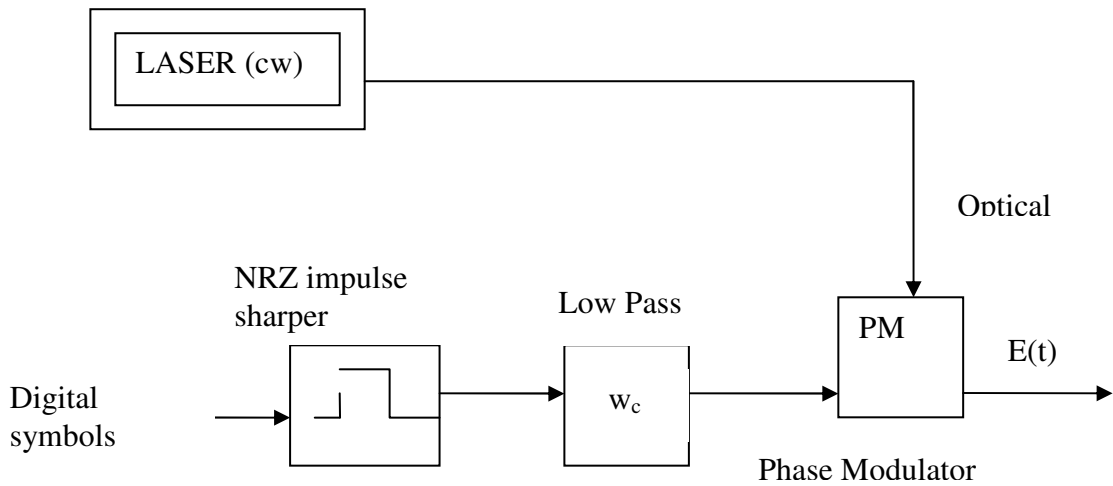


Fig.2.6. Block diagram of Phase shift key optical modulation

In the case of BPSK the transmitter produces the desired optical signal according to the block diagram in Fig.2.6 In the first stage, the electrical drive signal is passed in no return-to-zero (NRZ) pulse shaper, low-pass filtered, and modulates the phase of the light from a continuous-wave (CW) laser, representing the bit stream. The phase modulator generates the required angle (for bit "0") and (for bit "1"). The output of the transmitter in terms of the electric field can be represented as

$$E(t) = \sqrt{P} A_n \cos(\omega_c t + \phi_n) \quad [2.4.]$$

Where $\frac{\omega_0}{2\pi}$ is the optical carrier frequency, P is the mean power of the CW laser, and A_n stands for the amplitude.

2.2.3. Pulse Position Modulation (PPM)

Current designs for deep-space optical communication systems utilize Q-switched lasers, which can provide peak power levels sufficient for deep-space applications. Because the duration of the optical pulse generated by the Q-switched laser is difficult to modify, the toggle rate between the on and off states is limited by the time it takes to recharge the lasing material. Given this constraint, pulse-position modulation (PPM) has been

chosen over on/off keying as a more efficient signaling format. In M-array PPM signaling, one of M symbols is transmitted in the form of a laser pulse located in one of M time slots in order to transmit $\log_2 M$ bits of data, where $\log_2 M$, represent the information content. [22]

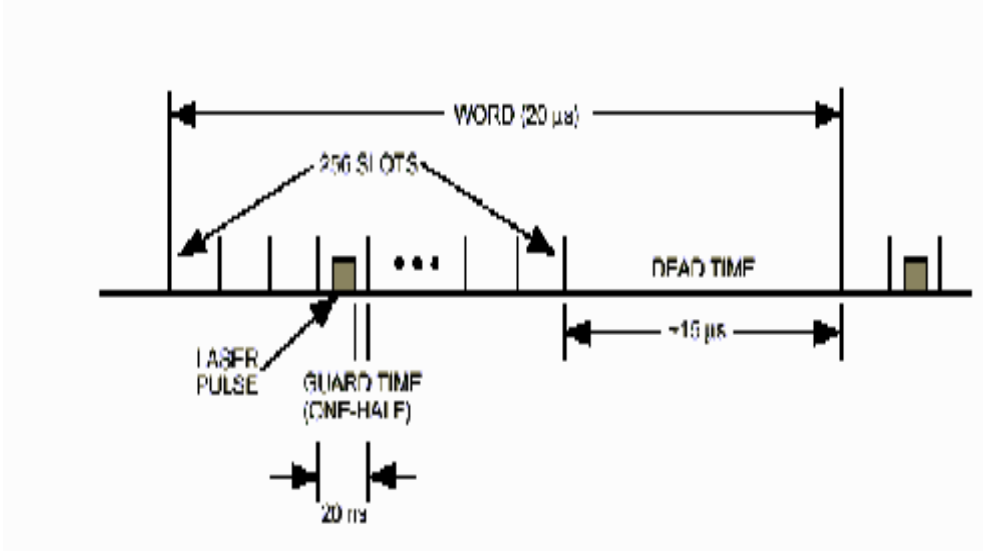


Fig.2.7. Pulse position optical modulation

The signal set of PPM represented in the Fig.2.7 can be expressed analytically as follows

$$S(t) = \sum_{i=-\infty}^{\infty} a_i p(t - (i - \frac{1}{2})T_f - l_i \tau - \varepsilon_i) \quad [2.5]$$

Where a_i is an independent, identically (uniform) distributed sequence of random intensity variation. in which a is a positive random variable. with $E\{a_i\} = \bar{a}_i$ and $E\{a_i^2\} = a^2_i$. p , is electrical power. l_i Is the PPM modulation corresponding to the i^{th} transmission, which takes the values $0, 1, \dots, M-1$, with equal probability of $1/M$ and the ε_i is an independent identically uniform time jitter.

2.3. Free Air Optical Channel

Transmission over free space features some advantages compared to the use of optical fibers. The atmosphere has a high transmission window at a wavelength of around 770 nm, where photons can easily be detected using commercial, and high-efficiency photon-counting modules. Furthermore, the atmosphere is only weakly dispersive and essentially non birefringent at these wavelengths. However, there are some drawbacks concerning free-space links as well. In contrast to the signal transmitted in a guiding medium where the energy is “protected” and remains localized in a small region of space, the energy transmitted via a free-space link spreads out, leading to higher and varying transmission losses. The general descriptions of transmitter, free air channel and receiver is illustrated by the figure shown below.

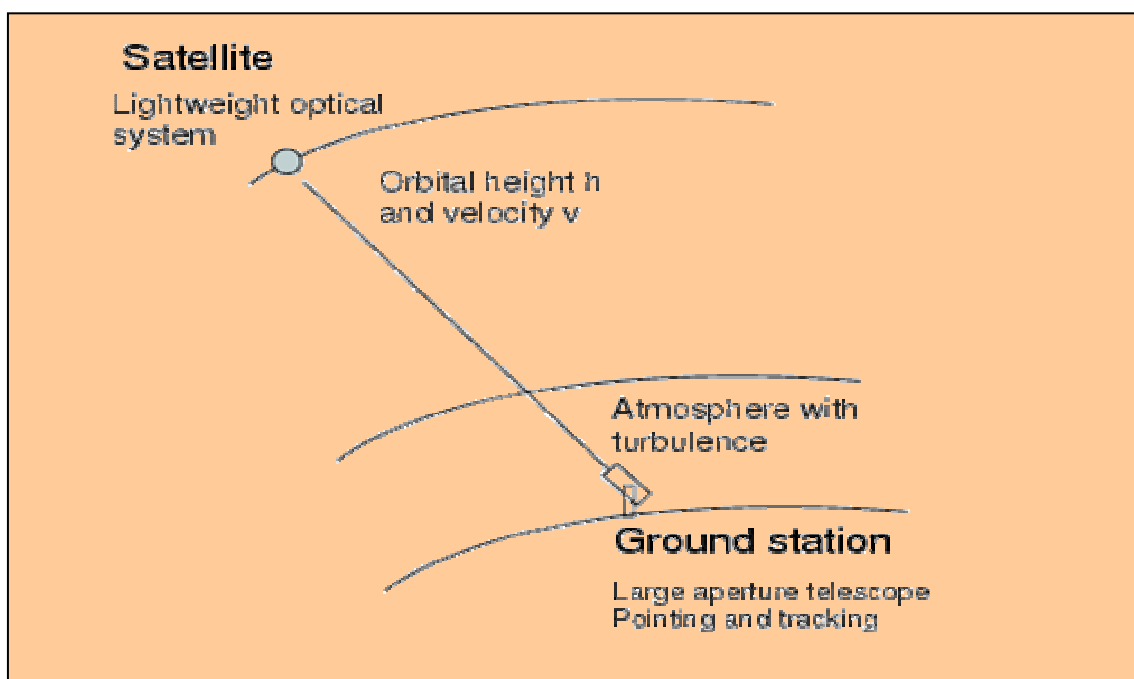


Fig.2.8 Free air optical Channel in relation to transmitter and receiver

In addition to loss of energy, ambient daylight, or even moonlight at night, can couple into the receiver, leading to a higher error rate. However, such errors can be kept to a reasonable level by using a combination of spectral filtering, spatial filtering at the receiver, and timing discrimination using a coincidence window of typically a few nanoseconds. Finally, it is clear that the performance of free-space systems depends dramatically on atmospheric conditions and is possible

only in clear weather. To comment on the different sources leading to coupling losses., a first concern is the transmission of the signals through a turbulent medium, leading to arrival-time jitter and beam wander (hence problems with *beam pointing*). However, as the time scales for atmospheric turbulences involved are rather small around 0.1–0.01 s—the time jitter due to a variation of the effective refractive index can be compensated for by sending a reference pulse at a different wavelength a short time (around 100 ns) before each signal pulse. Since this reference pulse experiences the same atmospheric conditions as the subsequent one, the signal will arrive essentially without jitter in the time window defined by the arrival of the reference pulse. In addition, the reference pulse can be reflected back to the transmitter and used to correct the direction of the laser beam by means of adaptive optics, hence compensating for beam wander and ensuring good beam pointing. Another issue is beam divergence; hence increase of spot size at the receiver end caused by diffraction at the transmitter aperture. Using, for example, 20-cm-diameter optics, one obtains a diffraction-limited spot size of 1m after 300 km. [26] This effect can in principle be kept small by taking advantage of larger optics. However, it can also be advantageous to have a spot size that is large compared to the receiver's aperture in order to ensure constant coupling in case of remaining beam wander.

2.4. Classical and Semi-Classical Optical Receiver

The overall task of the optical receiver is to extract the information that has been placed on the modulated light carrier by the distant transmitter and restores the information to its original form. The typical through-the-air communications receiver as shown in the Fig.2.9 below can be broken down into four separate sections. These are:

- ❖ Light collector (lens),
- ❖ Light detector (PIN, APD),
- ❖ Current to voltage converter,
- ❖ Signal amplifier and pulse discriminator.

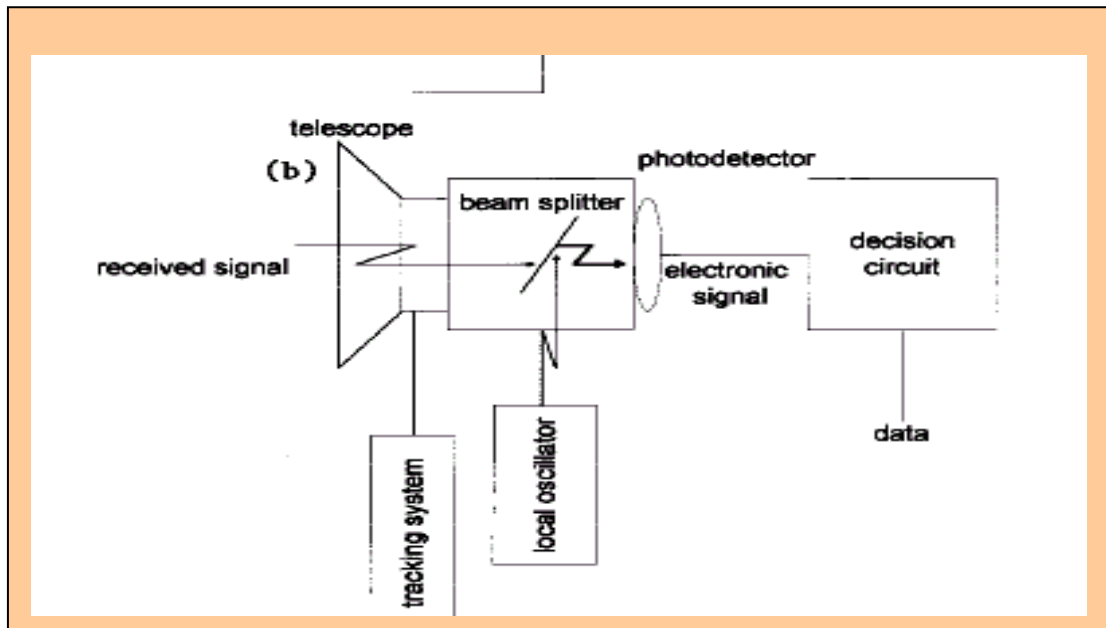


Fig.2.9. Optical receiver schematic diagram

There may also be additional circuits depending on the kind of the signal being received. But for mathematical analysis; it is convenient to model the receiver by sub dividing the receiver in to two parts-the signal demodulator and the detector-as shown below in Fig2.10. [22] The function of the signal demodulator is to convert the received waveform $r(t)$ in to an N-dimensional vector $r = [r_1, r_2, \dots, r_N]$ where N is the dimension of the transmitted signal waveform. The function of the detector is to decide which of the M possible signal waveform was transmitted based on the vector r . The two known realization of the signal demodulator are based on the use of *Signal Correlator* and the use of *Matched Filter*.

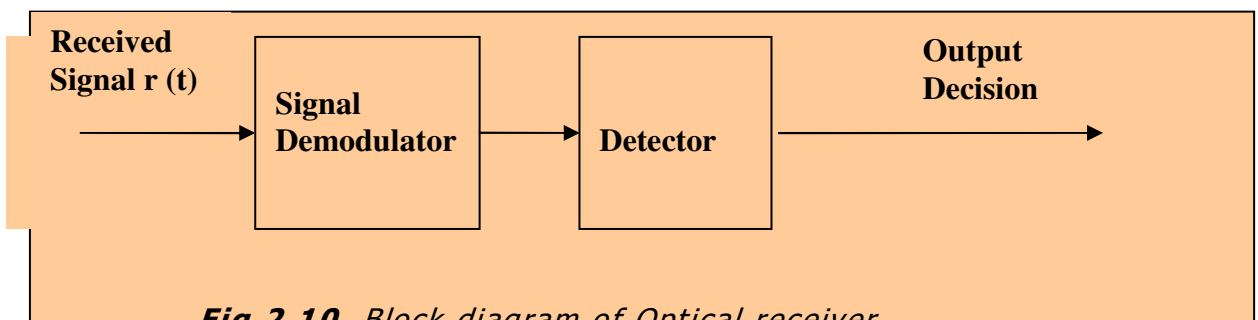


Fig.2.10. Block diagram of Optical receiver

2.4.1. Direct and Coherent Detection

At present, modulated optical fields are generally detected by means of energy detectors either directly (photon counting) or by the use of phase-sensitive coherent detection techniques. At the extremely high frequencies of optical signals, energy detection becomes a viable option that can be used even to discriminate between individual photons, due to the high energy of photons in the optical regime. [36]

Direct-detection receivers employ a square-law device, which produces an electrical signal proportional to the intensity of the incident optical signal (e.g., a photodiode) the signal's power is measured directly. As shown in Fig2.11 the electric field acting on the sensitive areas of the photo detector produce a current proportional to its intensity. Decision unit measures the output current from the photo-detector.

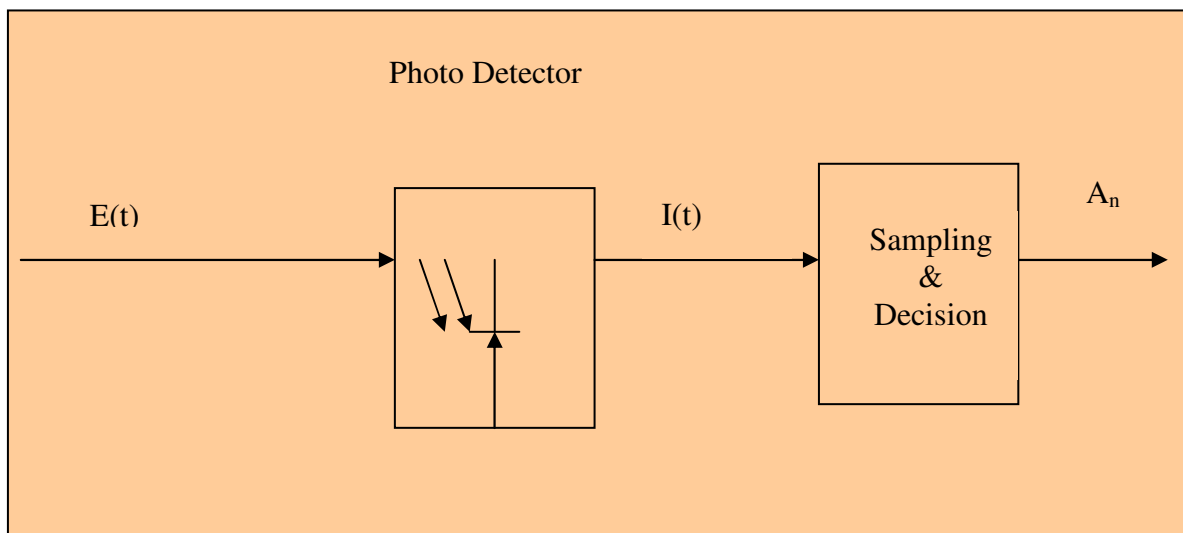


Fig.2.11. Block diagram for direct optical detection

2.4.1.1. Demodulation in direct detection

The demodulation in the direct detection is performed by single photo diode.[34] The photocurrent produced by the field of optical power $p(t)$ is

$$I(t) = \frac{e\eta}{h\nu} p(t) \quad [2.6]$$

With η = quantum efficiency of the detector, e = electron charge h = Planck constant and ν = optical frequency with

$$p(t) = \frac{|E|^2}{2Z_0} A \quad [2.7]$$

With A = photo detector surface, Z_0 = characteristics impedance, therefore

$$I(t) = \frac{e\eta A}{h\nu Z_0} |E|^2 \quad [2.8]$$

In substituting the electric field expression given by [Eq.2.2]

$$E(t) = \sqrt{p} A_n \exp(i\omega..t) \quad [2.9]$$

$$I(t) = \frac{e\eta A p}{h\nu 2Z_0} |A_n|^2 \quad [2.10]$$

If we substitute $I_0 = \frac{e\eta}{h\nu} p$ and the proportionality constant $K = \frac{A}{2Z_0}$ we get the simplified expression for the current out put of the photo detector as follows

$$I(t) = \frac{1}{2} K I_0 A_n^2(t) \quad [2.11]$$

This current is fed to a sampling and decision device, which provide the estimate of the bit sequence.

2.4.1.2. Demodulation in Coherent Detection

In contrast to IM/DD, in coherent detection the parameters of the received electrical field can be modulated, such as, its amplitude, frequency or phase. Coherent detection can be performed using two different techniques; heterodyne, i.e., different signal and local oscillator frequencies, or, homodyne detection, where the signal and local oscillator frequencies are equal.

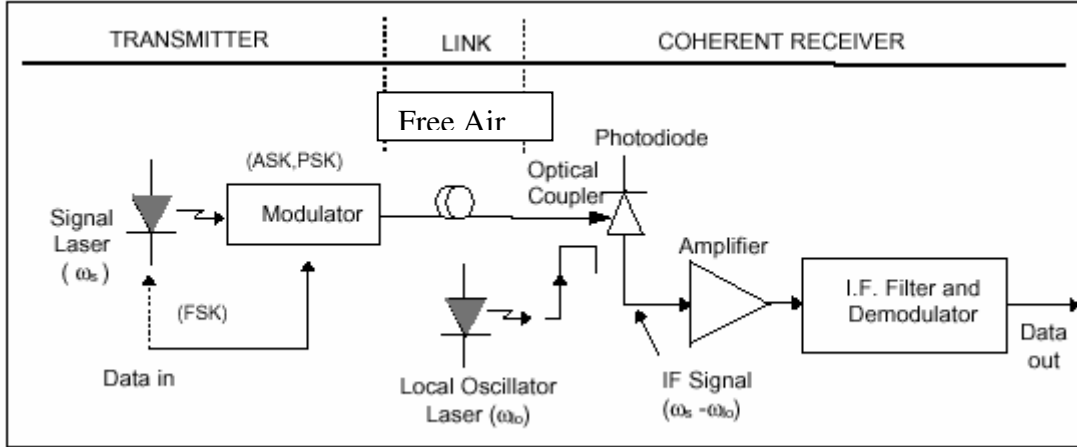


Fig.2.12.Block diagram of optical coherent detector

As shown in Fig.2.12, coherent reception consists of the photo detection of the beating between the received optical field E_{rec} and a locally produced wave (From optical local oscillator) E_{rec} . The optical beams mixing on a photodiode (square-law detector), and let the beams be given by:

$$E_{received} = E_r \cos(\omega_r t + \phi) \quad [2.12].$$

$$E_{Local - Oscillator} = E_L \cos(\omega_L t) \quad [2.13].$$

The photo detector current is given by:

$$I_{PD} = k(E_{received} + E_{L-O})^2 \quad [2.14].$$

Where k is the proportionality constant.

Inserting the field expression in Eq. [2.14]. One gets

$$I_{PD} = k[E_r \cos(\omega_r t + \phi) + E_L \cos(\omega_L t)]^2$$

$$I_{PD} = 0.5k(E_{received})^2[1 + \cos 2(\omega_r t + \phi)] + kE_r E_L [\cos(\omega_r - \omega_L)t + \phi] + kE_r E_L [\cos((\omega_r + \omega_o)t + \phi)] + 0.5kE_L^2[1 + \cos 2\omega_L t] \quad [2.15].$$

Rejecting all but the difference frequency term, the final expression or output of the photo detector becomes as follows

$$I_{PD} = kE_R E_L [\cos((\omega_R - \omega_L)t + \phi)] \quad [2.16].$$

Where $\omega_R - \omega_L = B_{IF}$ is the difference (intermediate) frequency. This current fed to a sampling and decision devices that provide the estimate of the bit sequence.

2.5. Optimum Detector

The starting point for signal detection theory is that nearly all decision-making takes place in the presence of some uncertainty. Signal detection theory provides a precise language and graphic notation for analyzing decision making in the presence of uncertainty. *i.e.*, the detector is designed to make a decision on the transmitted signal in each signal interval based on the observation of the demodulator output in each interval such that the probability of correct decision is maximized.

2.5.1. Maximum a Posteriori Probability (MAP)

The decision criterion is based on selecting the signal corresponding to the maximum of the set of posterior probabilities. $P(S_m / r)$. This decision criterion maximizes the probability of correct decision and, hence, minimizes the probability of error. This decision criterion is called the maximum a posteriori probability (MAP)[22]. Using Bayes rule, the posteriori probability is expressed as

$$P(S_m / r) = \frac{P(r / S_m)P(S_m)}{P(r)} \quad [2.17]$$

Where $P(r/S_m)$ the conditional probability distribution (pdf) is function of the observed vector, given S_m and $P(S_m)$ is the priori probability of the m^{th} signal being transmitted. The denominator of Eq[.2.12] can be expressed as

$$P(r) = \sum_{m=1}^M P(r / S_m)P(S_m) \quad [2.18.]$$

The computation of the posterior probability $P(S_m / r)$ requires a knowledge of the a priori probabilities $P(S_m)$ and the conditional probability distribution function $P(r / S_m)$, for $m=1, 2, 3 \dots M$.

2.5.2. Maximum Likelihood (ML)

The conditional Pdf, $P(r / S_m)$ or any monotonic functions of it is usually called the likelihood function. The decision criterion based on the maximum of $P(r / S_m)$ over the M signal is called the maximum likelihood (ML) criterion. A detector based on MAP criterion and one that is based on the ML criterion make the same decision as long as the a priori probabilities $P(S_m)$ are all equal, i.e., the signal $\{S_m\}$ are equiprobable.

2.6. Fluctuation in photon statistics and Classical interpretation

At this point one can ask what are the uncertainties associated with weak optical signal reception. What exactly one measures in an experiment to detect fluctuation? The answer, of course, is the electric current from a photo detector. Thus, any treatment of the subject must take into account the fact that we actually observe discrete electrons emitted by photo detector such as photo cathode or semiconductor devices. [14] According to the classical thought the source of fluctuations is the incoherence of light wave emitted by classical monochromatic light source. As they put it, the light we see at any moment comes from number of atoms, each making a transition between the same pair of energy level, but that the emission from any one atom in no way related to that from any other atom. Infact a careful spectroscopic measurement shows that the light is not really monochromatic in a strict sense of the word. It contains component of various wavelengths within a certain range, called the line width. If the line width is much less than the average wavelength one can use the term quasi monochromatic, for such radiation. Based on this argument now one can ask exactly what the wave looks like? The question

can be answered by performing a Fourier synthesis –i.e. take a number of sine waves, having frequencies randomly chosen within a specified range–the line width of the radiation –and add them together. As shown in Fig.2.13 the amplitude of three impure sine waves, which are constructed by adding five waves in a range of the line width is not constant, but fluctuate in rather haphazard fashion. [37]

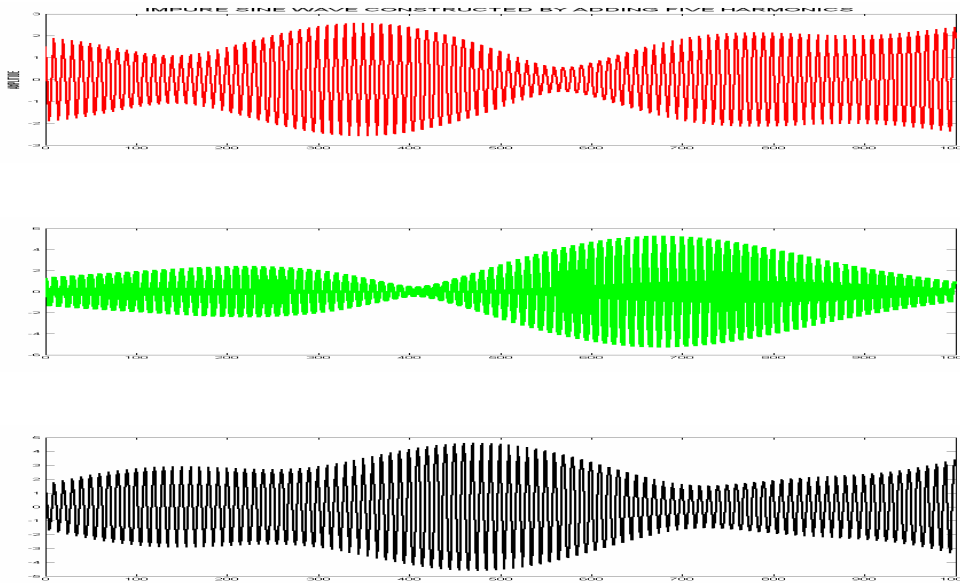


Fig.2.13. Amplitude variation of impure sine wave constructed by adding five Harmonics

The average or mean value of a quasi-monochromatic light beam that is represented at a given point in space by the superposition of a large number N of waves with equal amplitude of a . Each one has a random phase ϕ_n and frequency ω_n randomly chosen from within a range $\omega_0 \pm \frac{\epsilon}{2}$ where $\epsilon \ll \omega_0$, and ω_0 is the resonant frequency. One should note that the actual value of ϕ_n depend on the origin chosen for time. [37] The amplitude and intensity of the combined wave are

$$f(t) = a \sum_{n=1}^N \exp[i(\omega_n t + \phi_n)] \quad [2.19.]$$

$$I(t) = |f(t)|^2 = a^2 \left| \sum_{n=1}^N \exp[i(\omega_n t + \phi_n)] \right|^2 \quad [2.20]$$

Eq [2.20] can be written as double sum,

$$I(t) = a^2 \sum_n \sum_m \exp\{i[(\omega_n - \omega_m)t + \phi_n - \phi_m]\} \quad [2.21]$$

What is noticeable about the waves is that their amplitude and phase fluctuate with a typical beat period $\frac{2\pi}{\varepsilon}$, which contains about $\frac{\omega_0}{\varepsilon}$ waves.

[16] This effect should be brought out by a comparison of a long term and short-term averages. The average over the interval T_0 , long compared with the duration of a beat, should reflect out the fluctuation, whereas the interval T_1 short compared to the beat, should not. Hence evaluating the averages

$$\langle I(t) \rangle_T = \frac{a^2}{T_0} \int_{-\frac{T_0}{2}}^{\frac{T_0}{2}} \sum_n \sum_m \exp\{i[(\omega_n - \omega_m)t + \phi_n - \phi_m]\} dt \quad [2.22].$$

When the integration time T is T_0 the term $(\omega_n - \omega_m)t$ can have any value up to εT_0 which according to the definition of T_0 can be $\gg 2\pi$. Thus there is a tendency to cancellation of the oscillating parts of the integral. All of them going through many cycle at different rates during the long interval $|T_0$. Only the terms for which $n=m$ all of which have value $e^{i0} = 1$ make a consistent positive contribution to the integral in Eq [2.22]. Therefore one can write the final expression as follows,

$$\langle I(t) \rangle_{T_0} = \frac{a^2}{T_0} \int_{-\frac{T_0}{2}}^{\frac{T_0}{2}} \sum_{n=1}^N 1 dt = a^2 N \quad [2.23].$$

This equation simply tells us that because the waves are uncorrelated the intensity of their sum is equal to the sum of their intensities [27].

However when one takes the short-term average with $T = T_1$ the situation with the integral will be different from that in the long-term average.

When T_1 is short enough for the maximum phase $|(\omega_n - \omega_m)T_1|$, to be much less than $\frac{\pi}{2}$. This occurs if $\varepsilon T < \frac{\pi}{2}$. Then the short term average become

$$\begin{aligned} \langle I(t) \rangle_{T_1} &= \frac{a^2}{T_1} \int_{-\frac{T_1}{2}}^{\frac{T_1}{2}} \sum_n \sum_{m=1}^N \exp[i(\phi_n - \phi_m)] dt \\ &= a^2 N + 2a^2 \sum_n \sum_{m < n} \cos(\phi_n - \phi_m) \end{aligned} \quad [2.24].$$

Where in the last line separation is made on the term involving $n = m$ from the rest. One cannot predict the exact value of the second term. Simply know that it will generally have a non-zero value and that this value does not change during the interval T_1 , but has a value differing from a long term mean $a^2 N$. It is interesting to estimate the size of the fluctuating second term of Eq. [2.24], which contains about $\frac{1}{2} N^2$ terms in the summation \sum . Its square, when averaged over many intervals, has the expected values

$$\frac{1}{2} N^2 4a^4 \langle \cos^2(\phi_n - \phi_m) \rangle \equiv a^4 N^2 \quad [2.25].$$

Since the expectation value of the expression over a period $\langle \cos^2 \vartheta \rangle = \frac{1}{2}$. [37]. So the fluctuation term has root-mean square value $a^2 N$. The fluctuations are therefore comparable with the mean intensity found above, also $a^2 N$ even as $N \rightarrow \infty$. As can be seen from Fig. 2.14 and from the developed programme [Appendix-A] one can deduce that the short-term mean fluctuates macroscopically about the long-term mean $a^2 N$. The critical time which distinguishes the long term from the short term, is $\pi/2\varepsilon$, which is approximately equal the coherence time of the wave $\tau_c = 10^{-10}$.

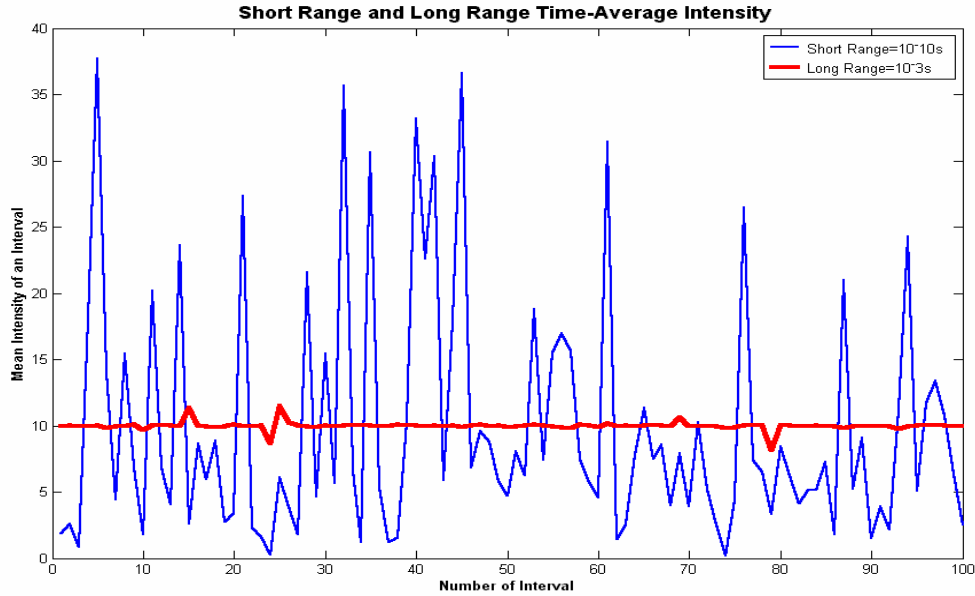


Fig.2.14. Mean Intensity variation of optical wave in short and long range

However during the short interval T_1 the wave behaves very much like a pure sine wave. [37] One can write the amplitude of $f(t)$ in a form

$$f(t) = a \exp(i\omega_0 t) \sum_n \exp[(\omega_n - \omega_0)t + i\phi_n] \quad [2.26]$$

During the period $t < T_1, |(\omega_n - \omega_0)t| \ll \pi/2$ and Eq [2.26] can be approximated as

$$f(t) \approx a \exp(i\omega_0 t) \sum_n \exp(i\phi_n) \quad [2.27]$$

The sum $\sum_n \exp(i\phi_n)$ will in general have a non-zero value $\alpha_1 \exp(i\Phi_1)$ where Φ_1 is quite indeterminate. Thus one concludes that during the interval T_1 the wave can be represented by a harmonic wave $a\alpha_1 \exp[i(\omega_0 t + \Phi_1)]$, whose phase Φ_1 and amplitude $a\alpha_1$ are constant but unknown. If one now repeats the measurement for an interval T_1 centered on a later time t_o should find the same result with new phase Φ_2 and $a\alpha_2$ With amplitude defined by:

$$\alpha_2 \exp(i\Phi_2) = \sum_n \exp[i(\omega_n - \omega_0)t_0 + i\phi_n] \quad [2.28]$$

Which in general are quite unpredictably different from Φ_1 and $a\alpha_1$ in view of ω_n s being randomly chosen. There is no correlation between the phase Φ_1, Φ_2 and amplitude $a\alpha_1, a\alpha_2$ measured in separate interval of length T_1 . From the Fig.2.15,16, Therefore, one can conclude that the measurement made during a short term T_1 indicate a simple harmonic wave of constant intensity. Observation continued for period much longer than $\frac{\pi}{2\varepsilon}$ will show this short-term intensity to fluctuate and there to be no correlation between the phases measured during intervals separated by much more than T_1 as can be seen from the Fig .2.17

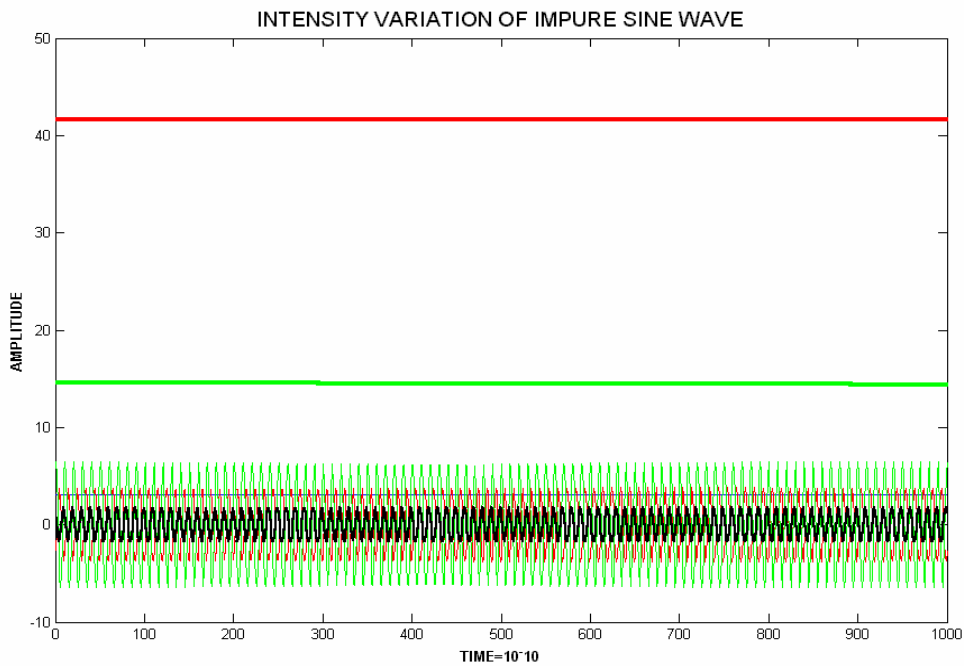


Fig.2.15. Intensity, amplitude and phase variation of optical wave near-coherence time

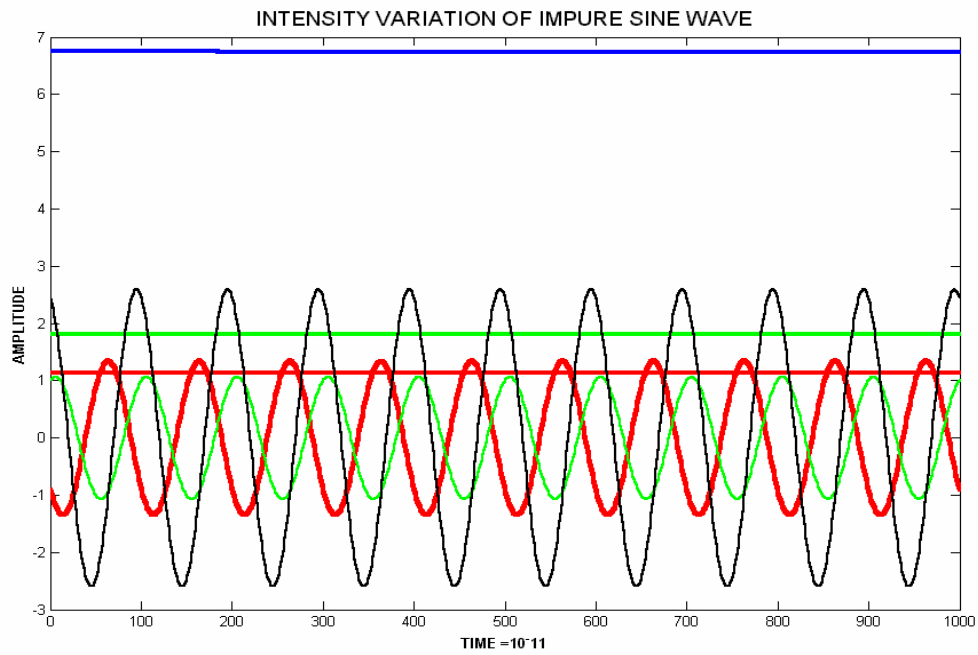


Fig.2.16. Intensity, amplitude and phase variation of optical wave near-coherence time

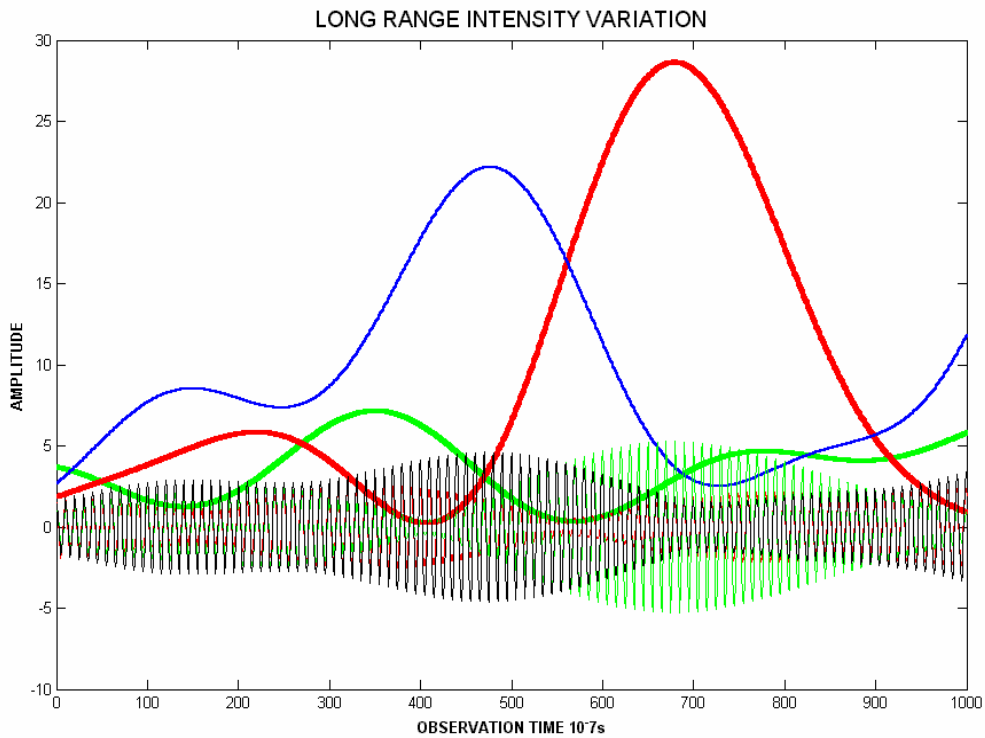


Fig.2.17. Intensity, amplitude and phase variation of optical wave near-coherence time

This conclusion implies that, if a measurement is made in a short-term interval then, the received signal can be considered as totally deterministic. Therefore, setting the condition of the absence of additive noise with the received signal the detector decides the bit sequence without making any error. This can be expressed mathematically:

Received Signal (r) = Transmitted signal(s) + Thermal Noise (n)

$$r(t) = S_m(t) + n(t), 0 \leq t \leq T \quad [2.29].$$

If $n(t) = 0$ in Eq [2.26], then

$$r(t) = S_m(t) \quad [2.30].$$

However experimental outcomes don't confirm the above theoretical result. Whatever intense a light beam is and coherent its intensity still appears to fluctuate when investigated with a fast enough detectors. To address this fallacy and to model optical detector that agree with the experimental result the classical approach of light needs to be supported by quantum thinking. It was that thinking that led to the development of Semi-classical receiver called "quantum mechanically correct" [13]

The simplified account of the classical argument for fluctuation in photon statistics was that, in observing optical signals we have two uncorrelated sources of fluctuation. The first arise because we are observing discrete electron emission whose average rate is proportional to the instantaneous intensity; the second because the instantaneous intensity itself is fluctuating about its long term mean value. Here the term instantaneous implies an average during a period $T_c < \tau_c$ Where t_c is the coherence time.

The mean number of electron emitted during a given interval $\delta t < T_1$ is

$$\bar{n} = \langle n \rangle = \langle I(t) \rangle_{T_1} \eta \frac{\delta t}{\hbar \omega}, \quad [2.31]$$

Where $\langle I(t) \rangle$ is the mean intensity and η is the quantum efficiency, which is the probability of an electron being emitted if a photon of energy falls on the photo detector-typically a few percent. Being the exact number of electron emitted given by Poisson distribution [8], thus the probability of n electron being emitted in δt is

$$P(n) = \frac{\bar{n}^n}{n!} e^{-\bar{n}} \quad [2.32]$$

The variance of mean square fluctuation for the Poisson distribution is well known to be equal to its mean value. [8]

$$\langle (\Delta n)^2 \rangle_{T_1} = \langle n^2 \rangle - \bar{n}^2 = \bar{n} \quad [2.33].$$

This is one source of fluctuation in current since \bar{n} depends on the mean intensity during the interval which is itself a fluctuating variable, one can also define $\bar{n} = \langle n \rangle = \langle I(t) \rangle_{T_0} \frac{\eta}{h\omega}$, [1] the average of \bar{n} over a long time T_0 and the expectation value of $\langle (\Delta n)^2 \rangle_{T_1}$ will equal \bar{n} .

The second source of fluctuation is mainly comes from $\langle I(t) \rangle$ it self. As stated above the light arrive at any moment in the photo detector comes from different particles [1]. The mean square difference

$$\langle (\langle I(t) \rangle_{T_1} - \langle I(t) \rangle_{T_0})^2 \rangle_{T_0} = a^4 N^2 = [\langle I(t) \rangle_{T_0}]^2 \quad [2.34]$$

In terms of electrons emitted in time δt , this can be written

$$\langle (\Delta \bar{n})^2 \rangle_{T_0} = \langle (\bar{n} - \bar{n})^2 \rangle_{T_0} = \bar{n} \quad [2.35].$$

Since $\Delta \bar{n}$ and Δn are not correlated one find that, the total variance in photoelectron count during T_1 is the sum of the individual variances.

$$\left\langle (n - \bar{n})^2 \right\rangle_{T_0} = \left\langle (\Delta n)^2 \right\rangle_{T_0} + \left\langle (\Delta n)^2 \right\rangle_{T_1} = \bar{n} + \bar{n} \quad [2.36]$$

The above argument, which is completely classical, shows that when a photo-detector is illuminated by a quasi-monochromatic wave, the emission of the electron is not a purely random process governed by Poisson statistics. Indeed photoemission events are correlated in some way, which is not seen in classical communication theory. [39]

2.7 Summary of the Chapter

Even though their simplicity makes them attractive and commonly used, direct detectors has some drawback. Since any optical phase information is lost in the process, direct detection cannot be used to measure the Doppler frequency shift of the radar echo, and direct detection is subject to thermal and dark current noises in the receiver and to background light incident on the detector. Under certain conditions of limited signal strength, direct detection therefore offers sensitivity inferior to that of coherent detection. However, direct detection has advantages over coherent detection when either source temporal coherence or the spatial phase characteristics of the received signal cannot be strictly controlled, or when complexity or cost is important design issues.

In the coherent detection case, where the local oscillator power $P_L \gg$ the received power P_R , the effective optical detection bandwidth that determines the noise floor of a signal, is the intermediate frequency (I.F) filter post-detection bandwidth BIF. Depending on the line width of the local-oscillator laser, this bandwidth could be as small as 1 kHz, so it can be made significantly smaller than the best incoherent optical filters. By employing dye lasers, which have wide tuneability, it is possible to effectively tune the receiver over the entire visible spectrum and part of the near infrared. While these detection techniques are very sensitive, they cannot realize the full advantages of optimum quantum detection, which typically performs much better in terms of the signal energy required to achieve a given detection performance. [See chapter 5]

What is remarkable about the conclusion of the semi-classical approach is that it is identical to the variance in the number of photons for a given state when they are considered as Bose-Einstein Particles. [1]. This event and its effect on the performance will be treated in the next chapter using quantum approach

Quantum Communication

Quantum information theory can be viewed as the generalization of the two major aspects of information theory. That is, quantum information theory includes the quantitative theory of how much we know about the quantum state of a physical system, and also the theory of the quantity of resources required to perform physical tasks- that are quantum analogues of classical tasks such as data compression, transmission and reception. Because of the differences between quantum states and classical states, the link between these two aspects is different in quantum information theory, and arguably less tight, than in classical information theory. Because of the differences between quantum and classical states, there are a variety of possible generalizations of each classical task.

One of the main reasons that led to the emergence of this rapidly developing field of communication is the inadequacy of classical ideas to explain all physical phenomena. The most notable problems arose from considerations of the electromagnetic wave spectrum in the cavity. The Heisenberg Uncertainty Principle forces us to introduce probabilities to and considers all possible paths taken by particles, with the classical path as a finite probability for a particle to deviate from its classical equation of motions. This deviation from a classical path is, on the scale determined by Planck's constant [6]. However, on the sub atomic scale, this deviation becomes the dominant aspects of a particle motions. In a microcosm, motions that are Infact forbidden classically determine the primary characterstics of the atom. The stability of the atom, the emission and absorption spectrum, radioactive decay, tunnelling, etc. are all manifestation of quantum behaviours that deviate from the classical equations of motions. [27]

3.1. Interaction of light with matter

Detection of light requires an interaction between the incident wave field and the electron in a sensitive element, the photo cathode, in which the electron have many states. To understand the interaction of light with matter let us see of the effect of an oscillating electromagnetic field on a single isolated one particle system with just two levels L_1 and L_2 . The particle in state $j = 1,2$ is described by an electronic wave function [36].

$$\psi_j(r, t) = \psi_j(r)e^{-i\omega_j t} \quad [3.1]$$

In which the spatial wave function $\psi_j(r)$ is separated from the temporal oscillation $e^{-j\omega t}$. The Eigen value of the two wave functions are $\hbar\omega_1$ and $\hbar\omega_2$ for $(\omega_2 > \omega_1)$, and the ψ is in each case a solutions of Schrödinger equations for the atomic potential $V(r)$. Each wave function corresponds to exact solutions of the Schrödinger equations and therefore the particle in either state will stay there forever. In each of the states described by the above equation will have a definite Eigenvalue. All the time dependence is in the $e^{-j\omega t}$. Any other possible electronic distribution can always be written as a superposition's of the wave function $\psi_j(r, t)$. Now if an oscillating electric field is applied to the system, the potential field is modified from $V(r)$ to $V(r) + e\Phi(r, t)$ where $\Phi(r, t)$ be the electric potential of the oscillating field. The stationary state wave function $\psi_j(r, t)$ corresponding to the new potential is no longer the same solution $\psi_j(r, t)$ of the Schrödinger equations. In these states the Eigen values no longer has a definite value-measurement will give either the Eigen value of state 1, or the Eigen value of state 2. The probabilities of the appearances of this values equals the square of the coefficients of a linear superposition of the $\psi_j(r, t)$.

$$\psi(r, t) = \alpha\psi_1(r, t) + \beta\psi_2(r, t) \quad [3.2]$$

Where, $|\alpha|^2 + |\beta|^2 = 1$

i.e. the probability of getting the eigen values of state 1 equal $|\alpha|^2$ and the probability of getting the eigen values of state 2 equal $|\beta|^2$. An important feature of the above expression is that, it accounts the quantum interference. When one calculates the electron density $|\psi(r, t)|^2$ will find a cross term which oscillates with the frequency $(\omega_2 - \omega_1)$.

Mathematically:

$$|\psi(r, t)|^2 = \alpha^2 \psi_1^2(r) + 2\alpha\beta \psi_1(r)\psi_2(r) \cos(\omega_2 - \omega_1) + \beta^2 \psi_2^2(r) \quad [3.3]$$

The above description leads directly to the most important concept involved in Laser. In the presence of an electromagnetic wave, no atomic electromagnetic wave functions are completely stationary-except the ground states in the presence of the vacuum field only. Otherwise transition occurs in which energy is transferred back ward and forward between the atom and the electromagnetic field. The atom behaves like an oscillating dipole antenna during a transition and the phase relation between this dipole and the electromagnetic field determine whether the atom absorb or emits.

3.2. State Space Representation

The concept of a state of a physical system constitutes one of the most important building stones of any physical theory. In classical physics the state of a system can be associated with a "point" in a corresponding phase space. Dynamical evolution of a classical system is then described as a trajectory in this phase space. Definition of a state in quantum physics is more abstract and complex Operationally; a state of a quantum-mechanical system is associated with particular probability distributions of measured physical observable. [5] These distributions are obtained via measurements over an ensemble of quantum-mechanical systems, which

are prepared in the same way (i.e., they are in the same state). Formally, the state of the quantum-mechanical system is described either as a vector in a Hilbert space $|\psi\rangle$ (in the case of pure states) or by a density operator $|\rho\rangle$.

The basic building block in quantum communications and information is the qubit that is a physical system with two orthogonal quantum states. A simple example is the horizontal and vertical states of polarization associated with a single photon. The quantum bit, or qubit, is the quantum generalization of the classical notion of the physical bit. It corresponds to a two-state quantum system, such as a two-state quantum system, the spin degree of freedom of an electron, or a nuclear spin [2]. The pure states of such a system are vectors in a two-dimensional Hilbert space. (More accurately, they correspond to rays in a two-dimensional Hilbert space, since the overall phase freedom is nonphysical, and states must be normalized.) Such a system can be used to carry classical information. Any pair of orthogonal basis vectors may be taken to represent the answers **"yes" or "no"** **"0" or "1"** to a single question. One might name these states $|0\rangle$ and $|1\rangle$.

Preparing the system in the appropriate one of these two states, one may store this information in the system. By measuring in this basis one may read the information out of the system accurately, or, by an appropriate unitary interaction, one may swap this information for the information stored in another qubit, or cause another bit to become correlated with this one. Therefore, the system can be used as a classical physical bit. Besides the two orthogonal states in a given basis, there is a continuum of states.

$$|\psi\rangle = \alpha_1|\phi_1\rangle + \beta_1|\phi_2\rangle \quad [3.5].$$

Which are superposition of the basis vectors $|0\rangle$ and $|1\rangle$ and orthogonal to neither of them. α_1 and β_1 are complex constants.

Equivalently, the state of a quantum-mechanical system can be described by a wave-function or, in the framework of the phase-space formalism, the state under consideration can be described with the help of phase-space

quasi-probability density distributions. [2] As mentioned above, classical dynamical variables can be measured to arbitrary accuracy in principle. This permits precise measurement of conjugated variables such as position and momentum, and allows joint probability density distribution to be constructed for a phase-space description of dynamics. However the lack of commutability of conjugated observable in quantum mechanics leads to the fact that the "point" in the quantum-mechanical phase space cannot be localized precisely, i.e., there is always a fundamental limit with which this "point" can be determined.

The statement that the product of the uncertainties in the values of two conjugate variables cannot be less than Planck's constant \hbar in the order of magnitude is called the Heisenberg uncertainty principle. [23]

Mathematically:

$$\Delta A \Delta B \geq \frac{\hbar}{2} \quad [3.6]$$

Where $\Delta A \Delta B$ are canonically conjugate variables and \hbar is Planck's constant.

It is well known that the wave function of a quantum-mechanical system cannot be measured directly [12]. Besides a single measurement does not yield enough information, which allows determining the state of the system uniquely [12]. In addition, due to the fact that conjugated observable do not commute, the quantum-mechanical measurement inevitably disturbs the state, so the information about the conjugated observable cannot be obtained from subsequent measurements. This result into a number of (quasi) probability density distributions associated with a phase-space description of a quantum-mechanical state The Wigner function plays an exceptional role among all quasiprobability density distributions. Firstly, it generates proper marginal distributions for individual phase-space variables. Secondly, under the action of linear canonical transformations the Wigner function behaves exactly in the same way as the classical probability density distributions [10] The Wigner function contains complete information about the state of the system, i.e.,

it carries the same information as the density operator or the corresponding wave function. From the Wigner function one can evaluate all (symmetrically-ordered) moments of the system operators. On the other hand, the inverse is also valid. It means that from the knowledge of the complete set of moments of system operators the Wigner function (as well as the density operator) can be determined uniquely [11].

In finding quantum mechanical representation of a single mode of a coherent optical field, the analogy between the photon and Simple harmonic oscillator give a better perspective. Consider a one-dimensional cavity of length L as shown in Fig.3.1. In, which the plane wave mode has an electric field described by,

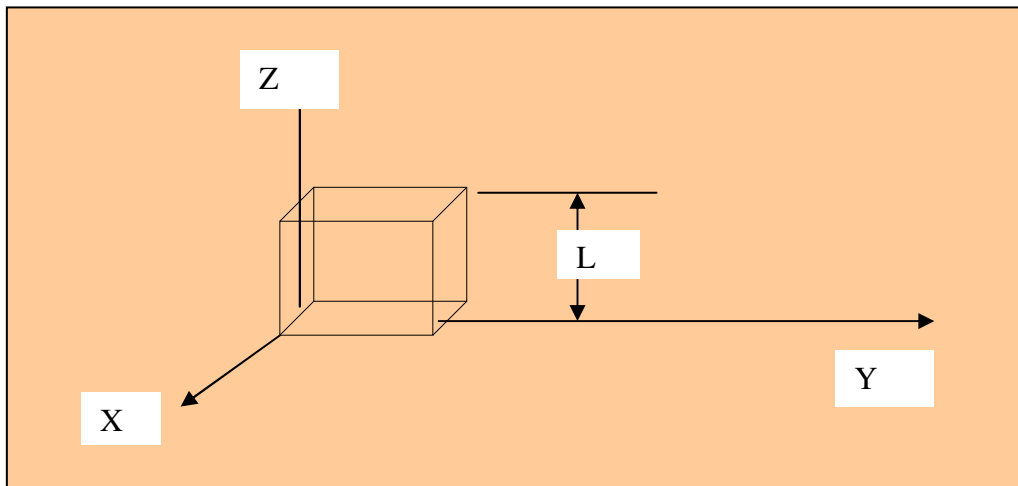


Fig.3.1. Cubic optical cavity

$$E = E_0 \cos(kx - \omega t - \phi) \quad [3.6]$$

Where the value of k and therefore ω are defined by L . The magnetic field B is not independent, and is always related to E **by** the impedance. Note that k and E will now be written as scalars, since the choice of particular mode (including its polarization) allows considering a single component of the field only. It is the magnitude of E_0 that will be shown to be quantized. [20]

First define two quantities

$$\begin{aligned}
q(t) &= \frac{E_0}{\omega} \cos(\omega t + \phi) \\
p(t) &= -E_0 \sin(\omega t + \phi)
\end{aligned}
\tag{3.7}$$

Noting that, $\frac{dq(t)}{dt} = p(t)$, and one can write the field

$$\begin{aligned}
E &= E_0[\cos(\omega t + \phi) \cos(kx) + \sin(\omega t + \phi) \sin(kx)] \\
&= \omega q(t) \cos(kx) - p(t) \sin(kx)
\end{aligned}
\tag{3.8}$$

The total energy per-unit cross-sectional area of the cavity [38] (including E and B fields) is then;

$$\begin{aligned}
U &= \int_0^L \epsilon_0 E^2 dx \\
&= \int_0^L \epsilon_0 (\omega q \cos(kx) - p \sin(kx))^2 dx \\
&= \frac{1}{2} \epsilon_0 L (\omega^2 q^2 + p^2)
\end{aligned}
\tag{3.9}$$

Using new variables again

$$\begin{aligned}
Q(t) &= (\epsilon_0 L)^{\frac{1}{2}} q \\
P(t) &= (\epsilon_0 L)^{\frac{1}{2}} p \\
U &= \frac{1}{2} (\omega^2 Q^2 + P^2)
\end{aligned}
\tag{3.10}$$

The above expression has the same form as the energy of a mechanical Simple harmonic oscillator [38], for which

$$U = \frac{1}{2} (Kx^2 + mv^2)
\tag{3.11}$$

Where K is the force constant and m is the mass. This can also be written in the same way as Eq [3.10], in which $\omega = \sqrt{K/m}$ is the classical vibration frequency, $\sqrt{m}x = Q$ and $\sqrt{m}v = \frac{dQ}{dt} = P$.

The energy of a simple harmonic oscillator is $U_n = \hbar \cdot \omega (n + \frac{1}{2})$.

Where n can be any non-negative integer. Thus one can deduce that the energy of the given mode of electromagnetic field is quantized in the same way. [7] An important non-classical feature is the existence of zero point energy.

$$U_0 = \frac{1}{2} \hbar \cdot \omega \quad [3.12]$$

Which is the lowest allowed energy level for that mode; it is not possible to eliminate field oscillation in any mode completely. [7] Even the lowest energy in every mode of the cavity contains this much energy. The actual electric field resulting from the zero point contributions of all the modes is their superpositions. Since their phase relation are unspecified they give rise to an inevitable fluctuating back ground field which adds noise to any physical measurements.

It is illustrative at this point to express the uncertainties on a $(P, \omega Q)$

Diagram (In quantum mechanics this is called a Wigner diagram[37]) by choosing P as horizontal and ωQ as a vertical axis as in Fig.3.2. The energy then is proportional to the square of the radius vector from the origin to $(P, \omega Q)$. However the point $(P, \omega Q)$ cannot be defined exactly

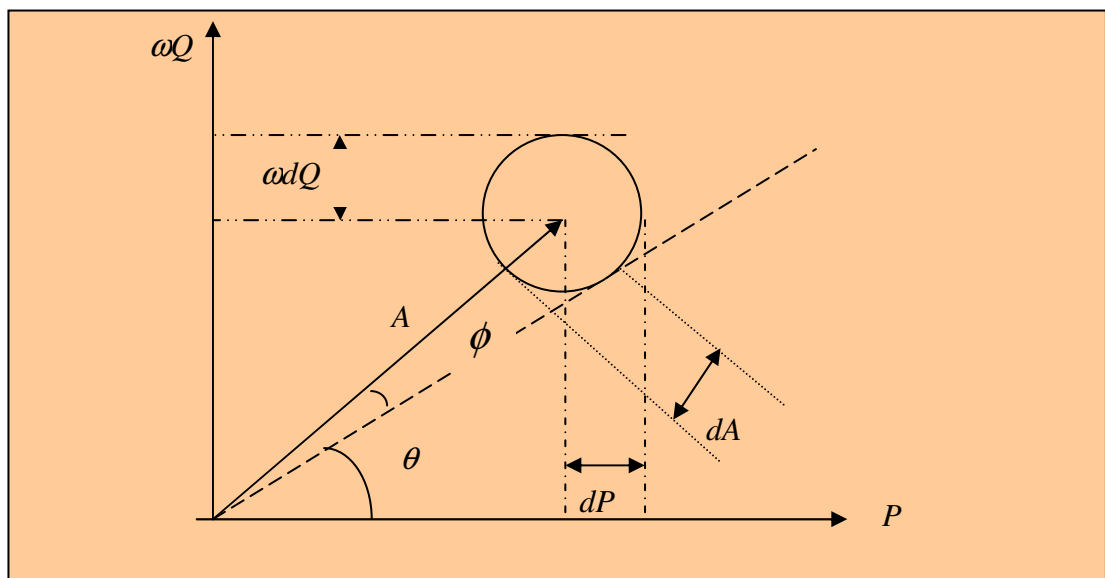


Fig 3.2. $(P, \omega Q)$ Diagram for light with minimum uncertainty (Chaotic light)

because of the uncertainty principle. All that can be known is the average position of the point, and the product of the uncertainty. When one defines the uncertainty region in the $(P, \omega Q)$ plane the construction of the wave become elementary. Taking coherent states and choosing randomly a number of points within the uncertainty region and draw one on top of the other we can clearly see the fluctuation in the field- depending on the choice.

Since P and ωQ appear symmetrically in Fig.3.2, one can expect the value of P and ωQ to be equal, so that the defined region is a circle. This is the situation that would normally be found, and to which any other situation that would normally be found, and which any other situation will naturally revert. Light with a single mode with this property is called coherent light.

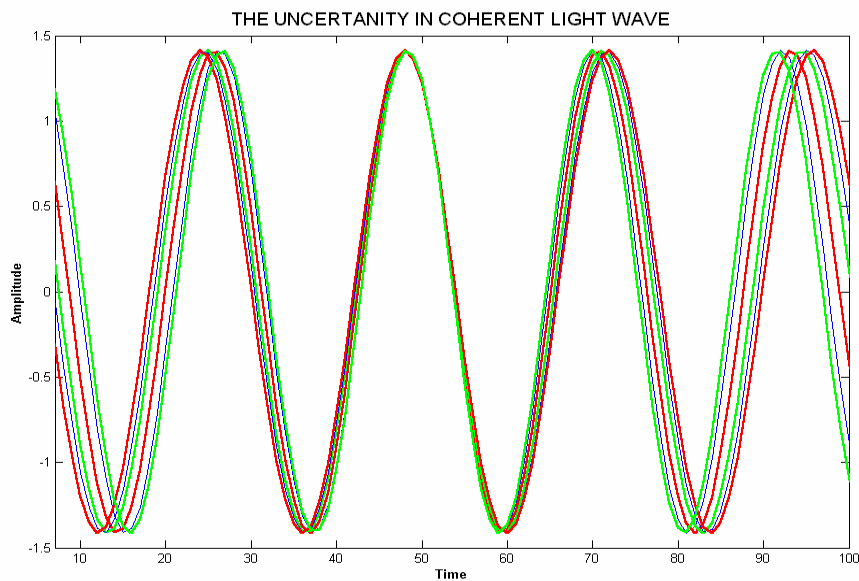


Fig.3.3 The uncertainty indicated by the range of superimposed waveforms

Each wave has amplitude and phase (A, ϕ)
 $A^2 = P^2 + \omega^2 Q^2 = 2U$ which are the polar coordinates of $(P, \omega Q)$ As shown in the Fig.3.3 in which the width covered by the resulting lines represent the uncertainties in the wave fields.

i.e.

$$\omega \delta P \delta Q = A \delta A \delta \phi = \frac{1}{2} \delta(A^2) \delta \phi \geq \hbar \omega \quad [3.13]$$

Chaotic light has the equilibrium [6] form $\delta P = \omega \delta Q = \sqrt{\hbar \omega}$. Then from Eq [3.9] putting $\phi = 0$, to simplify things

$$\begin{aligned} \delta U &= \omega^2 Q \delta Q + P \delta P \\ &= (\epsilon_0 L)^{\frac{1}{2}} \left[\omega^2 \frac{E}{\omega} \cos(\omega t / \omega)^{\frac{1}{2}} + E_0 \sin \omega t (\hbar \omega)^{\frac{1}{2}} \right] \\ &= (\epsilon_0 \hbar \omega L)^{\frac{1}{2}} (E_0 \cos(\omega t) + E_0 \sin(\omega t)) \end{aligned} \quad [3.14]$$

This shows that the contributions to δU from $\cos \omega t$ term and $\sin \omega t$ phases are equal. The root mean square fluctuation ΔU in each phase is

$$\Delta U = \langle (\delta U)^2 \rangle^{\frac{1}{2}} = (\epsilon_0 \hbar \omega L)^{\frac{1}{2}} E_0 \langle \cos^2 \omega t \rangle^{\frac{1}{2}} = E_0 \left(\frac{\epsilon_0 \hbar \omega L}{2} \right)^{\frac{1}{2}} \quad [3.15]$$

One can compare the fluctuation in mean intensity, when both are measured as numbers n of photon per unit area in a given time. Then one can have

$$\begin{aligned} \delta n &= \frac{\Delta U}{\hbar \omega} = E_0 \left(\frac{\epsilon_0 L}{2 \hbar \omega} \right)^{\frac{1}{2}} \\ \langle n \rangle &= \frac{U}{\hbar \omega} = \frac{1}{2} (\omega^2 Q^2 + P^2) \frac{1}{\hbar \omega} \\ &= \frac{1}{2} \left\langle \omega^2 \frac{E_0^2}{\omega^2} \cos^2 \omega t + E_0^2 \sin^2 \omega t \right\rangle \frac{\epsilon_0 L}{\hbar \omega} \\ &= E_0^2 \frac{\epsilon_0 L}{2 \hbar \omega} \\ (\delta n)^2 &\equiv \langle n \rangle \end{aligned} \quad [3.16]$$

Indeed chaotic light which is light with many photon in a single mode having $\delta P = \omega \delta Q = \sqrt{\hbar}$, fluctuate in a way corresponding to Poisson statistics, which also represent the smallest fluctuation possible in a semi classical model. Poisson statistics indicate the arrival of photon at a

detector is un correlated with that of the previous one. Which necessarily limit the accuracy of optical measurement .If one can force them to be correlated, the stream of arrival will be steadier and an improvement in accuracy is to be expected. Although this method is tried by semi classical approach, the essential point is that the trial exists because light is emitted as individual quanta, and therefore cannot be described classically.

3.3. The Coherent-State Representation of Optical Signals

Coherent states, representing electromagnetic radiation produced by physical devices such as lasers, are an important class of states for optical communications. Within the framework of the phase-space formalism Coherent states form a position-momentum patch of minimum area and may be regarded as the quantum analogue of classical points in phase space.[11] Coherent states of a single mode of radiation $|\alpha\rangle$ in quantum formulation expressed as

$$|\alpha\rangle = e^{-\frac{1}{2}|\alpha|^2} \sum_{n=0}^{\infty} \frac{\alpha^n}{(n!)^{\frac{1}{2}}} |n\rangle \quad [3.17]$$

Where the Eigen states $|n\rangle$, known as the number Eigen states. [36]: Each number Eigen state $|n\rangle$ contains n photons, where α is the complex number. The corresponding number density operator is also given by

$$\rho = |\alpha\rangle\langle\alpha| = e^{-|\alpha|^2} \sum_n \sum_m \frac{\alpha^n (\alpha^*)^m}{(n!m!)^{\frac{1}{2}}} |n\rangle\langle m| \quad [3.18]$$

Where the density operator viewed as an infinite dimensional matrix, and the diagonal terms are

$$\langle n|\rho|m\rangle = e^{-|\alpha|^2} \frac{|\alpha|^{2n}}{n!} \quad [3.19]$$

Which are recognized as Poisson probabilities for n , with an average number of photon $|\alpha|^2$ [12]. The off diagonal terms are,

$$\langle m | \rho | n \rangle = e^{-|\alpha|^2} \frac{\alpha^n (\alpha^*)^m}{(n!m!)^{\frac{1}{2}}} \quad [3.20]$$

Note that measuring photon is directly related to measuring of energy. Hence the probability of obtaining exactly n photons as the outcome of an experiment can be computed as

$$|\langle \alpha | n \rangle|^2 = \frac{1}{n!} e^{-|\alpha|^2} |\alpha|^{2n} \quad [3.21]$$

The quantum interference between coherent-state components in phase space, which is intrinsically related to the over incompleteness of the coherent-state basis, is what leads to purely quantum effects. As can be seen from the above description the off-diagonal elements of the density operator in the coherent-state basis carry information about the non-classical properties of quantum states of light. By considering the overlap between two arbitrary coherent states, $|\alpha_1\rangle, |\alpha_2\rangle$, one can easily show that coherent states are not orthogonal. Orthogonality requires the overlap between the states should vanish altogether; however, for coherent states, the squared magnitude of the overlap is not zero but instead is given by:

$$\begin{aligned} |\langle \alpha_1 | \alpha_2 \rangle|^2 &= \left| e^{-(|\alpha_1|^2 + |\alpha_2|^2)} \sum_n \sum_m \frac{\alpha_1^n \alpha_2^{*m}}{\sqrt{n!} \sqrt{m!}} \langle n | m \rangle \right|^2 \\ &= \left| e^{-\frac{1}{2} (|\alpha_1|^2 + |\alpha_2|^2 - 2\alpha_1 \alpha_2^*)} \right|^2 \\ &= e^{-|\alpha_1 - \alpha_2|^2} \end{aligned} \quad [3.22]$$

Eq [3.22] demonstrates that there is always some overlap between coherent states, regardless of how great the coherence between the states and average photon counts may be. This phenomenon accounts the quantum interference and the error one made in optical detection.

Quantum Signal Processing & Detection Operator

In this chapter we deal with the optimization problem that is, finding communication system for a given task that performs the best within the given class of all the possible system. In taking this approach one face with these basic problems:

- 1) What optimization criterion is to be used?
- 2) What is the optimum structure for a given problem under these criteria of optimization?
- 3) What is the performance of the optimum receiver?

One may formulate these problems as a quantum detection problem, and seek a measurement that minimizes the probability of a detection error [24]. Therefore, in this section, by briefly reviewing elements of linear algebra that are common to both signal processing and quantum communication we proceed to the problem of formulating detection operator.

In both signal processing and quantum mechanics, the setting one considers is a $|x\rangle$ finite-dimensional subspace U of a complex Hilbert space H . [24] The elements of H are called vectors. Assuming for notational convenience, H that is finite-dimensional, with $\dim(H) = k$; then, by appropriate choice of coordinates, one can identify H with C^k .

In the **bra-Ket** notation, the elements of H are "Ket" vectors, denoted, e.g., by $|x\rangle \in H$. The corresponding "bra" vector $\langle x| \in H^*$ is an element of the dual space and may be regarded as the Conjugate transpose of $|x\rangle$. The inner product of two vectors is a complex number denoted by $\langle x|y\rangle$. An outer product of two vectors such as $|x\rangle\langle y|$ is a rank-one matrix, which as an operator $z \in H$ takes to $|x\rangle\langle y||z\rangle = \langle y|z\rangle|x\rangle \in H$.

An operator on H is a continuous linear transformation A : The adjoint of a linear operator A is the unique operator A^* such that $\langle x | Ay \rangle = \langle A^*x | y \rangle$ for all $x, y \in H$. [41] If the elements of H are column vectors of A , then a linear operator is represented by a square matrix, and its adjoint is represented by the conjugate transpose A^* , since

$$\langle x | Ay \rangle = x^* Ay = (A^*x)^* y = \langle A^*x | y \rangle \quad [4.1]$$

An operator A is called *Hermitian* if it is self-adjoint; i.e., if $A = A^*$ [24]

In many quantum mechanics the term "observable" is used synonymously with "selfadjoint operator" (with no constraint like $0 \leq F \leq \mathbf{1}$). So one has to make the connection. In one direction it is easy: suppose the measuring device produces *real numbers as output*, i.e., the set X is a set of real numbers. Suppose if one is not interested about the entire probability distribution of the outcomes, but only about their *mean*. For each density operator $|\rho\rangle$ this mean is obviously [24]

$$\sum Tr(\rho F) = Tr(\rho A_1) \quad [4.2]$$

Using the linearity of the trace, and introduced the operator expression

$$A_1 = \sum_x x F_x. \quad [4.3]$$

This is the kind of operator usually called an "observable" [20]. Its expectation value $Tr(\rho A_1)$ is the mean value of the measured probability distribution.

Similarly, one can introduce an operator $A_2 = \sum_{xxx} x^2 F_x$ such that $Tr(|\rho\rangle F_x)$ is the second moment of the measured distribution. In general, A_2 has nothing to do with A_1 . However, there is an important special case, in

which A_2 can be computed from A_1 : the case of *spectral measures*, or more generally **projection-valued observable**. [20]

An observable is called projection valued, if each of its "values" F_x is a projection, i.e., $F_x^2 = F_x$. Since the projections F_x add up to the identity, they have to be orthogonal, so $F_x F_y = \delta_{xy} F$. From this relation one readily concludes that $A_2 = A_1^2$, where the square on the right hand side of this equation is formed using the operator product. Hence A_2 is determined by A_1 , and so are the F_x themselves. This is the content of the *Spectral Theorem*, [27] here in its fairly trivial finite dimensional version: Every Hermitian operator A on a finite dimensional Hilbert space has a unique decomposition $A = \sum_{x \in \Omega} x F_x$. The finitely many values x for which F_x is non-zero are the eigenvalue of A , and this confirms the usual phrase that the eigenvalue of an observable are the possible outcomes of measurements of that observable. .

Therefore, one can generalize the usual notion of observable in two ways: firstly, one shouldn't insist that the outcomes of measurements are real numbers; they can be labeled by any set one pleases. [15] Secondly, and more importantly, one shouldn't insist that the response of a single outcome (a yes/no measurement) is given by a projection. The effect of this generalization is discussed in chapter six. However the detection operators considered in this chapter are projection valued [20]

4.1. Basics of Quantum Detection Operator

Consider a quantum communication for sending M-array classical information $\{X_i / i = 0, 1, \dots, M - 1\}$. In this case the output of the transmitter are quantum states or probability density functions $\{\rho_i\}$ i.e. $[\rho_0, \rho_1, \dots, \rho_M]$ which corresponds to classical information.

$$\rho_i \geq 0 \tag{4.4}$$

$$\hat{Tr}(\rho_i) = 1 \tag{4.5}$$

Where Tr denotes trace, i.e., the sum of the diagonal element of the matrix. If the signal state is pure $\{\rho_i\}$ the state can be described by a unit vector $|\psi\rangle$ in the Hilbert space and the density operator expressed by $\rho = |\psi\rangle\langle\psi|$ and $Tr\rho^2 = 1$ is satisfied. If the signal state is mixed the state contains classical noise and $Tr\rho^2 < 1$ is satisfied.

A quantum receiver in which a quantum measurement is performed is generally described by a positive valued measure; (PVM) which is a set of non-negative Hermitian operator $\{\pi_j\}$ satisfies the resolution of the identity.

$$\sum_{j=0}^{M-1} \pi_j = \mathbf{I} \quad [4.6]$$

$$\pi_j \geq 0 \quad [4.7]$$

Where $\hat{\mathbf{I}}$ is the identity operator, $\hat{\pi}_j$ is called the detection operator and express measurement process which decides that the received states are ρ_j .

In general the number of detection operator shouldn't be equal to the number of signal sets. But one can suppose that they are equal-since the performance measure only treat probability of error as criteria.

If $\{\pi_j\}$ satisfies not only Eq [4-3] but also $\pi_j \pi_i = \delta_{ij} \pi_j$ where δ_{ij} is the kroncker delta, which is defined as.

$$\delta_{jj'} = \begin{cases} 0 & j \neq j' \\ 1 & j = j' \end{cases} \quad [4.8]$$

Then $\{\pi_j\}$ are called projection operator value measure (POVM)[20]. Therefore when the transmitted signal is ρ_i , the probability that the received signal is decided to be ρ_j , by π_j is

$$P(\rho_j | \rho_i) = \text{Tr}(\rho_i \pi_j) \quad [4.9]$$

Then the error probability is represented as

$$p = 1 - \sum_{j=0}^{m-1} \xi_j \text{Tr}(\rho_j \pi_j) \quad [4.10]$$

Where ξ_j is the priori probability of ρ_j , and the operator $\{\pi_j^{opt}\}$ by which P is minimized are called the optimum detection operator. [10]

4.2. Optimal Quantum Measurements

Obtaining a closed-form analytical expression for the optimal detection operator in Eq [4.10] is a difficult and unsolved problem. But when the signal state are simple or show certain symmetries alternative approach can be developed [3].

That is based on choosing a squared-error criterion and determining a measurement states that minimizes this criterion. Specifically, the measurement vectors $|\mu_i\rangle$ are chosen to be orthogonal and closest in least-squares (LS) sense to the given set of state vectors $|\psi_i\rangle$ so that the vectors $|\mu_i\rangle$ are chosen to minimize the sum of the squared norms of the error vectors.

In the simplest case, the measurement operators are rank-one operators and have the outer-product form $\Pi_i = \mu_i \mu_i^*$ for some nonzero vectors $\mu_i \in H$. Such measurements will be called rank-one

measurements, as shown in Fig.4.1 and the vectors μ_i will be called the measurement vectors.

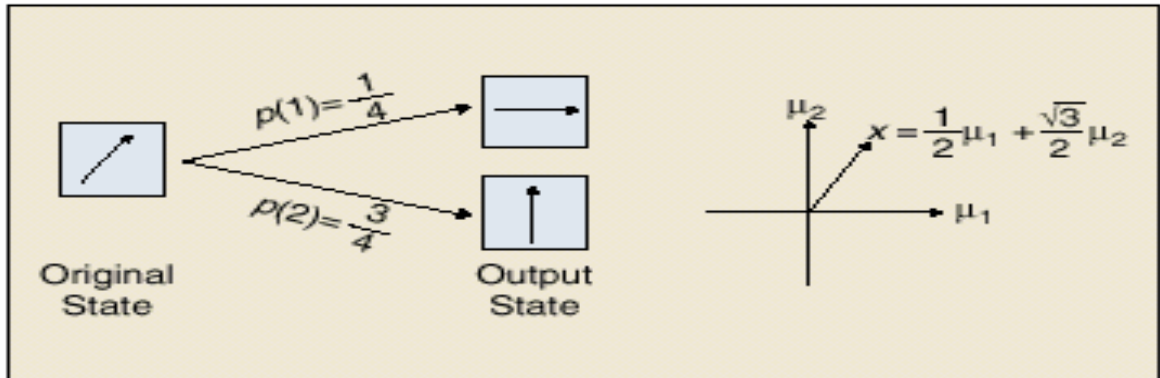


Fig4.1-illustration of a rank-one quantum measurement

If the state vector is ψ , then the probability of observing the i^{th} outcome is simply the squared projection of the states on the measurement states [24].

$$P(i) = \langle \psi_i, \Pi_i \psi_i \rangle = |\langle \psi_i, \mu_i \rangle|^2 \quad [4.11]$$

If the states are prepared with equal priori probabilities, then the probability of detection error using the measurement vectors is given by

$$P(E) = 1 - P(C) = 1 - \frac{1}{M} \sum |\langle \psi_i | \mu_i \rangle|^2 \quad [4.12]$$

If the vectors are orthonormal, then choosing $\psi_i = \mu_i$ results in $P(E) = 0$. However, if the given vectors are not orthonormal, then no measurement can distinguish perfectly between them. Therefore, a fundamental problem in quantum communication is to construct measurements optimized to distinguish between a set of nonorthogonal pure quantum states.

To construct a measurement vectors from a given set of vectors that span a signal set, a reasonable approach is to find a set of vectors that are

“closest” to the vectors in the least-squares sense. Thus, one seeks vectors that minimize the squared error defined as follows ,

$$E = \sum_{i=1}^n \langle e_i | e_i \rangle \quad [4.13]$$

Where the i^{th} error vector as illustrated by Fig. 4.2 in two-dimensional cases is given by the vector difference $|e_i\rangle = |\psi_i\rangle - |\mu_i\rangle$

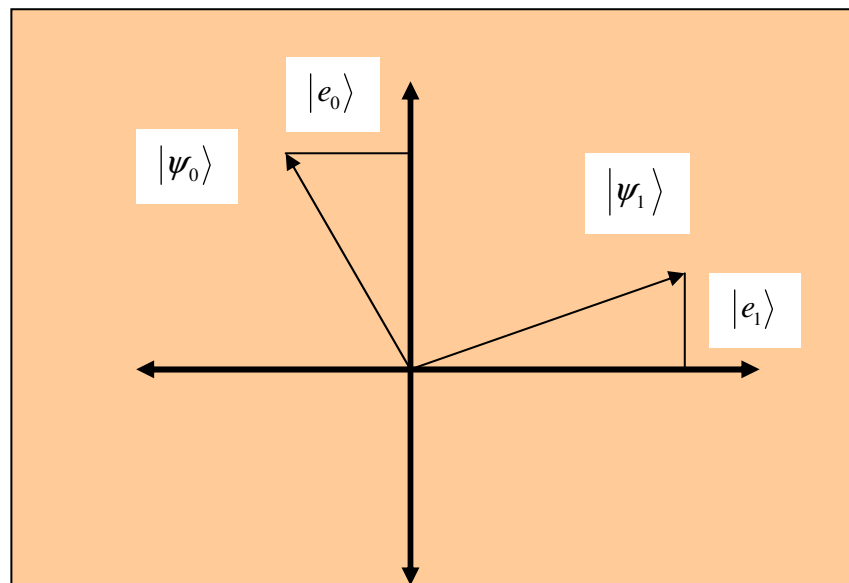


Fig-4-2. Two dimensional examples of LS measurement

The LS measurement problem in Eq [4.13] has a simple closed-form solution with many desirable properties. Its construction is relatively simple; it can be determined directly from the given collection of states. [24]

4.2.1 Optimal Detection Operator for Binary pure State Signal

The simplest quantum mechanical system has a two dimensional complex state space. In this case two possible quantum states are present that

needs modeling. Suppose the received electromagnetic field in states $|\psi_0\rangle$ is governed by the density operator ρ_0 , and the received electromagnetic field in state $|\psi_1\rangle$ governed by ρ_1 . i.e,

$$|\rho_0\rangle = |\psi_0\rangle\langle\psi_0| \quad [4.14]$$

$$|\rho_1\rangle = |\psi_1\rangle\langle\psi_1| \quad [4.15]$$

If one single out an orthonormal basis set in the state space of such a system, and label the basis vectors as $|\mu_0\rangle$ and $|\mu_1\rangle$ then the total probability of correct detection [8] is given by

$$P(C) = P(H_0)P(C/H_0) + P(H_1)P(C/H_1) \quad [4.16]$$

Where H_0 denotes the hypotheses that state $|\psi_0\rangle$ is transmitted and H_1 represent the hypothesis that state $|\psi_1\rangle$ is transmitted. $P(C)$ = The total probability of corrects detection, $P(H_0)$ = priori probability of hypothesis H_0 and $P(H_1)$ = priori probability of hypothesis H_1 and $P(C/H_i)$ is the probability of correct given Hypothesis H_i .

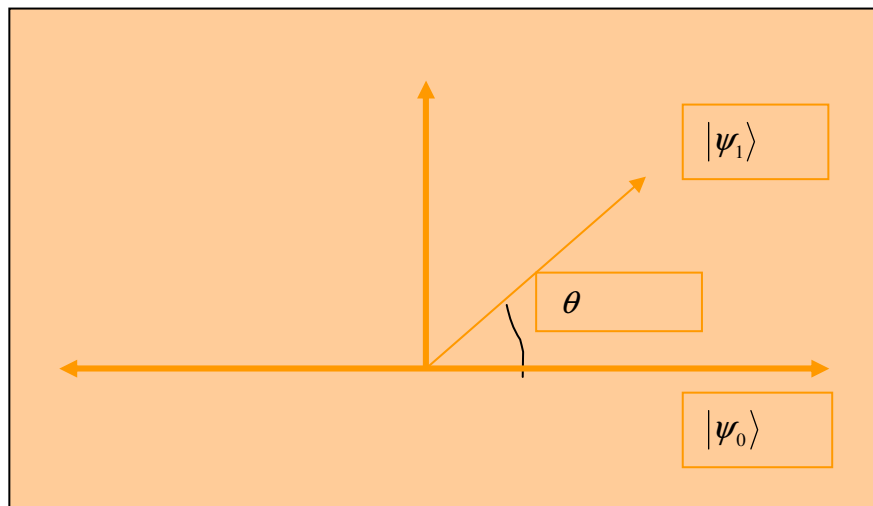


Fig.4.3. Binary signal state representation in a two dimensional Hilbert space

If one gives the geometrical interpretation to the signal set and measurement set as in Fig.4.3 the conditional probability denote nothing but the squared magnitude of the signal set on the respective measurement states.

Mathematically:

$$P(C) = P(H_0) |\langle \psi_0 | \mu_0 \rangle|^2 + P(H_1) |\langle \psi_1 | \mu_1 \rangle|^2 \quad [4.17]$$

If the signal state has equal priori probability, then the above expression can be simplified as

$$P(C) = \frac{1}{2} [|\langle \psi_0 | \mu_0 \rangle|^2 + |\langle \psi_1 | \mu_1 \rangle|^2] \quad [4.18]$$

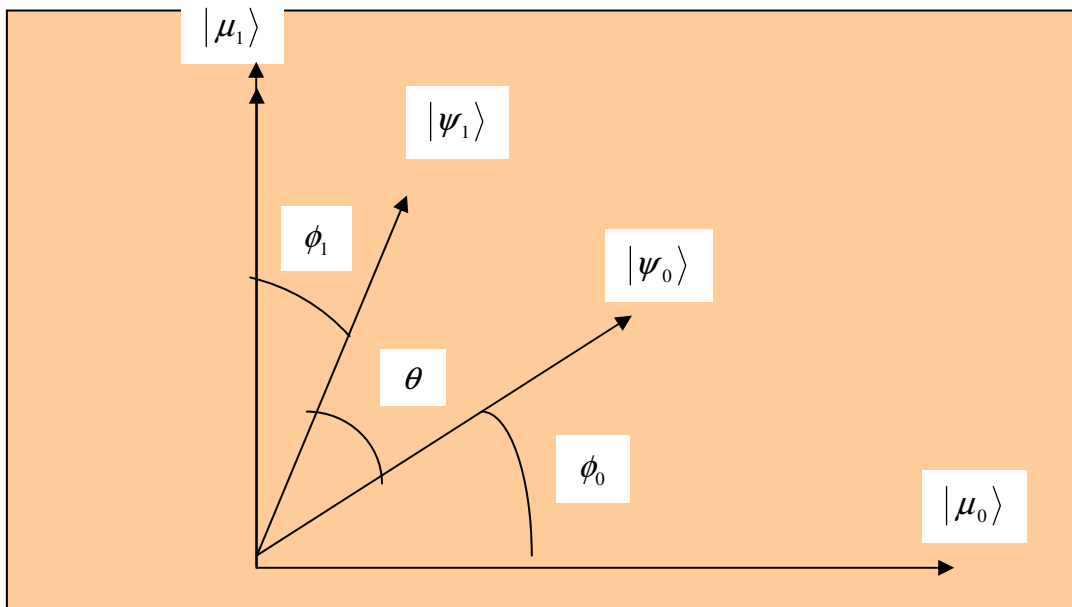


Fig.4.4 -Signal and Measurement states in 2-dimensional Hilbert space

Operating entirely in the plane determined by the signal states, it is possible to find the minimum average probability of error by rotating the

measurement states within the signal plane and calculating the error probability for each rotation until a minimum is reached. The plane defined by two signal states, and containing two orthogonal measurement states is shown in Fig.4.4. To simplify the steps of finding appropriate measurement axis lets define $0 \leq \phi_0, \phi_1 \leq \frac{\pi}{2}$ and we interpret $\cos(\theta) = |\langle \psi_i | \mu_i \rangle|, i = 0,1$ as the overlap between the signal and corresponding measurement states. Note from Fig.4.4 that. $\phi_0 = \frac{\pi}{2} - \theta - \phi_1$.

$$P(C / H_0) = |\langle \psi_0 | \mu_0 \rangle|^2 = \cos^2(\phi_0) \quad [4.19]$$

$$P(C / H_1) = |\langle \psi_1 | \mu_1 \rangle|^2 = \cos^2(\phi_1) \quad [4.20]$$

With equally probable signals the average probability of correct detection.

$$\begin{aligned} P(C) &= \frac{1}{2} [|\langle \psi_0 | \mu_0 \rangle|^2 + |\langle \psi_1 | \mu_1 \rangle|^2] \quad [4.21] \\ &= \frac{1}{2} [\cos^2(a - \phi_1) + \cos^2(\phi_1)] \end{aligned}$$

Where ,we define $a = \frac{\pi}{2} - \theta$ for convenience. The maximum value of the probability of correct detection, as a function of the rotation angle, can be easily found by differentiating $P(C)$ with respect to ϕ_1 and equating to zero:

$$\frac{\partial P(C)}{\partial \phi_1} = -2 \cos(a - \phi_1) \sin(a - \phi_1) + 2 \cos(\phi_1) \sin(\phi_1) = 0 \quad [4.22]$$

This yields the optimum rotation angle $\phi_1^* = a/2 = \frac{1}{2} \left(\left[\frac{\pi}{2} \right] - \theta \right)$. Substituting ϕ_1^* into the expression for $P(C)$ yields the maximum value of the probability of correct detection as

$$P^{opt}(C) = \frac{1}{2} \left[\cos^2\left(\frac{a}{2}\right) + \cos^2\left(\frac{a}{2}\right) \right] \quad [4.23]$$

$$= \frac{1}{2} [1 + \cos(a)]$$

$$= \frac{1}{2} [1 + \sin(\theta)] \quad [4.24]$$

But using Trigonometry it is easy to prove the expression $\sin(\theta) = \sqrt{1 - \cos^2(\theta)} = \sqrt{1 - |\langle \psi_0 | \psi_1 \rangle|^2}$ in Fig.4.4. Hence using the maximum value of $P(C)$, the minimum probability of error for this binary state signal becomes

$$P(E) = 1 - P(C) = \frac{1}{2} \left[1 - \sqrt{1 - |\langle \psi_1 | \psi_2 \rangle|^2} \right] \quad [4.25]$$

This is one of the developments of quantum detection principle. Rather than taking state zero as totally deterministic (as in the case of sub optimal detection) by associating quantization to the signal state develops a rotational algorithm that leads to the minimization of the average probability of error.

One can see the effect of this rotation in minimization of error through the Matlab programme output in Fig.4.5. Initially the signal state of $|\psi_0\rangle$ and $|\mu_0\rangle$ are aligned. Then by adding one degree the rotation of the measurement state $|\mu_0\rangle$ away from signal state $|\psi_0\rangle$ is performed. And calculation of the probability of average error is evaluated. By repeating the above step with equal interval till the measurement state $|\mu_1\rangle$ aligned with the signal state $|\psi_1\rangle$. In this way one gets the optimal orientation of the measurement state as in Fig.4.5. In this regard, the optimal quantum receiver can be viewed as a simple rotation of the measurement states in the plane defined by the signal states in the front end of the receiver [For the detailed programme see appendix-No.C.1 annexed to the thesis]

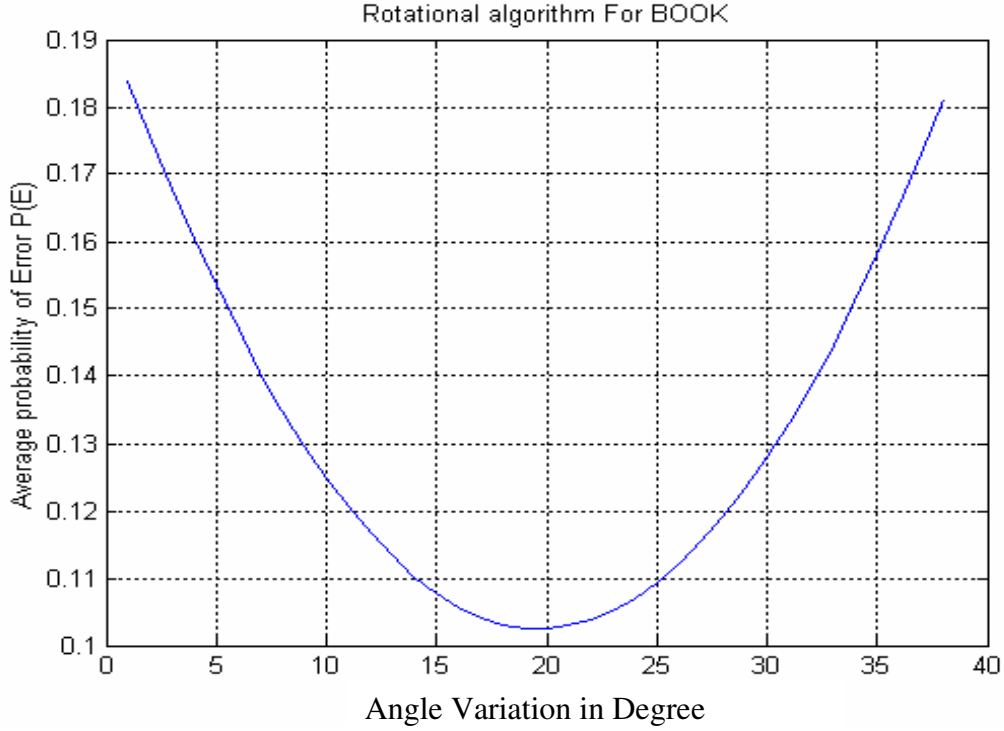


Fig 4.5. The dependence of average probability of error on variations of measurement states orientations for Book with $k_s=1$

Using similar steps it is also possible to find the orientation for the measurement states of Binary phase Shift Key optical modulation. [19] In this case the signal in a Hilbert space has a form

$$\begin{aligned} |\psi_0\rangle &= |\alpha\rangle \\ |\psi_1\rangle &= |-\alpha\rangle \end{aligned} \quad [4.26]$$

With average photon signal equals $k_s = |\alpha|^2$. The angle and the magnitude square overlap between the signals states expressed as follow respectively,

$$\begin{aligned} \cos(\theta_{01}) &= \langle \alpha | -\alpha \rangle = e^{-2|\alpha|^2} = e^{-2k_s} \\ \theta_{01} &= \cos^{-1}(e^{-2k_s}) \end{aligned} \quad [4.27]$$

$$|\langle \psi_0 | \psi_1 \rangle|^2 = |\langle \alpha | -\alpha \rangle|^2 = e^{-2|\alpha|^2} = e^{-4k_s} \quad [4.28]$$

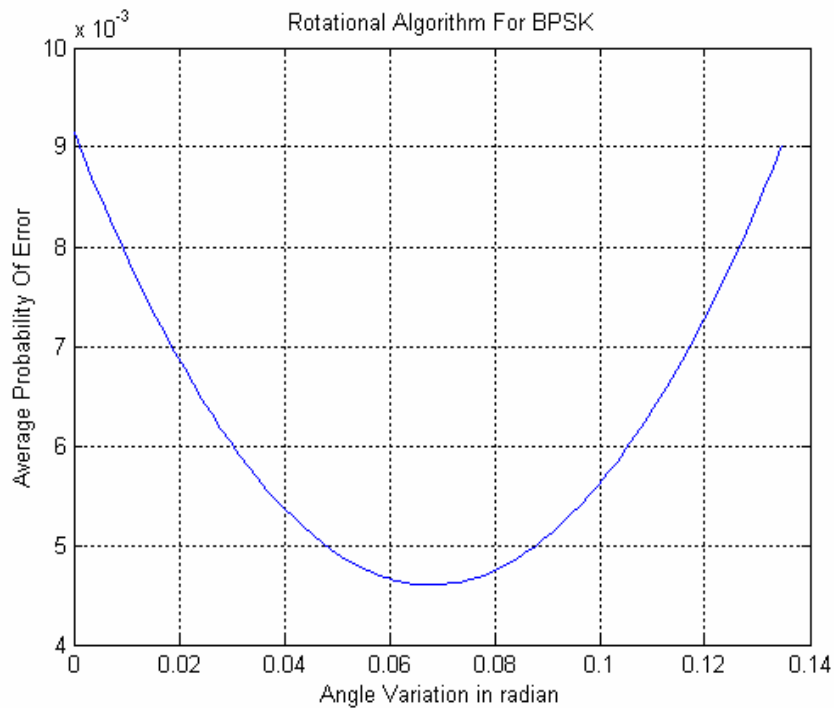


Fig 4.6. *The dependence of average probability of error on variations of measurement states orientations for BPSK with $k_s=1$*

Then, Using the rotational algorithm, i.e. by varying the orientations of the two measurement states in a plane defined by the signal state one can find the optimal point that minimize the error in a mean square sense as shown in the Fig.4.6. Since BPSK and BOOK are different modulation the orientation and the average probability of error *differs* [For the complete programme see appendix-No.B.2 annexed to the thesis]

4.2.2. Optimal Detection Operator for M-array optical modulation formats

There are situations where a single Hilbert space is not sufficient to describe the signal state. [19] According to the general rules of quantum mechanics a Hilbert space is associated with every kind of quantum mechanical system. A principal way of getting new systems from old is

putting two systems together into a "composite system" by rule of Tensor product.

The tensor product of $|\psi_a\rangle$ and $|\psi_b\rangle$ give us a large array formed by taking all possible product between $|\psi_a\rangle$ and $|\psi_b\rangle$ and denoted as follows

$$|\psi_a\rangle \otimes |\psi_b\rangle = |\psi_c\rangle \quad [4.29]$$

If $|\psi_a\rangle$ is $m \times n$ and $|\psi_b\rangle$ is $p \times q$ then the vector $|\psi_c\rangle$ will have a dimension $m \times p$ by $n \times q$ [35].

An important example of modulation format that requires a "product-state" description of the form shown above is M-array pulse-position modulation, or PPM. [41] This modulation format in quantum state space description can be found from the product of coherent states as follows,

$$|\alpha_k\rangle = |\alpha_{K,1}\rangle |\alpha_{K,2}\rangle \dots \dots \dots |\alpha_{K,M}\rangle \quad [4.30]$$

Where each of the $|\alpha_{K,j}\rangle$ are coherent states associated with the individual modes produced from the output of laser, with $|\alpha_{K,j}| = |\alpha| \delta_{K,j}$, and $K_s = |\alpha|^2$ is the average number of signal photons in each signal. For product states, the magnitude squared of the overlap is computed according to the tensor product rule. [41]

$$\begin{aligned} \langle \alpha_m | \alpha_k \rangle^2 &= \prod_{j=1}^M \langle \alpha_{m,j} | \alpha_{k,j} \rangle^2 \quad [4.31] \\ &= \langle \alpha_{m,1} | \alpha_{k,1} \rangle^2 \langle \alpha_{m,2} | \alpha_{k,2} \rangle^2 \dots \dots \dots \langle \alpha_{m,M} | \alpha_{k,M} \rangle^2 \end{aligned}$$

Using the expression for the magnitude squared of the overlap between two coherent states expressed in Chapter 3 Eq. [3.25]. The above quantity expressed as

$$\begin{aligned} \langle \alpha_m | \alpha_k \rangle^2 &= \exp\left(\sum_{j=1}^M 2\alpha_{mj}^* \alpha_{kj} - |\alpha_{mj}|^2 - |\alpha_{kj}|^2\right) \quad [4.32] \\ &= \begin{cases} 1 & m = k \\ e^{-2k} & m \neq k \end{cases} \end{aligned}$$

The M signals define an M -dimensional subspace. Since the M product states are linearly independent, the optimum strategy for minimizing the average probability of error is to project the received signal state onto M orthonormal measurement states spanning the same subspace, and to select the signal corresponding to the measurement state with the greatest projection. Mathematically, the average probability of symbol error for M-array PPM modulation format with equal priori probability can be written as

$$P(SE) = 1 - \frac{1}{M} \left[|\langle \psi_0 | \mu_0 \rangle|^2 + |\langle \psi_1 | \mu_1 \rangle|^2 + \dots + |\langle \psi_{M-1} | \mu_{M-1} \rangle|^2 \right] \quad [4.33]$$

4.2.3 Procedure For Optimization of Higher Order Detection Operators

Numerical optimization of the detection operators consists of finding the orientation of the orthogonal measurement states that yield the maximum probability of correct detection or, equivalently, the minimum probability of error. As shown in previous section, rotating the measurement states in a 2-dimensional Hilbert space, and calculating the probability of correct detection for each rotation until the maximum is found can find the solution to the general Binary -hypotheses problem. Actually such approach can be extended to M-hypothesis for the case of signal states that shows symmetries. Since PPM satisfies this condition

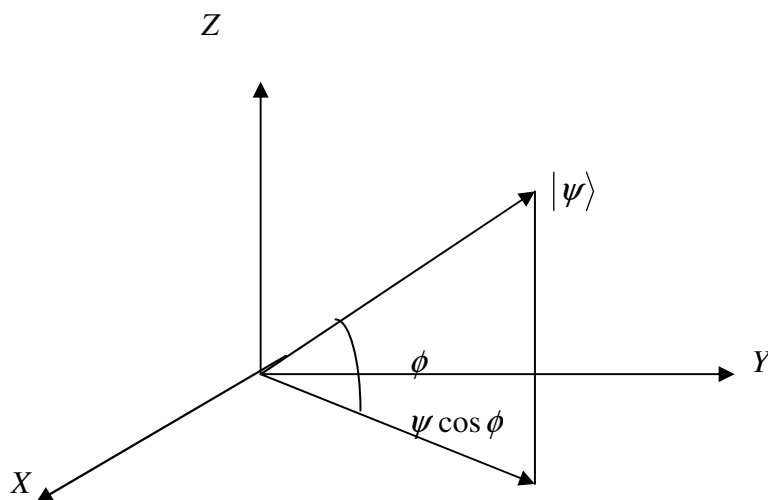


Fig-4-7 Projection of signal states in a lower measurement state

One can apply the above method. Indeed, the optimization problem of higher order can be solved iteratively starting with first two, randomly selected signal states. It is possible to rotate the projections of a vector in any lower dimension without affecting the projections of that vector onto the higher dimensions [7]. For example, this principle is illustrated in Fig.4.7, where the projection of an arbitrary state vector $|\psi\rangle$ in the X,Y plane is given by $|\psi\rangle \cos \phi$. The vector $|\psi\rangle$ can be rotated in the plane x, y such that the projection onto the z -axis is unchanged while the x -and y -projection components vary.

Generalizing this result to any arbitrary N -dimensional vector, the projections onto N coordinate axes can be varied by rotating each of the $(N-1)$ measurement coordinates without affecting the projection onto the next higher dimension. The application of these principles to measurement states is straightforward. Since measurement states are orthogonal and can be thought of as analogous to axes in an arbitrary Hilbert space. Making use of this dimensional independence, the measurement states are incrementally rotated and the error probability calculated until the angle yielding the minimum probability of error is found for each dimension. To further simplify the search, each dimension only requires a rotation in a single plane. The N^{th} dimensional axis and the $N-1$ dimensional bisectors easily define this plane. The optimum measurement state orientation for each dimension can be determined from the lower-dimensional solution, and this procedure is continued until the complete N -dimensional solution is obtained.

As a practical example here under presented the algorithm carried out for PPM-4 signals sets. The signal sets are defined as [41]

$$\begin{aligned}
 |\psi_0\rangle &= |\alpha\rangle|0\rangle \\
 |\psi_1\rangle &= |0\rangle|-\alpha\rangle \\
 |\psi_2\rangle &= |-\alpha\rangle|0\rangle \\
 |\psi_3\rangle &= |0\rangle|\alpha\rangle
 \end{aligned}
 \tag{4.34}$$

Initially, the measurement states are aligned with the Cartesian coordinate axes: $|\mu_0\rangle$ with the x-axis, $|\mu_1\rangle$ with the y-axis, $|\mu_2\rangle$ with the z-axis, and $|\mu_3\rangle$ with the w-axis as shown in Fig.4.8. For three dimensions.

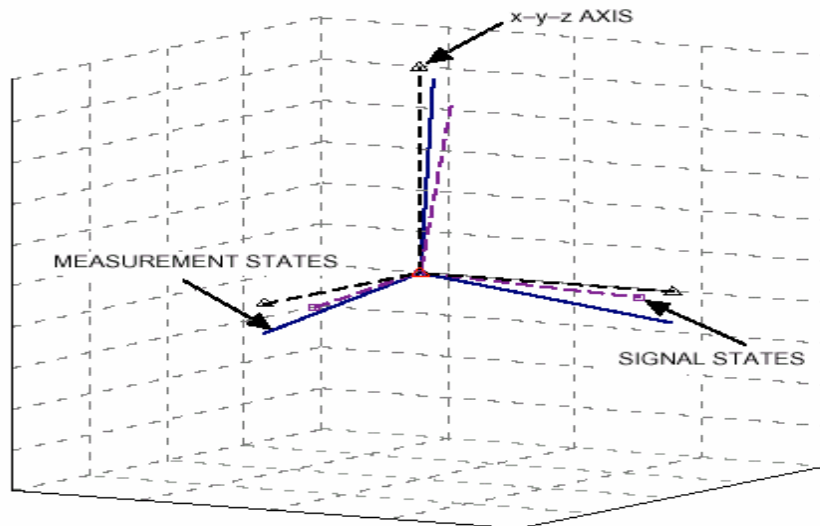


Fig.4.8. product space representation of PPM-3 in 3-dimensional number spaces

Step-1

Starting with the solution for $M = 2$, by choosing two signal randomly from the set which defines a plane containing two signal states and two measurement states. The rotation performed by the following sample Matlab programme written for the thesis.

```

-----// -----
ks=1;                                %average signal photons
a=acos(exp(-ks));                    %angle between the signal
sets                                  sets
b=pi/2-a;
c=0:0.0000175:b(1);                 %rotation angle in radian
c1=b(1)-c;
%-----M=2-Rotation-----
p1=1-0.5*(cos(c).^2+cos(c1).^2);    %Probability of error
p1opt=min(p1);                      %minimum error
                                     %...minimum error angular
                                     location.....
M_21=find(p1==p1opt);
M21=c(M_21);
M21opt=b(1)-M21;
%-----// -----

```

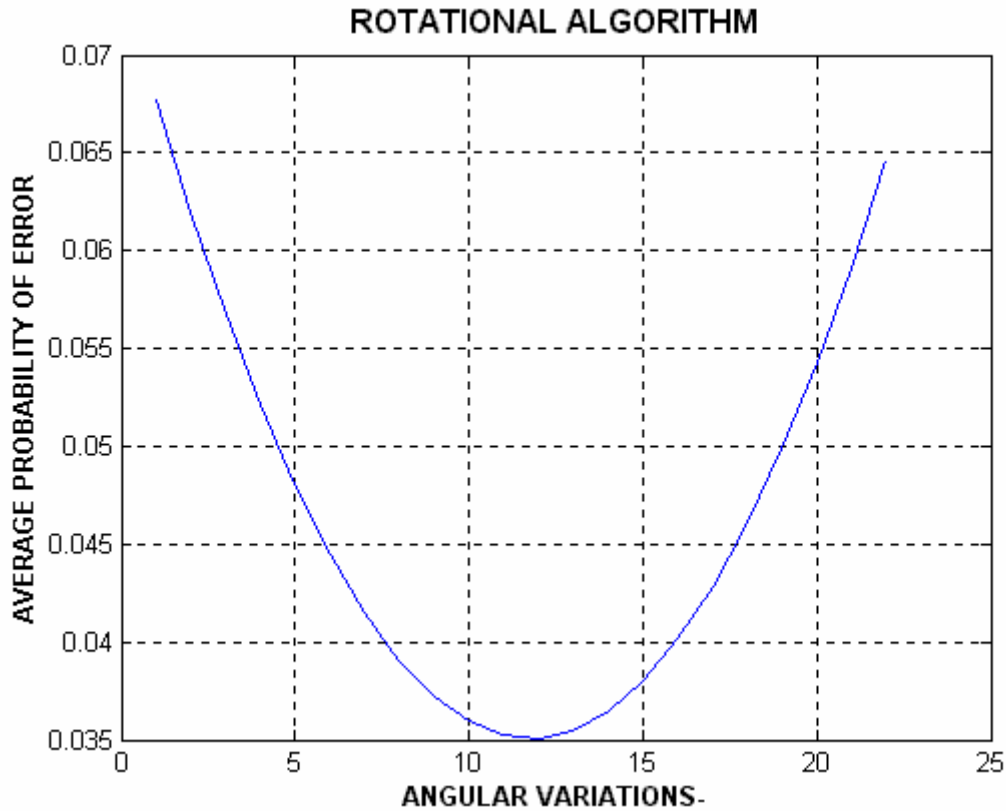


Fig 4.9. *The dependence of average probability of error on angular variations of measurement states for PPM-2*

Step-2

The three-dimensional optimal rotation will be in the plane defined by the z-axis and x-y bisector. As the states are rotated into the third dimension, the projections of $|\psi_0\rangle$ and $|\psi_1\rangle$ onto $|\mu_0\rangle$ and $|\mu_1\rangle$ must be kept equal to each other in order to keep their projections onto the fixed $|\mu_0\rangle$ and $|\mu_1\rangle$ measurement states maximum for any rotation. The reason for this is that the minimum probability of error is achieved when the average projection of all signal states onto their corresponding measurement states is maximum. Fig.4.8, illustrate that in order to keep the angles between $|\psi_0\rangle$; $|\psi_1\rangle$ equal, the rotation must be in the plane defined by the z-axis and x-y bisector. The rotation of the measurement states away from the z-axis towards the x-y bisector is accomplished with the use of the following unitary rotation matrix [27]

$$\begin{pmatrix} \cos(\frac{\pi}{4}) & -\sin(\frac{\pi}{4}) & 0 & 0 \\ \sin(\frac{\pi}{4}) & \cos(\frac{\pi}{4}) & 0 & 0 \\ 0 & 0 & 1 & 0 \\ 0 & 0 & 0 & 1 \end{pmatrix} x \begin{pmatrix} \cos \theta & 0 & \sin \theta & 0 \\ 0 & 1 & 0 & 0 \\ -\sin \theta & 0 & \cos \theta & 0 \\ 0 & 0 & 0 & 1 \end{pmatrix} x$$

$$\begin{bmatrix} \cos(\pi / 4) & -\sin(\pi / 4) & 0 & 0 \\ \sin(\pi / 4) & \cos(\pi / 4) & 0 & 0 \\ 0 & 0 & 1 & 0 \\ 0 & 0 & 0 & 1 \end{bmatrix} \quad [4.30]$$

Where θ is the rotation angle away from the z-axis towards the x-y bisector. As the measurements states are rotated, the probability of error is found for each incremental θ by computing the quantities p31 in the below programme: Thus, the measurement states are incrementally rotated and the error probability calculated until the angle that yields the minimum probability of error is determined-and that will be the optimum rotation angle for the dimension.

```
%.....PPM=3-Rotation.....

p31=(1-
(1/3)*[(cos(c).^2*(cos(M21)^2+cos(M21opt)^2)+cos(c1).^2]));

p31opt=min(p31); %Minimal Symbol error
% Minimum error angular location
M_31=find(p31==p31opt);
M31=c(M_31);
M31opt=b(1)-M31
-----//-----
```

Step-3

Next, the above three-dimensional solution is used to obtain the four-dimensional solution corresponding to four signal states. As before, the goal is to rotate the $|\mu_3\rangle$ measurement state away from the w-axis while keeping the projections of $|\psi_0\rangle, |\psi_1\rangle$ and $|\psi_2\rangle$ onto $|\mu_0\rangle, |\mu_1\rangle$, and

$|\mu_2\rangle$ maximal. The rotation that satisfies these conditions is the rotation within the plane defined by the w-axis and the x-y-z trisector. Defining Θ_1 as the angle between the x-y-z trisector and the x-y bisector, and Θ_{11} as the rotation angle away from the w-axis towards the x-y-z trisector, **c**(*angular variation symbol in the programme*) in the programme is incremented once again until the minimum probability of error **p41opt**(*Optimal error symbol in the programme*) is found. Using the four-dimensional extension of Eq [4.3]. The Matlab programme for evaluating fourth order is presented below.

```

-----//-----
p41=(1-
(1/4)*[cos(c).^2*[(cos(M31)^2*(cos(M21)^2+cos(M21opt)^2)+cos(M3
1opt)^2)]+cos(c1).^2]);
p41opt=min(p41);
M_41=find(p41==p41opt);
M41=c(M_41);
M41opt=b(1)-M41;
-----//-----
-----

```

This approach can be easily generalized to any higher dimensional signal sets by iteratively applying the above algorithm. *[For higher dimensional signal sets with different values of average signal photon look the mat lab programme N0.1D annexed to the thesis in the appendix-D]*

4.3. Summary of chapter

By looking what is presented in the above formulation one can summarize the result as follow;

Step. 1: Finding the Eigen value and Eigen vector of system even though not impossible is not a simple task. However for pure coherent state signal that has symmetries using the Eigen number state representation one can find the appropriate vector form.

Step.2: Using the vector representation by singular value decomposition one can find measurement vectors that minimize the error in a mean square sense. Since finding an Eigen value and an Eigen

vector of a state is equivalent to finding a unitary matrix that obey $U' = U^{-1}$. Thus in multiplying the state by U transform the signal set to a diagonal form. That can be used as the measurement vector.

Step.3: Therefore projection of the signal on the appropriate measurement vector will give the optimal value of correct detection

Performance Analysis of Optimal Quantum Receiver**5.1. Classical and Quantum Mechanical Derivation of a Photon-Counting Receiver (On/Off Keying)**

Binary On/Off optical modulation format as described in the Second chapter classically [one of the signals has zero amplitude, while the other signal has complex amplitude α] suppose there are two hypotheses, H_0 **and** H_1 , denoting absence and presence of signal, respectively. If the background radiation can be neglected, then either no photons or an average of $\lambda = |\alpha|^2$ photons are received. The received field is assumed to be from a coherent laser source; hence, the photons are Poisson distributed with conditional densities

$$P(n/H_0) = \begin{cases} 1 & n = 0 \\ 0 & n \geq 1 \end{cases} \quad [5-1]$$

$$P(n/H_1) = \frac{|\alpha|^{2n}}{n!} e^{-|\alpha|^2} \quad [5.2.]$$

At the end of each signaling interval, the receiver records the total number of detected photons and decides which hypothesis is true by computing the two likelihood functions, and selecting the hypothesis corresponding to the larger of the two. This decision rule [22] may be expressed as

If $\frac{P(n/H_0)}{P(n/H_1)} \geq 1$ then H_0 is selected. Otherwise $\frac{P(n/H_0)}{P(n/H_1)} < 1$ H_1 is selected

[5.3].

If no photon is counted, (in the absence of noise) H_0 is always decoded correctly, i.e. inserting the respective probability values in Eq [5.3] we get

$$P(C / H_0) = P(0 / H_0) = 1 \quad [5.4]$$

$$P(0/H_1) = e^{-\lambda} \quad [5.5]$$

In dividing the term result is always greater than one. If at least one photon is detected, (in the absence of noise), then H_1 is decoded correctly: i.e

$$P(C/H_0) = P(n \geq 1/H_0) = 0 \quad [5.5]$$

$$P(n \geq 1 / H_1) = 1 - e^{-|\alpha|^2} \quad [5.6]$$

Substituting this value in Eq [5-3] the result we get is always less than one. Therefore if one assumes equal a priori probabilities, for the two hypotheses $P(H_0) = P(H_1) = \frac{1}{2}$, then the probability of correct detection becomes

$$P(C) = \sum_{i=1}^{i=2} P(C/H_i)P(H_i) = 1 - \frac{1}{2}e^{-|\alpha|^2} \quad [5.7]$$

Similarly, putting the result found in Eq [5-6] the average probability of error for sub-optimal quantum receiver expressed as

$$P(E) = 1 - P(C) = \frac{1}{2}e^{-|\alpha|^2} \quad [5.8]$$

In the quantum mechanical formulation, the received field is in one of two states [12],

$$|\psi_1\rangle = |\alpha\rangle \quad \text{Or} \quad |\psi_0\rangle = |0\rangle \quad [5.9]$$

The signal field is assumed to be in a pure coherent state [no noise], which can be expressed in the number state representation as

$$|\psi_1\rangle = e^{-\frac{1}{2}|\alpha|^2} \sum_{n=0}^{\infty} \frac{\alpha^n}{\sqrt{n!}} |n\rangle \quad [5.10]$$

Where α is a complex number, the set $\{|n\rangle\}$ represents the number Eigen states, and $|\alpha|^2$ again represents the average number of photons in the signal. A measurement that determines whether or not the received state is the ground state corresponds to an application of the detection operator Π_0 . [27] Its action gives the optimal measurement states. Similarly the detection operator Π_1 determine the measurement state of the excited state. Mathematically the statement can be described as follows

$$\Pi_0|\psi_0\rangle = |0\rangle\langle 0|0\rangle = |\mu_0\rangle \quad [5.11]$$

$$\Pi_1|\psi_1\rangle = e^{-\frac{1}{2}|\alpha|^2} \sum_{n=1}^{\infty} \frac{\alpha^n}{\sqrt{n!}} |n\rangle \equiv |\mu_1\rangle \quad [5.12]$$

If the states are prepared with equal prior probability, to find the average probability of error by applying the result we get in Eq [4-19] first we calculate the average number of photon in the signal for this particular modulation format. $k = \frac{1}{2}|\alpha|^2$. Then we evaluate the squared magnitude of the overlap between the two states. (Since the error is caused by the quantum interference between the two states)

$$|\langle\psi_0|\psi_1\rangle|^2 = e^{-|\alpha|^2} = e^{-2k} \quad [5.13]$$

Finally by putting the result in Eq [4.19] we obtain the average probability of error for optimal quantum receiver for optical BPSK as expressed below.

$$P(E) = \frac{1}{2} \left[1 - \sqrt{1 - e^{-2k}} \right] \quad [5.14]$$

The performance of the two receivers in normal and semi log scale presented in Fig 5.1.and Fig.5.2.

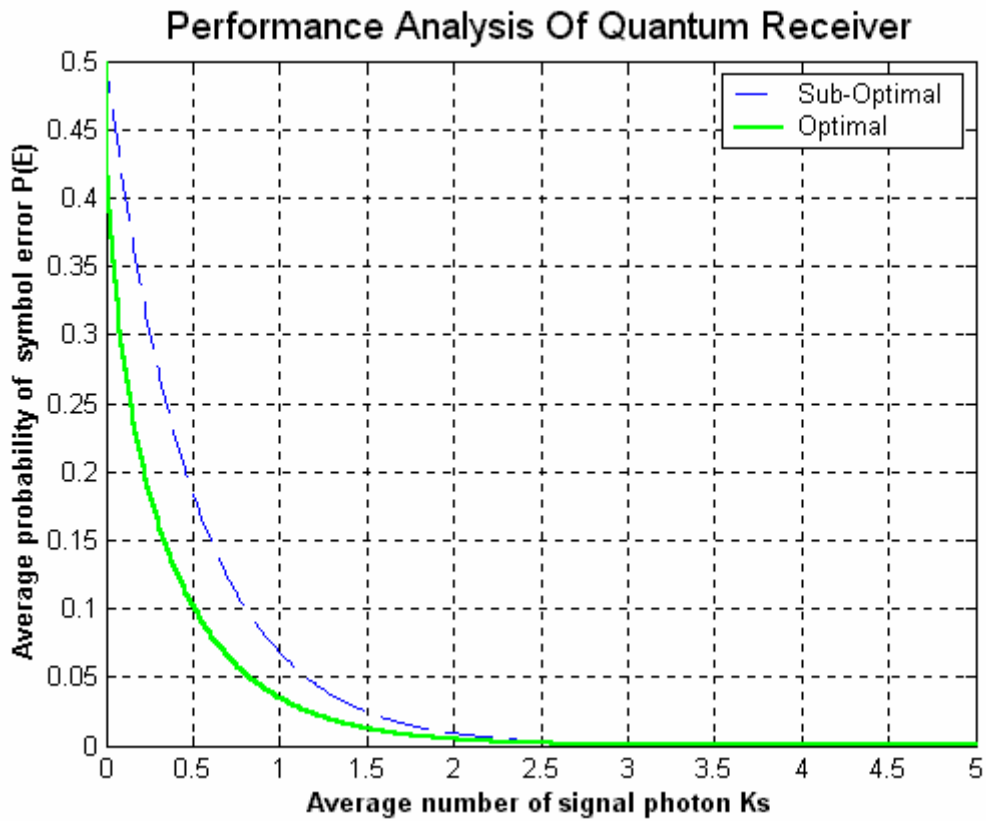


Fig.5.1. Performance graphs of optimal sub-optimal quantum receivers for BOOK

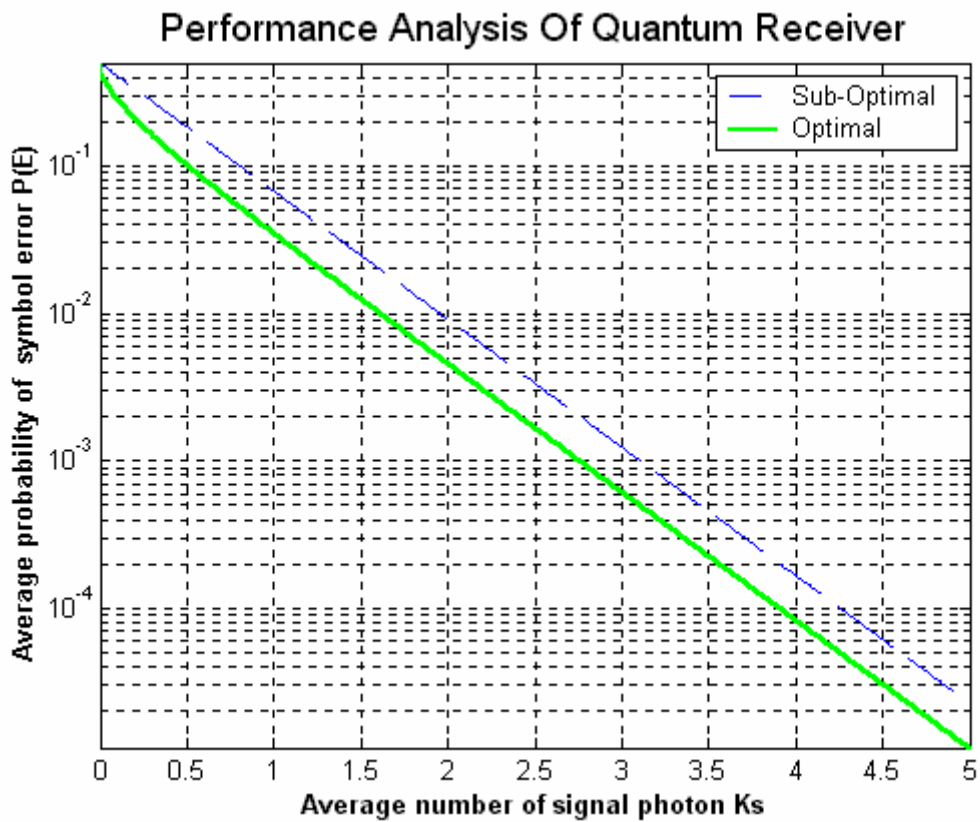


Fig.5.2. Semilog Performance graphs of optimal and sub-optimal quantum receivers for BOOK

5.1.1. Numerical performance comparison of Binary ON/OFF Keying

It is common to compare the performance of a receiver using probability of error as a measure of how precisely one can identify each signal states on average. Here and in the subsequent section the comparison of the receiver is made for the average probability of error 10^{-3} . Actually for deep space effective optical communication the theoretical average probability of error ought to lie in the range 0.001. And further to avoid the effect of atmospheric turbulence the receiver and the transmission position is assumed to lie at geostationary earth orbit satellites and Low orbit satellites (40000km).

Since average probability of error is taken as a measure of performance first the average the number of signal photon required must be calculated. Using Eq [4-6]and Eq[4-10] one can find the average signal photon for sub-optimal and optimal quantum receiver respectively as follows,

$$k_s = 0.5\log(2P(E)) \quad [5.15]$$

$$k_s = 0.5\log[1 - (1 - 2P(E))^2] \quad [5.16]$$

Performance Comparison Table for BOOK			
Average Signal Photon (Ks)	Average Probability of Error		
	Sub-Optimal Receiver	Optimal Quantum Receiver	Simulation Result
0.0	0.5000	0.5000	0.5000
0.5	0.1839	0.1025	0.1205
1.0	0.0677	0.0351	0.0305
1.5	0.0249	0.0126	0.0210
2.0	0.0092	0.0046	0.0075
2.5	0.0034	0.0017	0.0016
3.0	0.0012	0.0006	0.0002
3.5	0.0005	0.0002	0.0001
4.0	0.0002	0.0001	0.0000
4.5	0.0001	0.0000	0.0000
5.0	0.0000	0.0000	0.0000

Performance comparison Table 5-1

The comparison table above shows the average signal photon needed with respective error margins including the result found from the simulation. As can be seen from the table, when the average signal photon is one or less the performance difference is substantial. But for large value e.g. at $ks=5$, performance of both receiver converge to the value zero. This is also true for the simulation result. However the simulation output converges to zero faster than the theoretical result. One can see this result from the Fig.5.3 in which the performance of the two receivers with the simulation result presented. [For the detailed computer programme see in the appendix-D N0..D.1,D.2 annexed to the thesis]

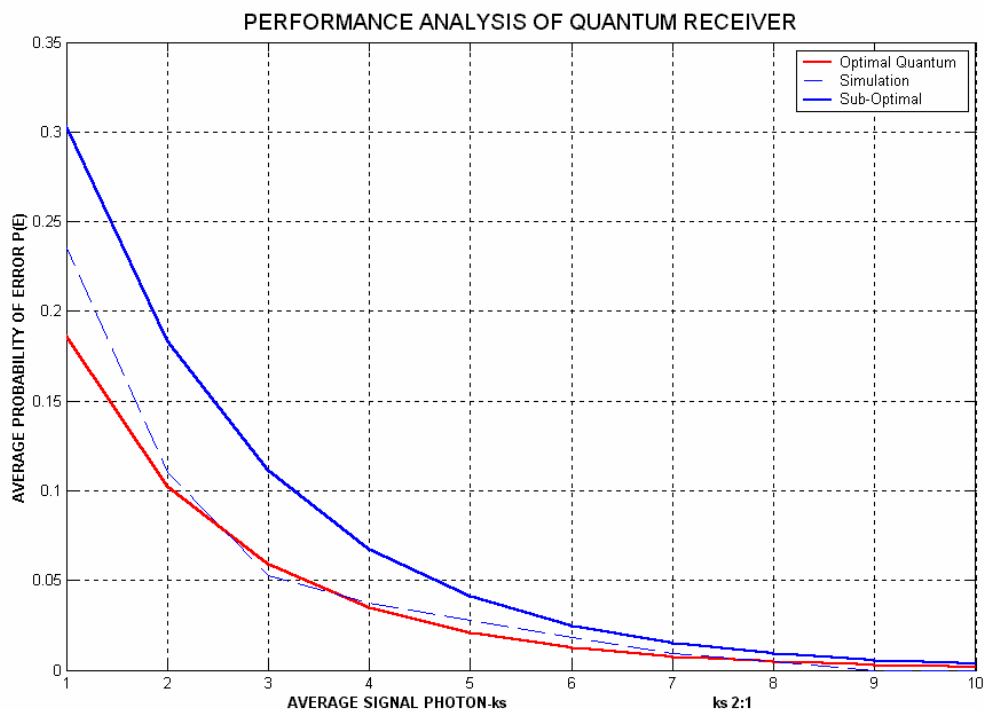


Fig.5.3. Performance graphs of Near-optimal and optimal quantum receivers for ON/OFF key modulation format with simulation result

Based on the result found in the above section it is also possible to evaluate the power gain in using optimal quantum receiver. The signal can be characterized in terms of the average power:

$$P_{av} = \frac{E_{av}}{T} = \frac{k_s h \nu}{T} \quad [5.17]$$

where k_{sw} is the average signal photon, h is Planck constant, ν optical frequency, and T is the signaling time. To achieve an error margin of $P(E) = 10^{-3}$, Sub-optimal photon counting receiver needs an average photon signal $k_s = \mathbf{3.1073}$. Similarly the required signal photon for the optimal quantum receiver is $k_s = \mathbf{2.7612}$. Thus substituting the values in Eq [5.18] one can easily compute the power ratio for the two receivers. and subsequently the gain.

$$Gain(db) = 10 \log_{10} \left(\frac{P_{OUT}}{P_{in}} \right) \quad [5.18]$$

$$Powergain(db) = 10 \log_{10} \left[\frac{3.1073}{2.7612} \right] = 0.5129db$$

5.2. Optical Binary Phase-Shift Keying (BPSK)

- **Coherent Detection and the Classical Limit.**

In this case, we have two coherent states with the same average photon energy $K_s = |\alpha|^2$ but π radians out of phase. As presented in chapter-2 classical coherent detection is performed by adding a local field of great amplitude, in phase, to the received field and detects the resulting sum field using classical energy detection, and then the performance of the classical coherent optical detector is obtained [22]. The error probability for this receiver is given by

$$P(E) = Q \left(\sqrt{\frac{2E_b}{N_0}} \right) \quad [5.19]$$

Where E_b and N_0 are the signal and noise energy respectively, and

$$Q = \frac{1}{\sqrt{2\pi}} \int_{-\infty}^{\infty} e^{-\frac{x^2}{2}} dx. \quad [5.20]$$

- **Near-Optimum Optical BPSK.**

Exponentially optimum (near-optimum) performance can be obtained by adding a local field of the same amplitude, in phase, to the received field followed by photon counting, [33]. With this technique, the field amplitude under one hypothesis is shifted to the ground state, but doubled under the other hypothesis. The error probability for this near-optimum detection scheme is

$$P(E) = \frac{1}{2} e^{-4K_s} \quad [5.21]$$

- **Optimal Quantum Receiver**

In the quantum mechanical formulation, the received field is in one of two states,

$$|\psi_0\rangle = |\alpha_0\rangle = |\alpha\rangle \quad [5.22]$$

Or.

$$|\psi_1\rangle = |\alpha_1\rangle = |-\alpha\rangle \quad [5.23].$$

The probability of correct detection is equivalent to the projection of squared magnitude of each state in their respective measurement states. [12]

$$P(C/H_0) = |\langle \psi_0 | \mu_0 \rangle|^2 = \cos^2(\phi_0) \quad [5.24.]$$

$$P(C/H_1) = |\langle \psi_1 | \mu_1 \rangle|^2 = \cos^2(\phi_1) \quad [5.25]$$

The squared magnitude of the overlap between this signal states can be computed using the coherent representation of $|\alpha\rangle$ [9]

$$|\langle \psi_0 | \psi_1 \rangle|^2 = |\langle \alpha_1 | \alpha_2 \rangle|^2 = e^{-2|\alpha|^2} = e^{-4K_s} \quad [5.26.]$$

Putting the expression found above in Eq [4.19] the average probability of error for optimal quantum receiver in the case of BPSK is given by

$$P(E) = \frac{1}{2} \left[1 - \sqrt{1 - |\langle \psi_0 | \psi_1 \rangle|^2} \right] = \frac{1}{2} \left[1 - \sqrt{1 - e^{-4K_s}} \right] \quad [5.27]$$

Fig.5.4. below shows the performance of Near-optimal and optimal quantum receiver for BPSK

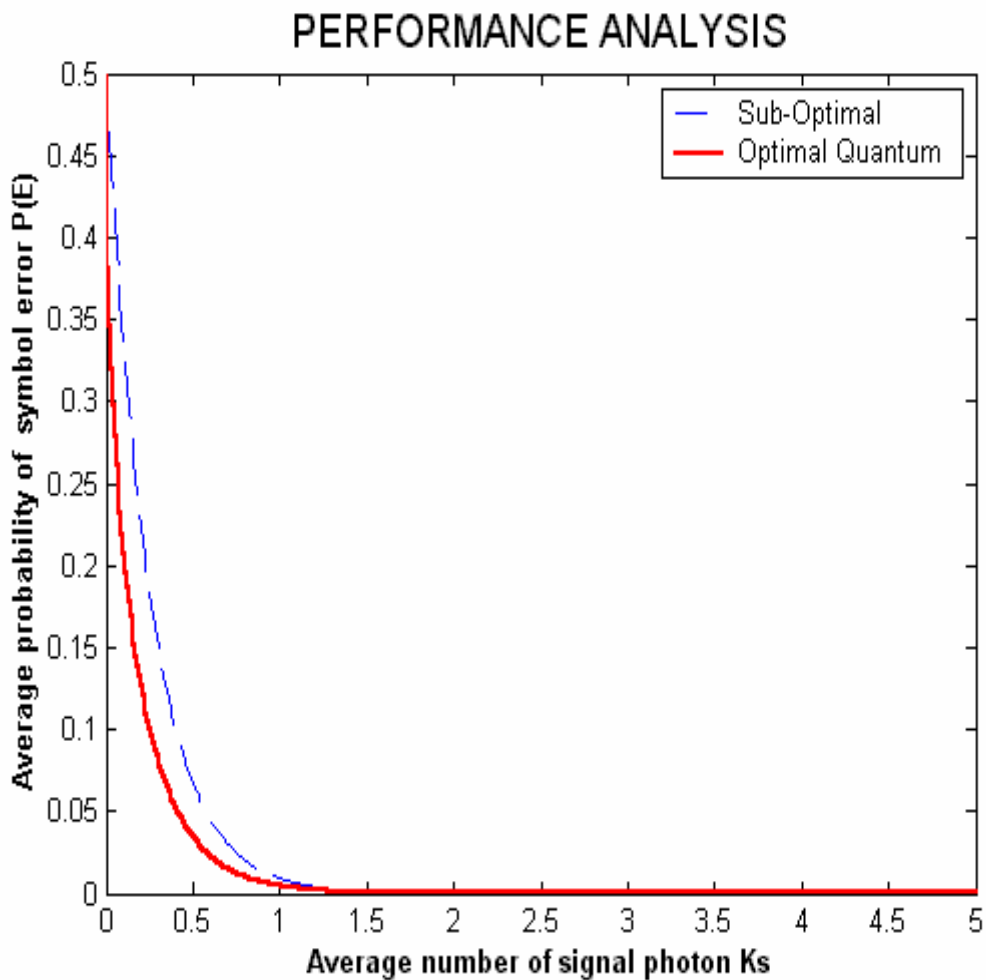


Fig.5.4. Performance comparison graphs of optimal and near optimal quantum receiver for BPS

5.2.1. Numerical performance comparison For Binary phase shift key (BPSK)

Using similar approach one can compute the required average signal photon to achieve an average probability of error to a certain limit. The comparison table below shows the performance of the three Receivers in relation to average signal photons.

Performance Comparison Table for BPSK			
Average Signal Photon(Ks)	Average Probability of Error		
	Classical Coherent Receiver	Sub-Optimal Receiver	Optimal Quantum Receiver
0.0	0.5000	0.5000	0.5000
0.5	0.1587	0.0677	0.0351
1.0	0.0786	0.0092	0.0046
1.5	0.0416	0.0012	0.0006
2.0	0.0228	0.0002	0.0001
2.5	0.0127	0.0000	0.0000
3.0	0.0072	0.0000	0.0000
3.5	0.0041	0.0000	0.0000
4.0	0.0023	0.0000	0.0000
4.5	0.0013	0.0000	0.0000

Performance comparison Table 5-2

To compute the power gain, once again has to express the required average signal photon in terms of average probability of error. In the case of sub-optimal and optimal quantum receiver no extra step is needed-as shown below.

$$k_s = 0.25 \log_{10}(2P(E)) \quad [5.28]$$

$$k_s = 0.25 \log[1 - (1 - 2P(E))^2] \quad [5.29]$$

However for classical coherent receiver the average signal photon required is determined by the required signal to noise ratio [22]. Mathematically, the signal to noise ratio can be expressed as

$$SNR = \frac{P_s}{P_N} = \frac{\frac{E_s}{T}}{\frac{E_N}{T}} = \frac{E_s}{E_N} = \frac{n_s h\nu}{n_N h\nu} = \frac{n_s}{n_N} \quad [5.30]$$

Where P_s and P_N are the signal and the noise power respectively. E_s , E_N denote the signal and noise energy accordingly. n_s , n_n represent the signal and noise photon number. h is the Planck constant, ν optical frequency, and T is the signaling time. Hence if we denote the ratio $k_s = \frac{n_s}{n_N}$ (where k_{sw} represent the average signal photon required to achieve a certain error margin.), then get an expression that relate directly the probability of error, average signal photon and power.

The semi log graph below presents the performance of the three receivers in relation to probability of error [For the complete programme look in the appendix-No.1.2.B.and N0.1.7.B]

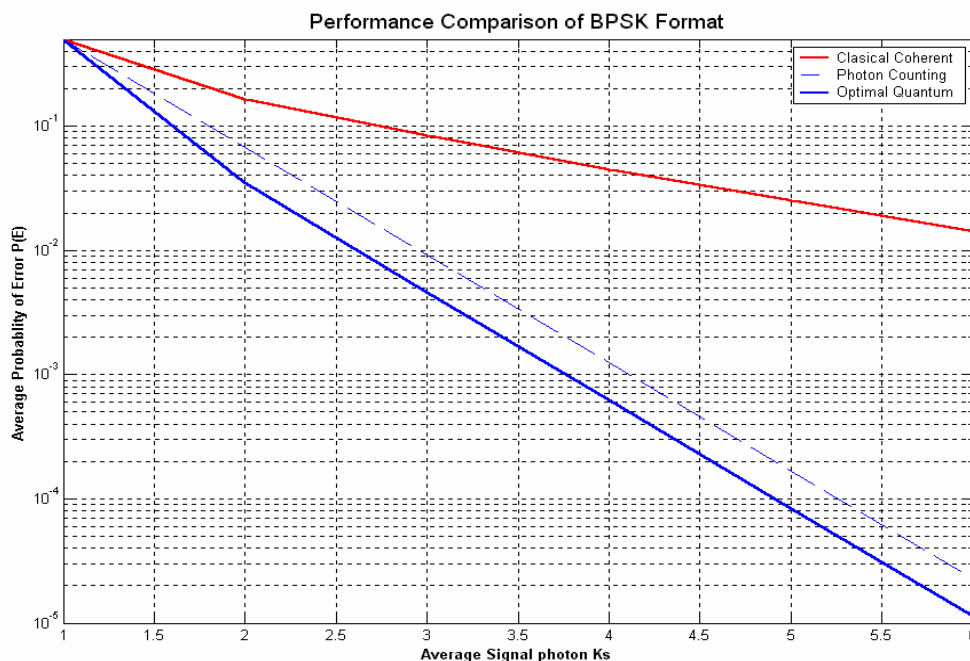


Fig.5.5. Performance graphs of classical t, Near-optimal and optimal quantum cohere receivers for BPSK

Thus to achieve an average probability of error $P(E) = 10^{-3}$ the classical coherent receiver needs $K_s = 3.000$. However the required average photon signals for optimal quantum receiver reduced by half-.i.e. $K_s = 1.500$.

$$\text{Power gain (db)} = 10 \cdot \log_{10} (3.0/1.5) = 3.0103 \text{db}$$

5.3. M-array Optical Pulse Position Modulation (PPM)

Using Poisson density distribution, semi-classical receiver counts the total number of photons in each slot and makes a decision by selecting the PPM word corresponding to the slot with the greatest photon count. The PPM word is decoded correctly if the photon count in the time slot containing the signal exceeds all others by at least one. However, correct detection also could occur if, all, slots contained the same number of photon i.e. Zero. Thus an equiprobable random selection was made among the slots. Pure Guessing among the M slots would lead to a correct decision $1/M$ times on the average. Considering all possible ways that equalities can occur, and accounting for the probabilities of correct resolution in each case, the probability of correct decision for signal without noise can be expressed as

$$P(n \geq 1/H_0) = 1 - [1 - \frac{1}{M}] e^{-K_s} = 1 - \frac{M-1}{M} e^{-K_s} = \frac{1}{M} e^{-K_s} \quad [5.31.]$$

$$P(n \geq 1/H_{M-1}) = 1 - [1 - \frac{1}{M}] e^{-K_s} = 1 - \frac{M-1}{M} e^{-K_s} = \frac{1}{M} e^{-K_s} \quad [5.32].$$

And the average probability of symbol error for photon counting receiver can be expressed as below

$$P(E) = 1 - P(C) = \frac{M-1}{M} e^{-K_s} \quad [5-33]$$

In the case of Optimal Quantum receiver as [10] theoretical result for the average probability of symbol error

$$p(SE) = \frac{M-1}{M^2} \left[\sqrt{1+(M-1)e^{-K}} - \sqrt{1-e^{-K}} \right]^2 \quad [5.34]$$

Based on the result found above the performance of the two receivers with the output of the developed programme presented in Fig. 5.6, Fig. 5.7 and Fig. 5.8. Note that the choice of order of modulation format is purely convenience [For details of the programme look in the appendix-D No.E.1 annexed to the thesis]

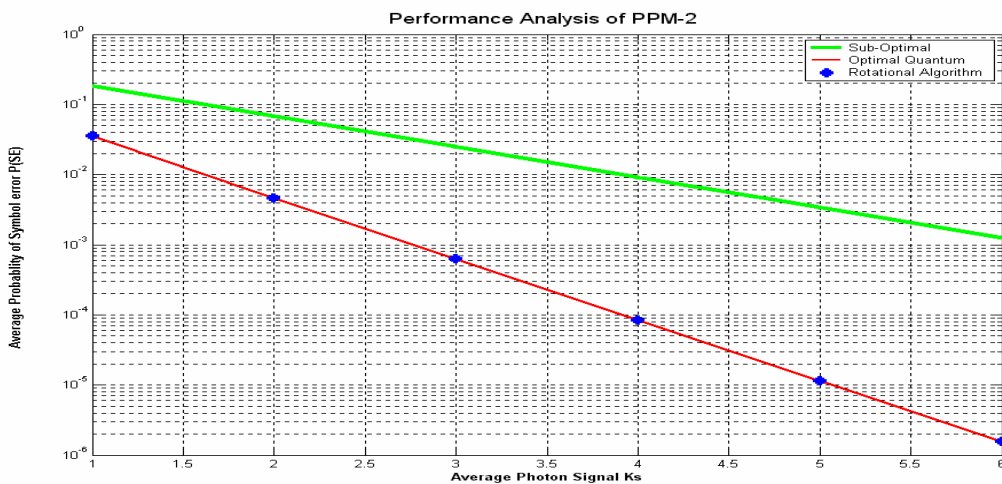


Fig.5.6 Semilog.Performance graphs Sub-optimal, optimal quantum receiver

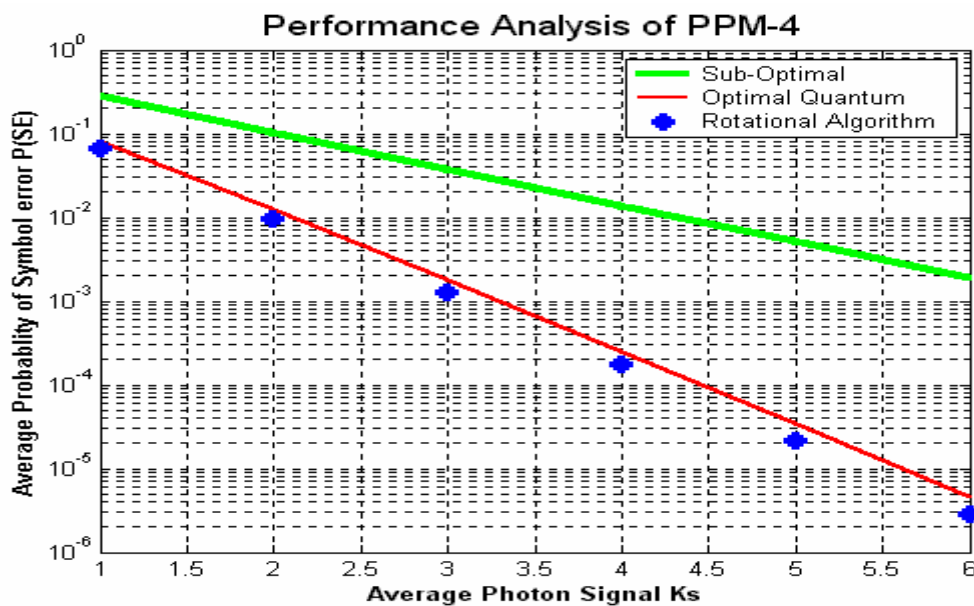


Fig .5.7 Performance graphs of Sub-optimal and Optimal quantum receiver

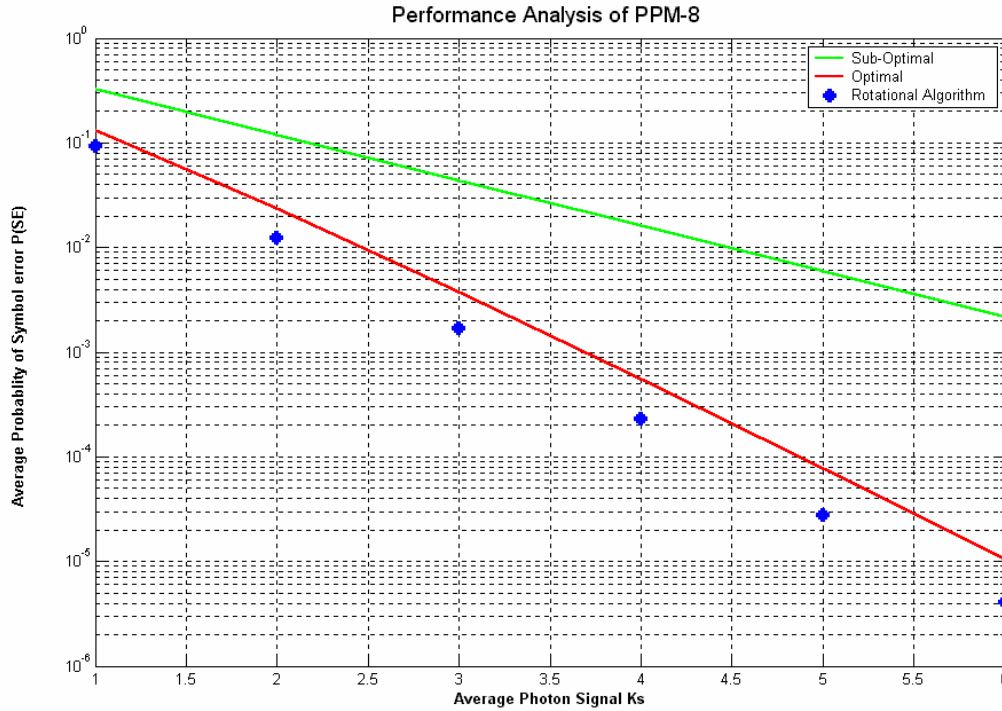


Fig.5.8. Performance graphs of Sub- optimal and Optimal quantum receiver

5.3.1 Numerical Performance evaluation of Pulse position Modulation

Using the result found in the previous section, it is possible to compare the two receivers numerically. Since average probability of error is taken as a measure of performance first the average signal photon required must be calculated. Using Eq [4-6] and [4-10] one can find the average signal photon for sub-optimal and optimal quantum number respectively, using iterative method. The result presented as follows. As can be seen from the table, at lower order formatting the result of the rotational algorithm and the theoretical values coincides. But at higher order a little variation start to appear.

5.3.1.1. Pulse position Modulation (PPM-2)

For $P(E) = 10^{-3}$ we get the average photon signal in photon counting receiver $ks=6.17$ and in optimal quantum receiver needs only $ks=2.76$. Hence the gain

$$Gain(db) = 10 \log_{10}\left(\frac{P_{OUT}}{P_{in}}\right) = 3.4938db$$

Average Signal Photon (ks)	Order of Modulation	Average Probability of symbol Error		
		Sub-optimal Classical	Optimal Quantum theoretical	Rotational Algorithm
1	2	0.1839	0.0351	0.0351
2	2	0.0677	0.0046	0.0046
3	2	0.0249	0.0006	0.0006
4	2	0.0092	0.0001	0.0001
5	2	0.0034	0.0000	0.0000
6	2	0.0012	0.0000	0.0000
PPM-4				
1	4	0.2759	0.0805	0.0662
2	4	0.1015	0.0123	0.0094
3	4	0.0373	0.0018	0.0013
4	4	0.0137	0.0002	0.0002
5	4	0.0051	0.0000	0.0000
6	4	0.0019	0.0000	0.0000
PPM-8				
1	8	0.3219	0.1313	0.0926
2	8	0.1184	0.0237	0.0124
3	8	0.0436	0.0038	0.0017
4	8	0.0160	0.0006	0.0002
5	8	0.0059	0.0001	0.0000
6	8	0.0022	0.0000	0.0000

Performance comparison Table 5.3

5.3.1.2. Pulse position Modulation (PPM-4)

For $P(E) = 10^{-3}$ we get the average photon signal in photon counting Receiver $ks=6.57$ and in optimal quantum receiver $ks=3.29$.

$$Gain(db) = 10 \log_{10}\left(\frac{P_{OUT}}{P_{in}}\right) = 3.0103db$$

5.3.1.3. Pulse position Modulation (PPM-8)

For $P(E) = 10^{-3}$ we get the average photon signal in photon counting receiver $K_s=6.75$ and in optimal quantum receiver $K_s=3.69$

$$Gain(db) = 10 \log_{10}\left(\frac{P_{OUT}}{P_{in}}\right) = 2.6228db$$

5.4. Summary of the chapter

Although the procedure for optimizing the measurement states and detection operation in both modulation formats (i.e. OOK & BPSK) is the same, the modulation formats are completely different. As we have observed in the thesis ON OFF KEY (OOK) represent an intensity modulation; it can be detected using direct techniques such as photon counting; however BINARY PHASE SHIFTING KEY (BPSK) is a phase modulation format and therefore needs coherent detection techniques. It is also evident that BPSK modulation actually requires twice as many photon per symbol, on the average as does OOK modulation. When compared on the basis of average transmitted power, both modulation formats exhibit similar performance as shown above. Note that photon counting exhibits the same exponential behavior as optimum quantum detection (both semi log curves have the same slope), implying that photon counting is nearly optimal for the detection of OOK signals. However, quantum detection of optical BPSK signals is exponentially 3 dB better than classical coherent detection, practically achieving a 2.6-dB reduction in the required signal energy at an error probability of 10^{-5} .

Unlike OOK, where the average symbol energy is half of the average pulse energy, PPM symbol contains a pulse; with average signal and pulse energy is both equal to K_s . Note that, for high-dimensional signaling and modest error probabilities in the order of $P(SE) \gg 10^{-3}$, As can be seen from the comparison table optimal quantum receiver performs approximately 2.6 dB better than the conventional photon counting receiver.

Realization of Optimal Quantum Receiver

In this section presented the realization method of a quantum receiver of which the detection operators are described by a positive value measure. (PVM). Generally, the expression of detection operators $\{\hat{\pi}_j\}$ of quantum receiver is abstract and the physical correspondence of the operator is not obvious. On the other hand detection operator, which corresponds to measurement of signal observable, are called standard detection operator. [operator value based on single outcome (Yes/No)] Its physical correspondence is obvious. Needless to say, physical correspondence of the other well-known observable (operator response with three outcomes at most regardless of the signal component) $\{\hat{E}\}$ is also obvious [28]. However in the generalized measurement one does not insist that the outcomes of measurements should be real numbers; they can be labeled by any set. [13] Secondly, and more importantly, one does not insist that the response of a single outcome (a yes/no measurement) is given by a projection. [14] Therefore to realize such optimal quantum receiver one has to develop a relation which connect the well-known operator \hat{E}_j with the optimal detection operator $\hat{\pi}_j$. i.e.

$$\hat{\pi}_j = \hat{U}^* \hat{E}_j \hat{U} \quad [6.1]$$

In this chapter the realization of the optimal quantum receiver for M – array linearly independent signal, which are not based on two state systems like PPM, is considered. The realization procedure is divided into two steps. The first step is to decompose each detection operator $\{\hat{\pi}_j\}$, which describe the quantum receiver in to a unitary operator \hat{U} and a

detection operator \hat{E}_j corresponding to a well known operator measurement. The second step is to derive a mathematical objects needed to describe devices which take some quantum system as an input and transforming it in some way, possibly producing some classical readout information in the process. Considering that input or output may be composite quantum systems, as well as classical ones, this is about the most general component of a quantum experiment one can think of. With a reasonable description of some basic operations of this kind, one obtains a theoretical construction kit for a large variety of experiment.

6.1. Decomposition of Detection Operator

In general the dimensions "d" of the Hilbert space of the physical system are not always equal to M . Indeed the dimensions of optical system are infinite. [11] In contrary to this the dimension of the well-known detection operators are defined on finite d-dimensional space and projection of them on the signal space are not generally a positive Operator Value Measure (POVM). [27] Therefore it is impossible to derive the unitary operator that expresses the received quantum state controller on M-dimensional space. However by introducing an extended space so that detection operator of well-known measurement becomes orthogonal on the extended space. For this end, first we apply the identity operator on a d -dimensional space. Then using the detection operator of the well-known measurement we project each signal states $\{|\psi_i\rangle / i=0,1,2,\dots,M-1\}$ in to M states as follows

$$|\psi_j\rangle = \sum_{j=0}^{M-1} \hat{E}_j |\psi_j\rangle = \sum_{j=0}^{M-1} \sqrt{\epsilon_{ij}} |A_{ij}\rangle \quad [6.2]$$

Where $|A_{ij}\rangle = \frac{1}{\sqrt{\epsilon_{ij}}} \hat{E}_j |\psi_i\rangle$ are the components of the vector in Hilbert Space.

Here ϵ_{ij} express the probability that the received signal is decided to be ρ_j by \hat{E}_j when the transmitted signal is ρ_i [20].

$$\epsilon_{ij} = \langle \psi_i | E_j | \psi_i \rangle \quad [6.3].$$

and satisfies

$$\sum_{j=0}^{M-1} \mathcal{E}_{ij} = 1 \quad [6.4]$$

In this way M signal vectors can be described by M^2 vectors. $\{|A_{ij}\rangle, |ij = 0,1,2,\dots,M-1\}$. By applying Schmidt Orthonormalization to N linearly independent vectors of M^2 . $\{|A_{ij}\rangle, |ij = 0,1,2,\dots,M-1\}$. One can introduced N -dimensional extended space spanned by this orthonormal set. Clearly the set, $\{|A_{j0}\rangle, \dots, |A_{j(M-1)}\rangle\}$, is orthogonal for any i . On the other hand the set $\{|A_{0j}\rangle, \dots, |A_{(M-1)j}\rangle\}$ is not orthogonal and sometimes they can be linearly dependent.[28] However if n_j vectors of $\{|A_{0j}\rangle, \dots, |A_{(M-1)j}\rangle\}$ are linearly independent, then we orthonormalize these vectors and derive an orthonormal set denoted by $\{|r_{j+l}\rangle, l = 0,1,2,\dots,n_{j-1}\}$ ($j' = \sum_{m=0}^{j-1} n_m$). This operation for all j , $N = (\sum_{j=0}^{M-1} n_j)$ derives orthogonal vectors $\{|r_k\rangle, k = 0,1,\dots,N-1\}$. Where $M \leq N \leq M^2$. These N vectors construct an orthonormal set in N -dimensional space.[19] Besides the well-known observable. E_j related ,to this Orthonormal set as follows

$$\hat{E}_j = \sum_{k=j'}^{j+n_j-1} |r_k\rangle\langle r_k| \quad [6.5]$$

$$j' = \sum_{m=0}^{j-1} n_m$$

Since the detection operator Π_j of the quantum receiver for M-array signals are PVM it can be represented as

$$\pi_j = |\mu_j\rangle\langle\mu_j| \quad [6.6]$$

Where $\{|\mu_j\rangle, j=0,1,2,\dots,M-1\}$ are called measurement basis vector. By extending these bases vector to basis vector in $N-1$ dimensional extended spaces. One can make an orthonormal set $\{|\mu'_k\rangle, k = 0,1,2,\dots,N-1\}$ in N -dimensional

extended space [24]. [The $N-M$ basis vectors are obtained from Schmidt orthonormalization process]

$$|\mu_j\rangle = |\mu_k\rangle \quad \text{If } j = k \quad [6.7]$$

In this way, both $\{\pi_j\}$ and $\{\hat{E}_j\}$ become a *PVM* in N -dimensional space. This confirms that realization of detection operators will be in principle possible by combining a quantum circuit which plays a role of unitary operator \hat{U} and the detection operator $\{\hat{E}_j\}$. As can be seen from the Fig.6.1. Shown below the operation of Optimal quantum receiver can be thought as the transformation of the signal observable from one form to other so as to maximize the process of distinguishing one quantum state from others. The transmitter produces quantum state using either photon number states or polarization states basis and sends it through quantum channel- for photons the quantum communication channel can be either free space or optical fibers—special fibers or the ones used in standard telecommunications.

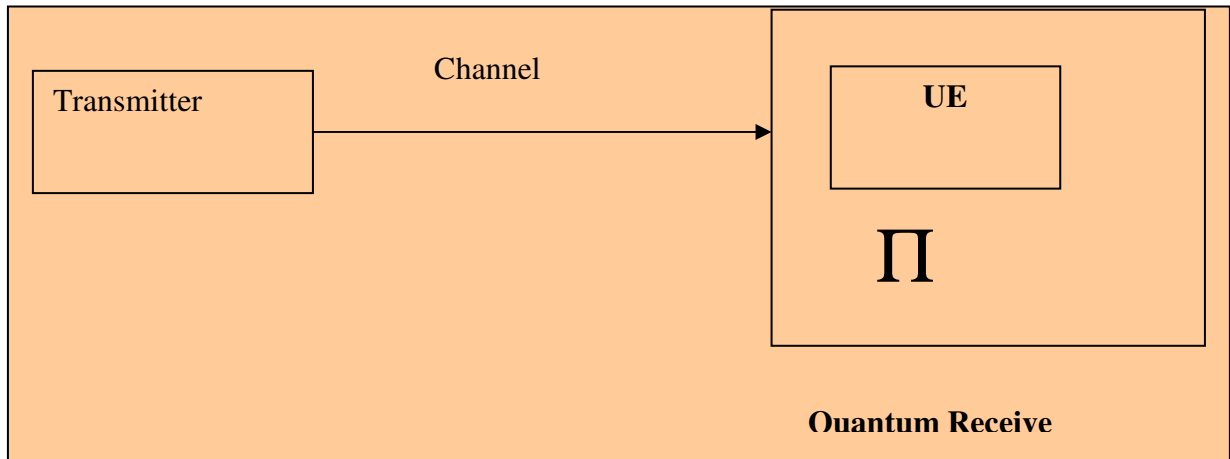


Fig.6-1- Block diagram optimal quantum receiver

The communication channel is thus not really quantum. What is quantum are the information carriers. The code is written on the individual photon not in the ensemble. At the receiver side through unitary transformation (the transformation that keeps the (metric) distance from the origin constant) new signal sets and measurement are developed to minimize the

average probability of error. [27] Here in our case the transformation of measurement states defined as follows.

$$| \mu'_k \rangle = \hat{U} | r_k \rangle \quad [6.8]$$

6.2. Decomposition of Unitary Operator

In order to construct the quantum receiver one needs to derive the Hamiltonian, an energy operator that correspond to \hat{U} and clarify the structure quantum circuit, which corresponds to the unitary operator defined in Eq [6.8] is the operator on N -dimensional space. Therefore it is also difficult to derive the Hamiltonian that corresponds to \hat{U} and to construct a quantum circuit. However if one can decompose a unitary operator on N -dimensional space in to one or two-dimensional operation it will be possible to construct the quantum circuit. According to stones spectral decomposition theorem [27] \hat{U} on N - dimensional space can be decomposed as

$$U = \sum_{i=0}^{N-1} e^{j\theta_i} | \phi_i \rangle \langle \phi_i | \quad [6.9]$$

Where $e^{j\theta}$ and $| \phi_j \rangle$ are an Eigen values and Eigen vector of \hat{U} , respectively and $\{ | \phi_j \rangle \}$ is an orthonormal set in N -dimensional space. Then \hat{U} is expressed as

$$U = \prod_{i=0}^{N-1} R_i(\theta) \quad [6.10].$$

$$R_i(\theta_i) = \exp(i\theta) | \phi_i \rangle \langle \phi_i | \quad [6.11]$$

In this way \hat{U} can be decomposed into $N-1$ dimensional rotations. Thus it will be possible in principle to construct quantum circuit if we are able to find the Hamiltonian (Energy operator) for 1-dimensional rotation. [29]The Hamiltonian for optical signal in coherent state space representation is given by

$$H_{R_t} = -\hbar g \rho_j \quad [6.12]$$

$$\rho = |\phi_j\rangle\langle\phi_j| \quad [6.13].$$

$$\rho = \sum_{m=0}^{\infty} \frac{C_{jm}}{\sqrt{m!}} \hat{a}^{*m} \sum_{i=0}^{\infty} \frac{(-\hat{a}^*)^i (a)^i}{\sqrt{i!}} \sum_{n=0}^{\infty} \frac{C_{jn} \hat{a}^n}{\sqrt{n!}} \quad [6.14]$$

Where, a, a^+ are the annihilations and creation Operators

$$C_{jn} = \langle n | \phi_j \rangle$$

$$\sum_m \sum_n C_{jm} C_{j'n} = \begin{cases} 0 & j \neq j' \\ 1 & j = j' \end{cases}$$

and $g = \frac{\theta_t}{\tau}$ the coupling constant of a physical process is represented by a Hamiltonian $H_{R_t} \cdot \tau$ is the interaction time, and $|n\rangle$ is a photon number state with photon number n . The Hamiltonian in Eq.[6.12] corresponds to nonlinear multiphoton process.

Based on the above procedure let us see the realization for 3 - arrays phase shift keyed (**3-PSK**) signal state which cannot be represented by product of coherent state signals as PPM.[30] Since this quantum state is optical signal its dimension is infinite. Therefore the dimensions of the quantum system are much higher than the signal space ($M \ll d$)

The signal states of 3 - PSK in quantum formulation are expressed as

$$|\psi_0\rangle = |\alpha\rangle$$

$$|\psi_2\rangle = \left| \alpha e^{-j\frac{2\pi}{3}} \right\rangle \quad [6.15]$$

$$|\psi_1\rangle = \left| \alpha e^{j\frac{2\pi}{3}} \right\rangle$$

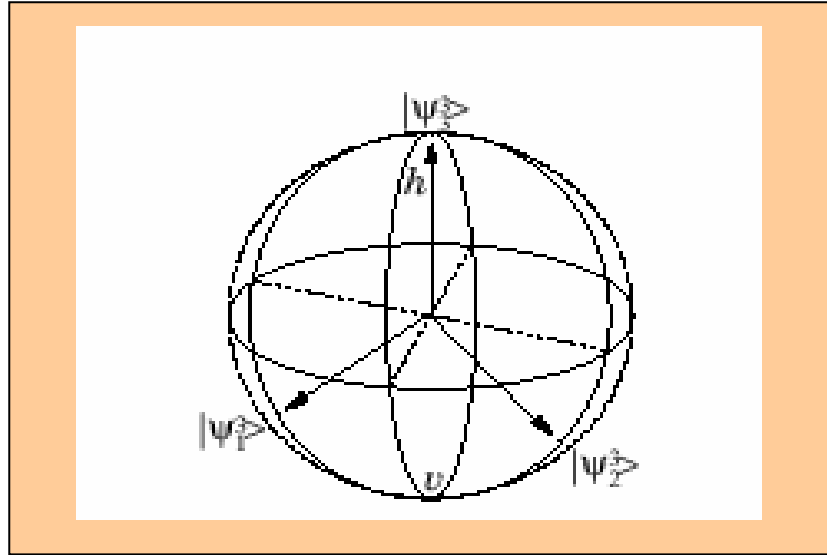


FIG.6.2 The PSK-3 states shown as polarization directions on the Poincaré sphere

One can assume that α is real since no generality is lost by the assumption. [30] Hence an orthonormal set $\{|e_j\rangle\}$ on 3-dimensional Hilbert space spanned by these signal states can be described as follows

$$\begin{aligned}
 |e_0\rangle &= \frac{1}{\sqrt{3u_0}} \left(|\psi_0\rangle + e^{-j\frac{2\pi}{3}} |\psi_1\rangle + e^{j\frac{2\pi}{3}} |\psi_2\rangle \right) \\
 |e_1\rangle &= \frac{1}{\sqrt{3u_1}} \left(|\psi_0\rangle + e^{\frac{j2\pi}{3}} |\psi_1\rangle + e^{-\frac{j2\pi}{3}} |\psi_2\rangle \right) \\
 |e_2\rangle &= \frac{1}{\sqrt{3u_2}} (|\psi_0\rangle + |\psi_1\rangle + |\psi_2\rangle)
 \end{aligned} \tag{6.16}$$

Where u_i are the Eigen values found from Gram-matrix [24]

$$\begin{aligned}
 u_0 &= 1 - k_i + \sqrt{3}k_j \\
 u_1 &= 1 - k_i - \sqrt{3}k_j \\
 u_2 &= 1 + 2k_i \\
 k_i &= e^{\frac{-3}{2}|\alpha|^2} \cos \frac{\sqrt{3}}{2} |\alpha|^2 \\
 k_j &= e^{\frac{-3}{2}|\alpha|^2} \sin \frac{\sqrt{3}}{2} |\alpha|^2
 \end{aligned} \tag{6.17}$$

For signal set that has equal priori probability, a measurement process, which is called the Square Root Measurement (SRM), gives the optimum

detection operator corresponds to the measurement basis vectors $\{|\mu_i\rangle\}$ [24] expressed as follow

$$|\mu_m\rangle = \frac{1}{\sqrt{M}} \sum_{j=0}^K e^{-i\frac{2\pi m}{M}j} |J\rangle \quad [2.18]$$

Where $|J\rangle$ is the orthonormal basis found from Schmidt orthogonalization, M is the signal set size and m specify each signal. Thus applying the above formula, the three measurement state that satisfy the SRM as follows,

$$\begin{aligned} |\mu_0\rangle &= \frac{1}{\sqrt{3}}(|e_0\rangle + |e_1\rangle + |e_2\rangle) \\ |\mu_1\rangle &= \frac{1}{\sqrt{3}}\left(e^{\frac{2\pi i}{3}}|e_0\rangle + e^{-\frac{2\pi i}{3}}|e_1\rangle + |e_2\rangle\right) \\ |\mu_2\rangle &= \frac{1}{\sqrt{3}}\left(e^{-\frac{2\pi i}{3}}|e_0\rangle + e^{\frac{2\pi i}{3}}|e_1\rangle + |e_2\rangle\right) \end{aligned} \quad [6.19]$$

Since square root measurement doesn't give the optimal performance limit allowed by quantum mechanics for this particular modulation format one must continue the transformation. [5] Hence each of the signal states is projected into three states.

$$|\varphi_i\rangle = \sum_{j=0}^2 \hat{E}_j |\psi_{ij}\rangle = \sum_{j=0}^2 \sqrt{\mathcal{E}_{ij}} |A_{ij}\rangle, i, j = 0, 1, \quad [6.20]$$

A detection of well known observable is a photon counting [12] (Energy Measurement) and can be described as

$$\begin{aligned} \hat{E}_0 &= |0\rangle\langle 0| \\ E_1 &= |1\rangle\langle 1| \\ \hat{E}_2 &= I - |0\rangle\langle 0| - |1\rangle\langle 1| \end{aligned} \quad [6.21]$$

Where $|0\rangle$ and $|1\rangle$ are vacuum states and photon number states with photon number 1 respectively.

The sub space spanned by $H_0 \{ |A_{i0}\rangle \}$, the sub space spanned by $H_1 \{ |A_{i1}\rangle \}$, the sub space spanned by $H_2 \{ |A_{i2}\rangle \}$ are orthogonal to each other.

But $\{A_{0j}\}$, $\{A_{1j}\}$ and $\{A_{2j}\}$ are not. Both $\{A_{i0}\}$ and $\{A_{i1}\}$ are linearly dependent sets. [29], since they can be represented by linear combination of the other vectors;

$$\{A_{00}\} = \{A_{10}\} = \{A_{20}\} = |0\rangle$$

$$\{A_{01}\} = e^{-j\frac{2\pi}{3}} |A_{11}\rangle = e^{j\frac{2\pi}{3}} |A_{21}\rangle = |1\rangle \quad [6.22]$$

So determining $|r_0\rangle$ and $|r_1\rangle$ as

$$|r_0\rangle = \{A_{00}\} = |0\rangle$$

$$|r_1\rangle = |A_{01}\rangle = |1\rangle \quad [6.23]$$

On the other hand $\{A_{i2}\}$ are linearly independent sets. So by applying Schmidt orthonormalization to $\{A_{i2}\}$ one can determine the remaining $|r_2\rangle$, $|r_3\rangle$ and $|r_4\rangle$.

$$|r_2\rangle = |A_{02}\rangle$$

$$|r_3\rangle = \frac{|A_{12}\rangle - \langle r_2 | A_{12} | r_2 \rangle}{\sqrt{1 - |\langle r_2 | A_{12} \rangle|^2}} \quad [6.24].$$

$$|r_4\rangle = \frac{|A_{22}\rangle - \langle r_2 | A_{22} | r_2 \rangle - \langle r_3 | A_{22} | r_3 \rangle}{\sqrt{1 - |\langle r_2 | A_{22} \rangle|^2 - |\langle r_3 | A_{22} \rangle|^2}}$$

Where,

$$|A_{m2}\rangle = \frac{\left| \alpha e^{\frac{2\pi j}{3}} \right\rangle - e^{\frac{|\alpha|^2}{2}} |0\rangle - \alpha e^{\frac{2\pi j}{3} - \frac{|\alpha|^2}{2}} |1\rangle}{\sqrt{1 - e^{|\alpha|^2} - |\alpha|^2 e^{-|\alpha|^2}}} \quad [6.25]$$

The pair overlaps between the components of $|A_{j2}\rangle$ can be computed using tensor rule as follows [27]

$$\langle A_{02} | A_{12} \rangle = \langle A_{12} | A_{22} \rangle = \langle A_{02} | A_{22} \rangle^*$$

$$= \frac{e^{\frac{-3+\sqrt{3}j}{2}|\alpha|^2} - e^{\frac{|\alpha|^2}{2}(1+\frac{\sqrt{3}j}{2})|\alpha|^2}}{1 - e^{-|\alpha|^2}(1+|\alpha|^2)} \quad [6.26]$$

From the above calculation one can obtain an orthonormal set $\{r_k\}$ ($k = 0, 1, 2, 3, 4$) in a five dimensional Hilbert space. The well known energy operator $\{E_j\}$ is now expressed by these transformed orthonormal sets as follows

$$\begin{aligned} \{E_0\} &= |r_0\rangle\langle r_0| \\ \{E_1\} &= |r_1\rangle\langle r_1| \\ \{E_2\} &= \sum_{k=2}^4 |r_k\rangle\langle r_k| \end{aligned} \quad [6.27]$$

Similarly the measurement vectors [27] of the optimal detection Operators in the extended spaces are expressed as follows

$$|\mu_j\rangle = \sum_{k=0}^4 C_{jk} |r_k\rangle \quad [6.26]$$

Where $C_{jk} = \langle r_k | \mu_j \rangle$, which using the above formulas can be easily solved.

Thus by adding the two-basis vector $|\mu_3'\rangle$ and $|\mu_4'\rangle$ to the original basis vector one can construct an orthonormal sets $\{\mu_k'\}$. [24]

Here $\{\hat{\pi}_j^{opt}\}$ is expressed as follows.

$$\begin{aligned} \hat{\pi}_0^{opt} &= |\mu_0'\rangle\langle \mu_0'| \\ \hat{\pi}_1^{opt} &= |\mu_1'\rangle\langle \mu_1'| \\ \hat{\pi}_2^{opt} &= \sum_{j=2}^4 |\mu_k'\rangle\langle \mu_k'| \end{aligned} \quad [6.28]$$

Where the expression for $|\mu_3'\rangle$ and $|\mu_4'\rangle$ can be found as follows

$$\left| \mu_k' \right\rangle = \frac{\mathbf{r}_{k-3} - \sum_{m=0}^{k-1} \langle \mu_m | \mathbf{r}_{k-3} \rangle | \mu_m \rangle}{\sqrt{1 - \sum_{m=0}^{k-1} \langle | \mu_m | \mathbf{r}_{k-3} | \rangle^2}} \quad [6.29]$$

Where $k = 3, 4$

These two-basis vectors don't affect the measurement result since they are orthogonal to signal states. But give a new dimension to account the pair overlap between the three states. Therefore by defining the unitary operator \hat{U} which relates $\hat{\Pi}_j^{opt}$ and \hat{E}_j^{opt} as

$$\hat{\Pi}_j^{opt} = \hat{U} \hat{E}_j^{opt} \hat{U}^\dagger \quad [6.30]$$

Here is \hat{U} expressed as $\hat{U} = [C_{jk}] \quad j, k = 0, 1, 2, 3, 4$,

$$\text{Where } C_{jk} = \langle r_k | \mu_j' \rangle \quad [6.31]$$

One can form the required transformation. As mentioned in the beginning now \hat{U} should be decomposed in to some 1 dimensional rotation to derive the Hamiltonian.

Using stones theorem

$$\hat{U} = \sum_{j=0}^4 e^{i\theta_j} | \phi_j \rangle \langle \phi_j | \quad [6.32]$$

Then \hat{U} can be decomposed into five 1 dimensional rotation as follows

$$\hat{U} = \prod_{j=0}^4 R(\theta_j) \quad [6.33]$$

$$R(\theta_j) = e^{i\theta} | \phi_j \rangle \langle \phi_j | \quad [6.34]$$

In order to derive the five rotational angles $\{\theta_j\}$ first the Eigen value of \hat{U} must be found. Then the five angles will be computed numerically. Finally, by using these five angles and the corresponding five Eigen vectors one can evaluate the performance of the Optimal Quantum receiver. Once \hat{U} **and** ϕ_t is expressed, the rotational matrix and the Hamiltonian can be expressed by the annihilation and creation operators. There fore the physical correspondence of the optimal quantum receiver in 3-PSK (which are not based on two system) signal is realizable. This method can be applied to any higher order since detection operator is expressed as PVM.

Here under, by using the simplified theoretical result [12] presented the performance comparison graphs for near optimum and optimal quantum receiver for 3-PSK.

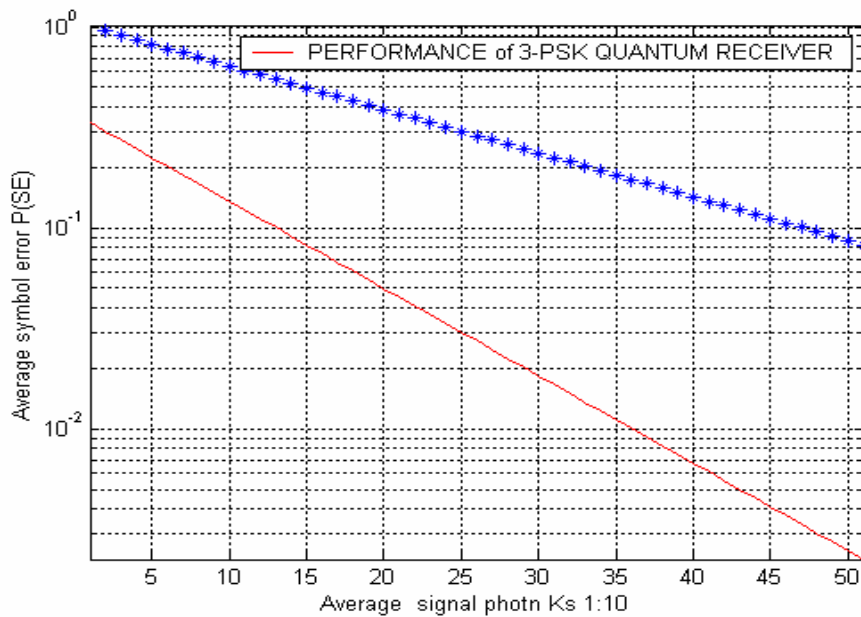


Fig. 6.2. *Semilog Performance Analysis graph for Near-optimal and optimal quantum receiver for 3-array PSK*

From the figure above one can see the performance improvement in optimal quantum receiver. [For detail see the programme annexed to the thesis in appendix-F. NO.1.F].

6.3. Summary of the chapter

Although a substantial progress has been achieved in the quantum state estimation, it is still a difficult and open problem how to find explicit and physically realizable solutions for optimal strategies in an algorithmic way, especially in the case of higher dimensional systems and larger numbers of samples. Moreover, discussions given so far in the literatures for ensuring the optimality of discrete and finite POMs were focused only on the condition for externality and not on the full conditions for the existence of a global maximum. In general, seeking all extreme and picking up the point corresponding to the global maximum is not necessarily a trivial task for complex systems.

Conclusion & Recommendations

When a communication system operates in quanta, the physical carrier conveying a letter X_i should explicitly be described by a quantum state $|\psi_i\rangle$, which usually referred as the letter state. Thus, if the letters 0, 1 are conveyed by weak pulses of laser light, the corresponding quantum states $|\psi_0\rangle, |\psi_1\rangle$ are usually non orthogonal coherent states. Such non-orthogonal states can never be distinguished perfectly, even in principle. Therefore even if a channel and a detector are completely noiseless, quantum mechanics imposes an inevitable source of error or ambiguity in signal detection. These factors are fundamental to quanta as distinct from classical information theory and make quantum key distribution possible.

In this thesis, taking average probability of error as a measure of performance, comparison was made on optical receiver using both Classical and Quantum Detection Techniques. The comparison was carried out in two parts,

(1) In the first part by taking Binary On /Off keying (OOK) and Phase Shift keying optical modulation format for noise free cases, performance comparison and simulation were carried out by changing both average signal photon AND ERROR MARGINS.

(2) Following the same procedure as in (1) an algorithm development for Pulse position Modulation (PPM) were carried out.

Results & Discussion

- ❖ Photon counting receiver exhibits the same exponential behavior as optimum quantum receiver. The power gain was only 0.5129db. (Both

performance curves have the same slope), implying that photon counting is nearly optimal for the detection of BOOK signals.

- ❖ However, quantum detection of optical BPSK signals is exponentially 3 dB better than classical coherent detection, practically achieving a 2.6 dB reduction in the required signal energy at an error probability of 10^{-5} . Besides classical coherent detection performs both photon counting and real time phase processing to reach decision.
- ❖ For large value of signal photon the performance of photon counting receiver and optimal quantum receiver tend to converge.
- ❖ In the case of PPM, at a lower dimensional signaling, optimal quantum receiver performs approximately 3 dB better than the conventional photon-counting receiver.
- ❖ For high-dimensional signaling and modest error probabilities in the order of $P (SE) \gg 10^{-3}$, optimal quantum receiver performs approximately 2.6 dB better than the conventional photon-counting receiver.

Injecting the effect of quantum interference and developing a successful simulation program that evaluate the performance of optimal quantum receiver is one of the main achievements of this thesis. The small variation between the theoretical values and the simulation result for BOOK might come from unseen constraints and also due to the approximations taken in expressing the vectors for injecting the quantum effect in the simulation. Moreover the simulation is carried out only ten times for limited 10000 data. Increasing the simulation data range, larger than what is taken in the thesis, could lessen the variation.

In the case of higher order modulation format, its inherent complexity hinders the development of simulation programmes that truly reflect the effect of quantum interference. However, a rotational algorithm, which was used to evaluate the performance of the optimal quantum receiver for PPM was developed. It agrees with the empirical results developed by experiment. The small variations between the empirical values and the rotational algorithm for

higher order can be accounted mostly to the round of error injected to the algorithm in calculating the optimal orientation. And increasing the division of angular variation to much lower value can minimize this effect.

Conclusion

From the results of this thesis, it can be concluded that the detection process of communication systems operating at optical frequencies will be determined by the rules of quantum mechanics. The analysis pointed out that looking optically transmitted signal through the eyes of quantum mechanics could increase the performance of the receiver.

There is one other remark connected with Quantum information worth making. Even though its principles rooted with strong and rich mathematical foundation, its physical realization is still a tabletop experiment. It is not done in present information-processing systems, as the technology for addressing and manipulating single atoms, even in a fixed basis, is too primitive for designing and constructing practical devices. But this should not discourage scholars as Albert Einstein put it, "... the creative principle resides in mathematics. In a certain sense, therefore, I hold it true that pure thought can grasp reality, as the ancients dreamed..." Therefore, with the drive toward miniaturization in classical computation and communication devices continues, and the cost of small devices continues to drop, classical computation will reach this quantum limit in the foreseeable future. In this event, engineers and computer scientists will have waiting for them as one of the best-developed parts of quantum information theory: the theory of - the use of quantum devices for storage, transmission and reception of classical information in a more reliable and effective way.

In this thesis work, quantum receiver performance analysis was carried out for a noise free channel, which is not the case in most of communication systems. Thus, the results obtained from the thesis can be used as the basis for future research works, which consider the performance of quantum communication under additive noise and other channel effects like scattering and dispersion. Quantum Coding and Error correction algorithm, Quantum Channel Capacity and Quantum Cryptology are also possible areas of future research.

References

- [1] A. Arvizu, F. J. Mendieta, R. Chavez, *Balanced Coherent Photo receiver for Coherent Optical Communication*, Harvard University, 1999
- [2] A. Peres, *Quantum Theory: Concepts and Methods*, Kluwer Academic Publishers, Dordrecht, 1993.
- [3] A. Peres and W. Wootters, "*Phys. Review Letter*, 66", 1992.
- [4] A. S. Holevo, *Problems of Information Transmission*, USSR, 1973.
- [5] A. S. Holevo, *Multivariate Analysis*, 1973.
- [6] A. Chees ,and S. M. Barnett, *Modern Optics*, 1998.
- [7] A.S.Kompanyets,*A course of Theoretical Physics*, Vol. 2, Mir Publishers, Moscow, 1978.
- [8] A. Papoulis, *Probability, Random Variables, and Stochastic Processes*, McGraw-Hill Series, 1989.
- [9] B.Huttner, A.Muller,J.D.Gautier,H. Zbinden, and N. Gisin, "*Phys. Review Letter*, A", 1996.
- [10] C. F. Fuchs, "*Phys. Review Letter*, 79(6), 1162", 1997
- [11] C. W. Helstrom, J. W. S. Liu, and J. P. Gordon, "*Quantum Mechanical Communications Theory Proceedings of the IEEE*", Vol. 58, No. 10, pp. 1578-1598, October 1970.
- [12] C.W.Helstrom, "*Quantum Detection and Estimation Theory, Mathematics in Science and Engineering*", Vol.123,NewYork, Academic Press, 1976.
- [13] David A.Johnson, *Optical Through-the-Air Communications Handbook - PE* 1988.
- [14] Dungan.Frank.R, *Electronics Systems, USA*, 1998.
- [15] E. B. Davies, *IEEE Transactions on Information Theory*, Aug. 1978 pp. 24, 596.
- [16] E.Hecht, *Optics*, Addison-Wesley, Mass, 1987.

- [17] Frank, P.Tedeschi and Margaret, R. Taber, *Solid State. Electronics*, Delmar Publisher Inc., 1976.
- [18] G. Jaeger and A.Shimony, "*Phys. Review Letter, A 197, 83*",1995.
- [19] H. P. Yuen, R. S. Kennedy, and M. Lax, "*Optimum Testing of Multiple Hypotheses in Quantum Detection Theory*", IEEE Transactions on Information Theory, Vol. IT-21, No. 2, pp. 125-134, March 1975.
- [20] Howard N.Barnum, *Quantum Information Theory*, Harvard University, 1983.
- [21] I.D.Ivanovic, "*Phys. Review Letter A123, 257*", 1987.
- [22] J. Proakis, *Digital Communication*, McGraw-Hill International Editions, 1990.
- [23] J. W. S. Liu, "*Reliability of Quantum-Mechanical Communications Systems*", Massachusetts Institute of Technology, Research Laboratory of Electronics, Technical Report 468, Cambridge, Massachusetts, December 31, 1968.
- [24] Michael A. Armen, "*Phys. Review Letter, A 13, 89*", 2002.
- [25] M. Born and E. Wolf, *Principles of Optics*, Pergamon Press, Oxford, 1987.
- [26] M. Edelve, *Optical Instrumentation*, USSR, 1988.
- [27] Michio Kaku, *Quantum Field Theory*, Oxford University Press Inc., 1993.
- [28] M. Osaki, M. Ban, and O. Hirota, "*Proceedings of the 4th Conference on Quantum Communication, Measurement, and Computation*", Evanston, Illinois, USA, 1998, (Plenum Press, New York, 2000)
- [29] M. Sasaki and O. Hirota, "*Phys. Review Letter, A 54(4), 2728*", 1996.
- [30] M. Sasaki, S. M. Barnett, R. Jozsa, M. Osaki, and O. Hirota, "*Phys. Review Letter, A 59(5), 3325*", 1999.
- [31] M.Ban,K. Kurokawa, R. Momose, and O. Hirota, "*Phys. Review Letter, 36(6), 1269*", Information Theory,1997.
- [32] N. Abramson, *Information Theory and Coding*, McGraw Hill, New York, 1963.

- [33] P. Hausladen and W. K. Wootters, J. *Modern Optics*, 1994.
- [34] P. Horowitz and W. Hill, *The Art of Electronics*, Cambridge University Press, Cambridge UK, 1989.
- [35] R. B. M. Clarke, A. Ches, S. M. Barnett, and E. Riis, "*Phys. Review Letter, A*", February 2001.
- [36] R. J. Glauber, "*Coherent and Incoherent States of the Radiation Field*", *The Physical Review*, Vol. 131, No. 6, pp. 2766-2788, 1963.
- [37] S.G.Lipson H.Lipson and D.S. Tannhauser, *Optical Physics*, 3rd Ed, Cambridge University Press, 1998.
- [38] S. J. D. Phoenix and P. D. Townsend, *Contemporary Physics*, 1995.
- [39] S. M. Barnett and E. Riis, J., *Modern Optics*, 1997.
- [40] T. Cover and J. Thomas, *Elements of Information Theory*, John Wiley and Sons, New York, 1991.
- [41] V. Vilnrotter and C. W. Lau, "*Quantum Detection Theory for the Free-Space Channel*", *The Inter-Planetary Network Progress Report*, pp. 42-146, Jet Propulsion Laboratory, Pasadena, California, June 2001.

Appendix-A

This Matlab Programme computes the intensity variation of coherent light wave both in amplitude and phase in relation to coherence time

```
sample_len=1000;
cen_freq=10^15;
Coh_T=10^-10;
freq_Har=5%Frequency Harmonics;
gg=100;
ph0=zeros(1, sample_len);
ph1=zeros(1, sample_len);
I=zeros(1, sample_len);
rr=zeros(gg, sample_len);
zz=zeros(gg, sample_len);
xx=zeros(gg, sample_len);
temp=zeros(1, freq_Har);
wp=zeros(1, freq_Har);
wq=zeros(1, freq_Har);
% alpha=zeros(1,3);
for p=1:1:gg;
k=rand(1, freq_Har);
k=k;%/sqrt(mean(k.*k));
c=(1/2)*ones(1, freq_Har);
d=(k-c)*2*pi;
w=randn(1, freq_Har);
w=w/sqrt(mean(w.*w));
ww1=sqrt(0.08*cen_freq)*w;
ww=ww1+cen_freq*ones(1, freq_Har);
del=Coh_T/999;

for n=1:1:sample_len;
for m=1:freq_Har;
temp(m)=(exp(i*(2*pi*ww(m)*(n-1)*del+d(m))));
wp(m)=exp(i*(2*pi*(ww(m)-(cen_freq))*((n-1)*del)+d(m)));
wq(m)=exp(i*d(m));
end;
%INTENSITY VARIATION
I(n)=(abs(sum(temp(1:end))))^2;
ph0(n)=phase(sum(wp(1:end)));
    ph1(n)=phase(sum(wq(1:end)));
end;
rr(p, :)=I;
zz(p, :)=ph0;
xx(p, :)=ph1;
% alpha(p)=abs(sum(wq(1:end)));
end;
```

```

% Mean Intensity Time average
for p=1:gg;
    CC(p)=mean(rr(p,:));
end;
% plot(rr(1,:), 'g')
% hold on
% plot(rr(2,:), 'r')
% hold on
% plot(rr(3,:), 'b')
%.....Impure Sine waves constructed by adding 5-quasi-monochromatic waves.....
for aa=1:sample_len;
    fg2(aa)=cos((2*pi*(10^15*del*(aa-1))+zz(1)));
end
fg2=sqrt(rr(1,:)).*fg2;
plot(fg2, 'r')
hold on
for aa=1:sample_len;
    fg1(aa)=cos((2*pi*(10^15*del*(aa-1))+zz(2)));
end
fg1=sqrt(rr(2,:)).*fg1;
    plot(fg1, 'g')
for aa=1:sample_len;
    fg3(aa)=cos((2*pi*(10^15*del*(aa-1))+zz(3)));
end
fg3=sqrt(rr(3,:)).*fg3;
plot(fg3, 'k')
for aa=1:sample_len;
    fg2(aa)=cos((2*pi*(10^15*del*(aa-1))+xx(1)));
end
fg2=sqrt(rr(1,:)).*fg2;
plot(fg2, 'r')
hold on
    for aa=1:sample_len;
    fg1(aa)=cos((2*pi*(10^15*del*(aa-1))+xx(2)));
end
    fg1=sqrt(rr(2,:)).*fg1;
plot(fg1, 'g')
    for aa=1:sample_len;
    fg3(aa)=cos((2*pi*(10^15*del*(aa-1))+xx(3)));
end
    fg3=sqrt(rr(3,:)).*fg3;
plot(fg3, '

```

Appendix-B

In this part of the appendix Presented seven Matlab programs that used to Compute the average probability of error for Binary On/Off and Binary Phase Shift Keying optical modulation Format in relation to Optimal quantum and photon counting receiver.

Input: k, average number of signal photon

P_C=Average probability of error for OOK in photon
Counting
P_Q=Average probability of error for OOK in optimal
Quantum receiver
P_C1=Average probability of error for BPSK photon
Counting
P_Q2=Average probability of error for BPSK in optimal
Quantum receiver

No.1.1.B

```
k=0:0.01:5;
plot(k,0.5*(exp(-2*k)), '--');
hold on
plot(k,0.5*(1-sqrt(1-exp(-2*k))), 'g')
legend('P_C','P_Q')
xlabel('Average number of signal photon Ks')
ylabel('Average probability of symbol error P(E)')
axis ([0 5 0 0.5])
```

No.1.2.B

```
k=0:0.01:5;
plot(k,0.5*(exp(-4*k)), '--');
hold on
plot(k,0.5*(1-sqrt(1-exp(-4*k))), 'g')
legend('P_C1','P_Q1')
xlabel('Average number of signal photon Ks')
ylabel('Average probability of symbol error P(E)')
axis ([0 5 0 0.5])
```

No.1.3.B

```
k=0:0.01:5;
P_C=0.5*(exp(-2*k));
P_Q=0.5*(1-sqrt(1-exp(-2*k)));
P_C1=0.5*(exp(-4*k));
P_Q1=0.5*(1-sqrt(1-exp(-4*k)));
plot(P_C, 'r')
hold on
plot(P_Q, 'g')
hold on
plot(P_C1, 'b')
hold on
plot(P_Q1, 'y')
title('Top Right Plot')
title('Performance Analysis')
legend('Bottom Right Plot')
legend('P_C','P_Q','P_C1','P-Q1')
xlabel('Average number of signal photn Ks')
ylabel('Average probablity of symbol error P(E)')
axis ([0 5 0 0.5])
```

No 1.4.B

```

k=0:0.1:5;
semilogy(0.5*(exp(-2*k)), '--');
hold on
semilogy(0.5*(1-sqrt(1-exp(-2*k))), 'r');
Legend(' P_C', 'P_Q')
xlabel('Average number of signal photons Ks')
ylabel(' Average probability of error P(E)')
title('Top Right Plot')
title('Performance Analysis Quantum Receiver')
axis ([0 5 0 0.5])

```

NO.1.5.B

```

k=0:0.1:4;
semilogy(0.5*(exp(-4*k)), '--');
hold on
semilogy(0.5*(1-sqrt(1-exp(-4*k))), 'r')
grid on;
Legend('SubOptimalPhoton counting', 'Optimal Quantum')
xlabel('Average number of signal photons Ks')
ylabel(' Average probability of error P(E)')
title('Top Right Plot')
title('Performance Analysis Quantum ReceiverFor BPSK')
axis tight

```

NO.1.6. B

```

k=0:0.1:5;
semilogy((0.5*(exp(-2*k))), 'r');
hold on
semilogy((0.5*(1-sqrt(1-exp(-2*k)))), '--')
hold on
semilogy((0.5*(exp(-4*k))), '*');
hold on
semilogy((0.5*(1-sqrt(1-exp(-4*k)))), '-ro')
legend(' P_C', 'P_Q', 'P_C1', 'P_Q1')
xlabel('Average number of signal photn Ks')
ylabel(' Average probability of symbol Error P(E)')
text(5,0.5*(exp(-2*k(5))), '\leftarrow 0.5*(exp(-2*k)=photon counting')
text(30,0.5*(exp(-4*k(30))), '\leftarrow 0.5*(exp(-4*k)=coherent
detection')
axis tight;

```

N01.7 B. This Matlab programme compute performance of Optimal, Sub Optimal quantum and classical coherent receiver.

```

Ks=0.5:0.5:6; %Average Signal Photon
Kb=1.38*10^-23; %Boltzmal constant
T=300; %degree in kelvin
N=Kb*T; %Themal Noise
h=1.054*10^-34; %Planck Constant
f=3*10^12:5*3*10^12:10^15;
E=h*2*pi.*f; %Signal Energ
g=E./N; %SNR
r=10*log10(g); %Power Gain
t=g(1):g(10);
DD=t';
for i=1:13;

P(i,1)=quadl('sqrt(2*pi)^-1*exp(-
0.5*x.^2)',sqrt(2.*DD(i,1)),inf);%Average Probability of error
classical coherent detection.

```

```
end;
semilogy(P, 'r')
hold on
semilogy(0.5*exp(-4*Ks), '--')%photon counting
hold on
semilogy(0.5*(1-sqrt(1-exp(-4*Ks))))%optimal quntum
grid on
title('Performance Comparison of BPSK Format')
xlabel('Average Signal photon Ks')
ylabel('Average Probablity of Error P(E)')
legend('Clasical Coherent', 'Photon Counting', 'Optimal Quantum')
```

Appendix-c

NO.C.1.This Matlab programme using Rotational algorithm compute the optimal orientation of the measurement axis that minimize the average probability of error for On/Off key Optical Modulation Format with average signal photon $k=1$.

```
S1 -quantum State vector approximation for single qubit
S2 -quantum State vector approximation for single qubit

S1=[1 0 0 0 0 0 0 0 0 0]
S2=[0.6065 0.6065 0.4289 0.2476 0.1238 0.0554 0.0226 0.0085 0.0030
0.0010]
c = sum(S1.* S2);
d=norm(S1);
e=norm(S2);
f=d*e;
g=c/f;
h=acos(g);
i=180*h/pi;
j=90-i;
m=0:1:j;
m1=pi*m/180;
s=j-[m];
s1=pi*s/180;
w=s1';
z=m1'
p=1-0.5*(cos(w).^2+cos(z).^2);
min(p);%minimal probability of error
plot(p);
title('Top Right Plot')
title('Rotational algorithm For BOOK')
xlabel('Angle Variation "tet"')
ylabel('Average probability of Error P(E)')
plot(p);
```

No.C.2.This Matlab programme using Rotational algorithm compute the optimal orientation of the measurement axis that minimize the average probability of error for Binary Phase Shift key Optical Modulation Format with average signal photon $k=1$.

```
k=1;
a=acos(exp(-2*k));angle between signal states
b=pi/2-a;
tet=0:0.00175:b;%angular variation in measurement states
e=b-tet;
p=1-0.5*(cos(tet).^2+cos(e).^2);
plot(tet,p);
grid on
xlabel('Angle Variation')
ylabel('Average Probability Of Error')
Title('Rotational Algorithm For BPSK')
```

Appendix-D

No.D.1. .This programme Using Matlab 6.1.Simulate the quantum effect using Poisson approach and compare the performance of Optimal quantum receiver with photon counting receiver for ON/OFF keying optical modulation format.

```

clc;
clear all;
for mm=1:10;
for r=1:10;
data_len=10000;
%-----Average photon number
ks=mm/2;
%.....Optimal Quantum Theoretical
Qu_OP(mm)=0.5*(1-sqrt(1-exp(-2*ks)));

%.....Photon counting theoretical.
CLL(mm)=0.5*exp(-2*ks);
x=randn(1,data_len);
x=(x>=0);
%.....Quantum state

p=sqrt(poissrnd(2*ks,data_len,2));
for i=1:1:data_len;
q(i,:)=(p(i,:).*(norm(p(i,:)).^-1);
end;
z0=[1,0];%.....State zero measurement
%.....Transmission mapping
for i=1:1:data_len;
if x(i)==0;
y(i,:)=z0;
else
y(i,:)=q(i,:);
end;
end;
%.....Rotational algorithm
for i=1:1:data_len;
a(i)=acos(sum(y(i,:).*z0));
k1(i)=cos(a(i)+0.3).^2;
k2(i)=1-k1(i);
end;
%.....Receiver Mapping
for i=1:1:data_len;
if y(i,:)==z0;
z(i)=0;
else k1(i)<k2(i);
z(i)=1;
end;
end;
[num_err,err_rate]=symerr(x,z);
mean_err_rate(r)=err_rate;
end;
mean_err_rates(mm)=mean(mean_err_rate);
end;
CLL(:)
Qu_OP(:)
mean_err_rates(:)
plot(CLL,'b')
hold on
plot(mean_err_rates,'k')
hold on
plot(Qu_OP,'r')
grid on;
legend('SUB-OPTIMAL CO','SIMULATION','OPTIMAL')
title('PERFORMANCE COMPARISON OF QUANTUM RECEIVER')
xlabel('Average number of signal photon Ks-2:1')
ylabel(' Average probability of symbol error P(E)')
axis tight

```

Appendix-D-2

No.D.2. .This programme Using Matlab 6.1.Simulate the quantum effect and compare the performance of optimal quantum receiver with photon counting receiver for ON/OFF keying optical modulation format Polarization basis.

```

for mm=1:1:10;
for n=1:2;
data_len=5000;
i=sqrt(-1);
%-----Average photon number-----
ks=mm/2;
%.....Optimal Quantum Receiver Theoretical...
Qu_OP(mm)=0.5*(1-sqrt(1-exp(-ks)));
%.....Sub-Optimal photon counting theoretical .....
CLL(mm)=0.5*exp(-ks);
a=[exp(-0.5*ks) exp(-0.5*ks)]';
%.....Polarization or Spin Eigen Space Basis.....
ph_0=[exp(-i*(pi+pi/3)/6)*cos((pi-(2*pi/3))/2) ;exp(i*(pi+pi/3)/6)*sin((pi-(2*pi/3))/2)];
ph_1=[ exp(-i*pi/6)*cos(pi/3) ; exp(i*pi/6)*sin(pi/3) ];
b=ph_0;
c=abs(angle((sum(a.*b))));
x=randn(1,data_len);
x=(x>=0);
beta_r=randn(1,data_len);
beta_i=randn(1,data_len);
alphaa_r=randn(1,data_len);
alphaa_i=randn(1,data_len);
%.....Complex amplitude.....
alpha=(alphaa_r+j*alphaa_i);
betta=(beta_r+j*beta_i);
nrm_alpha=cos(alpha).^2;
nrm_alpha1=1-cos(alpha).^2;
nrm_beta=exp(I*betta);
%.....Transmission Mapping...
phi_1=[ph_0(1,1)*nrm_alpha+ph_1(1,1)* nrm_alpha *nrm_beta;ph_0(2,1)* nrm_alpha +ph_1(2,1)* nrm_alpha
*nrm_beta];
for k=1:data_len;
    phi_11(:,k)= phi_1(:,k).*(norm(phi_1(:,k))).^-1;
    if x(k)==0;
        data_Tx(:,k)=ph_0;
    else data_Tx(:,k)=phi_11(:,k);
    end;
end;
%-----receiver part-----
for l=1:data_len;
    teta(1)=0.5*(pi/2-acos(sum(abs(data_Tx(:,l)).*ph_0)/sqrt(sum(abs((data_Tx(:,l)))))));
    C(1)=acos(sum(abs(data_Tx(:,l)).*ph_0)/sqrt(sum(abs((data_Tx(:,l)))))));
    rr1(1)=cos(teta(1)+C(1))^2;
    rr2(1)=1-rr1(1);
    if data_Tx(:,l)==ph_0;
        data_rec(l)=0;
    elseif rr1(1)<=rr2(1);
        data_rec(l)=1;
    else data_rec(l)=0;
    end;
end;
[num_err,err_rate]=symerr(data_rec,x);
mean_err_rate(n)=err_rate;
end;
mean_err_rates(mm)=mean(mean_err_rate);
end;
plot(Qu_OP,'r')
hold on
plot(mean_err_rates,'--')
plot(CLl,'b')
CLl(:)
Qu_OP(:)
mean_err_rates(:)

```

Appendix-E

No.E.1. This programme Using Matlab 6.1. Compute the optimal orientation of the measurement axis and performance of the optimal quantum receiver for optical Pulse Position Modulation (PPM) format using the iterative rotational algorithm

```

ks=1:1:6;
C=0.5*exp(-ks);%photon counting average probability of symbol error
CC=C';
Q=0.25*(sqrt(1+exp(-ks))-sqrt(1-exp(-ks))).^2;%quantum Theoretical
QQ=Q';
a=acos(exp(-ks));
b=pi/2-a;
c=0:0.0000175:b(1);
d=0:0.0000175:b(2);
e=0:0.0000175:b(3);
f=0:0.0000175:b(4);
g=0:0.0000175:b(5);
h=0:0.0000175:b(6);
c1=b(1)-c;
d1=b(2)-d;
e1=b(3)-e;
f1=b(4)-f;
g1=b(5)-g;
h1=b(6)-h;
%-----M=2-Rotation-----
p1=1-0.5*(cos(c).^2+cos(c1).^2);
p2=1-0.5*(cos(d).^2+cos(d1).^2);
p3=1-0.5*(cos(e).^2+cos(e1).^2);
p4=1-0.5*(cos(f).^2+cos(f1).^2);
p5=1-0.5*(cos(g).^2+cos(g1).^2);
p6=1-0.5*(cos(h).^2+cos(h1).^2);
%.....minimum error.....
p1opt=min(p1);
p2opt=min(p2);
p3opt=min(p3);
p4opt=min(p4);
p5opt=min(p5);
p6opt=min(p6);
%.....minimum error angular location.....
M_21=find(p1==p1opt);
M21=c(M_21);
M21opt=b(1)-M21;
M_22=find(p2==p2opt);
M22=d(M_22);
M22opt=b(2)-M22;
M_23=find(p3==p3opt);
M23=e(M_23);
M23opt=b(3)-M23;
M_24=find(p4==p4opt);
M24=f(M_24);
M24opt=b(4)-M24;
M_25=find(p5==p5opt);
M25=g(M_25);
M25opt=b(5)-M25;
M_26=find(p6==p6opt);
M26=h(M_26);
M26opt=b(6)-M26;
PROT=[ p1opt p2opt p3opt p4opt p5opt p6opt]';
semilogy(ks,CC,'g');
hold on
semilogy(ks,QQ,'r');
hold on
semilogy(ks,PROT,'*');
title('Performance Analysis of PPM-2')
xlabel('Average Photon Signal Ks')
ylabel('Average Probability of Symbol error P(SE)')

```

```

%.....PPM3-Rotation .....
C3=(2/3)*exp(-ks);
CC3=C3';
Q3=(2/9)*(sqrt(1+2*exp(-ks))-sqrt(1-exp(-ks))).^2;
QQ3=Q3';
p31=(1-(1/3)*[(cos(c).^2*(cos(M21)^2+cos(M21opt)^2)+cos(c1).^2]);
p32=(1-(1/3)*[(cos(d).^2*(cos(M22)^2+cos(M22opt)^2)+cos(d1).^2]);
p33=(1-(1/3)*[(cos(e).^2*(cos(M23)^2+cos(M23opt)^2)+cos(e1).^2]);
p34=(1-(1/3)*[(cos(f).^2*(cos(M24)^2+cos(M24opt)^2)+cos(f1).^2]);
p35=(1-(1/3)*[(cos(g).^2*(cos(M25)^2+cos(M25opt)^2)+cos(g1).^2]);
p36=(1-(1/3)*[(cos(h).^2*(cos(M26)^2+cos(M26opt)^2)+cos(h1).^2]);
%.....Minimal Symbol Error.....
p31opt=min(p31);
p32opt=min(p32);
p33opt=min(p33);
p34opt=min(p34);
p35opt=min(p35);
p36opt=min(p36);
%..... Minimum error angular location.....
M_31=find(p31==p31opt);
M31=c(M_31);
M31opt=b(1)-M31;
M_32=find(p32==p32opt);
M32=d(M_32);
M32opt=b(2)-M32;
M_33=find(p33==p33opt);
M33=e(M_33);
M33opt=b(3)-M33;
M_34=find(p34==p34opt);
M34=f(M_34);
M34opt=b(4)-M34;
M_35=find(p35==p35opt);
M35=g(M_35);
M35opt=b(5)-M25;
M_36=find(p36==p36opt);
M36=g(M_36);
M36opt=b(6)-M26;
PROT3=[ p31opt p32opt p33opt p34opt p35opt p36opt]';
semilogy(ks,CC3,'g');
hold on
semilogy(ks,QQ3,'r');
hold on
semilogy(ks,PROT3,'*');
title('Performance Analysis of PPM-3')
xlabel('Average Photon Signal Ks')
ylabel('Average Probability of Symbol error P(SE)')

%.....PPM4-rotation.....
C4=(3/4)*exp(-ks);
CC4=C4';
Q4=(3/16)*(sqrt(1+3*exp(-ks))-sqrt(1-exp(-ks))).^2;
QQ4=Q4';
p41=(1-(1/4)*[cos(c).^2*[(cos(M31)^2*(cos(M21)^2+cos(M21opt)^2)+cos(M31opt)^2)]+cos(c1).^2]);
p42=(1-(1/4)*[cos(d).^2*[(cos(M22)^2*(cos(M32)^2+cos(M32opt)^2)+cos(M22opt)^2)]+cos(d1).^2]);
p43=(1-(1/4)*[cos(e).^2*[(cos(M23)^2*(cos(M33)^2+cos(M33opt)^2)+cos(M23opt)^2)]+cos(e1).^2]);
p44=(1-(1/4)*[cos(f).^2*[(cos(M24)^2*(cos(M34)^2+cos(M34opt)^2)+cos(M24opt)^2)]+cos(f1).^2]);
p45=(1-(1/4)*[cos(g).^2*[(cos(M25)^2*(cos(M35)^2+cos(M35opt)^2)+cos(M25opt)^2)]+cos(g1).^2]);
p46=(1-(1/4)*[cos(h).^2*[(cos(M26)^2*(cos(M36)^2+cos(M36opt)^2)+cos(M26opt)^2)]+cos(h1).^2]);
%.....Minimal Symbol Error.....
p41opt=min(p41);
p42opt=min(p42);
p43opt=min(p43);
p44opt=min(p44);
p45opt=min(p45);
p46opt=min(p46);
%..... minimum error angular location.....

```

```

M_41=find(p41==p41opt);
M41=c(M_41);
M41opt=b(1)-M41;
M_42=find(p42==p42opt);
M42=d(M_42);
M42opt=b(2)-M42;
M_43=find(p43==p43opt);
M43=e(M_43);
M43opt=b(3)-M43;
M_44=find(p44==p44opt);
M44=f(M_44);
M44opt=b(4)-M44;
M_45=find(p45==p45opt);
M45=g(M_45);
M45opt=b(5)-M45;
M_46=find(p46==p46opt);
M46=h(M_46);
M46opt=b(6)-M46;
PROT4=[p41opt p42opt p43opt p44opt p45opt p46opt];
semilogy(ks,CC4,'g');
hold on
semilogy(ks,QQ4,'r');
hold on
semilogy(ks,PROT4,'*');
title('Performance Analysis of PPM-4')
xlabel('Average Photon Signal Ks')
ylabel('Average Probability of Symbol error P(SE)')
%.....PPM=5-rotation.....
C5=(4/5)*exp(-ks);
CC5=C5';
Q5=(4/25)*(sqrt(1+4*exp(-ks))-sqrt(1-exp(-ks))).^2;
QQ5=Q5';
p51=1-
[(1/5)*[[cos(c).^2*[cos(M41)^2*[(cos(M21)^2*(cos(M31)^2+cos(M31opt)^2)+cos(M21opt)^2)]+cos(M41opt)^2]]+cos(c1).^2]];
p52=1-
[(1/5)*[[cos(d).^2*[cos(M42)^2*[(cos(M22)^2*(cos(M32)^2+cos(M32opt)^2)+cos(M22opt)^2)]+cos(M42opt)^2]]+cos(d1).^2]];
p53=1-
[(1/5)*[[cos(e).^2*[cos(M43)^2*[(cos(M23)^2*(cos(M33)^2+cos(M33opt)^2)+cos(M23opt)^2)]+cos(M43opt)^2]]+cos(e1).^2]];
p54=1-
[(1/5)*[[cos(f).^2*[cos(M44)^2*[(cos(M24)^2*(cos(M34)^2+cos(M34opt)^2)+cos(M24opt)^2)]+cos(M44opt)^2]]+cos(f1).^2]];
p55=1-
[(1/5)*[[cos(g).^2*[cos(M45)^2*[(cos(M25)^2*(cos(M35)^2+cos(M35opt)^2)+cos(M25opt)^2)]+cos(M45opt)^2]]+cos(g1).^2]];
p56=1-
[(1/5)*[[cos(h).^2*[cos(M46)^2*[(cos(M26)^2*(cos(M36)^2+cos(M36opt)^2)+cos(M26opt)^2)]+cos(M46opt)^2]]+cos(h1).^2]];
%.....Minimal Symbol Error.....
p51opt=min(p51);
p52opt=min(p52);
p53opt=min(p53);
p54opt=min(p54);
p55opt=min(p55);
p56opt=min(p56);

%..... Minimum error angular location.....

M_51=find(p51==p51opt);
M51=c(M_51);
M51opt=b(1)-M51;
M_52=find(p52==p52opt);
M52=d(M_52);
M52opt=b(2)-M52;
M_53=find(p53==p53opt);
M53=e(M_53);
M53opt=b(3)-M53;
M_54=find(p54==p54opt);
M54=f(M_54);

```

```

M54opt=b(4)-M54;
M_55=find(p55==p55opt);
M55=g(M_55);
M55opt=b(5)-M55;
M_56=find(p56==p56opt);
M56=h(M_56);
M56opt=b(6)-M56;
PROT5=[p51opt p52opt p53opt p54opt p55opt p56opt];
semilogy(ks,CC5,'g');
hold on
semilogy(ks,QQ5,'r');
hold on
semilogy(ks,PROT5,'*');
title('Performance Analysis of PPM-5')
xlabel('Average Photon Signal Ks')
ylabel('Average Probability of Symbol error P(SE)')
%.....PPM-5 rotation.....
C6=(5/6)*exp(-ks);
CC6=C6';
Q6=(5/36)*(sqrt(1+5*exp(-ks))-sqrt(1-exp(-ks))).^2;
QQ6=Q6';
p61=1-
[(1/6)*[(cos(c).^2*([cos(M51).^2*[cos(M41)^2*(cos(M21)^2*(cos(M31)^2+cos(M31opt)^2)+cos(M21opt)^2
)+cos(M41opt)^2])+cos(M51opt).^2))+cos(c1).^2];
p62=1-
[(1/6)*[(cos(d).^2*([cos(M52).^2*[cos(M42)^2.*[(cos(M22)^2*(cos(M32)^2+cos(M32opt)^2)+cos(M22opt)^2
)+cos(M42opt)^2])+cos(M52opt).^2))+cos(d1).^2];
p63=1-
[(1/6)*[(cos(e).^2*([cos(M53).^2*[cos(M43)^2.*[(cos(M23)^2*(cos(M33)^2+cos(M33opt)^2)+cos(M23opt)^2
)+cos(M43opt)^2])+cos(M53opt).^2))+cos(e1).^2];
p64=1-
[(1/6)*[(cos(f).^2*([cos(M54).^2*[cos(M44)^2.*[(cos(M24)^2*(cos(M34)^2+cos(M34opt)^2)+cos(M24opt)^2
)+cos(M44opt)^2])+cos(M54opt).^2))+cos(f1).^2];
p65=1-
[(1/6)*[(cos(g).^2*([cos(M55).^2*[cos(M45)^2.*[(cos(M25)^2*(cos(M35)^2+cos(M35opt)^2)+cos(M25opt)^2
)+cos(M45opt)^2])+cos(M55opt).^2))+cos(g1).^2];
p66=1-
[(1/6)*[(cos(h).^2*([cos(M56).^2*[cos(M46)^2.*[(cos(M26)^2*(cos(M36)^2+cos(M36opt)^2)+cos(M26opt)^2
)+cos(M46opt)^2])+cos(M56opt).^2))+cos(h1).^2];

%.....Minimal Symbol Error.....
p61opt=min(p61);
p62opt=min(p62);
p63opt=min(p63);
p64opt=min(p64);
p65opt=min(p65);
p66opt=min(p66);

%..... Minimum error angular location.....
M_61=find(p61==p61opt);
M61=c(M_61);
M61opt=b(1)-M61;
M_62=find(p62==p62opt);
M62=d(M_62);
M62opt=b(2)-M62;
M_63=find(p63==p63opt);
M63=e(M_63);
M63opt=b(3)-M63;
M_64=find(p64==p64opt);
M64=f(M_64);
M64opt=b(4)-M64;
M_65=find(p65==p65opt);
M65=g(M_65);
M65opt=b(5)-M65;
M_66=find(p66==p66opt);
M66=h(M_66);
M66opt=b(6)-M66;
PROT6=[p61opt p62opt p63opt p64opt p65opt p66opt];
semilogy(ks,CC6,'g');
hold on
semilogy(ks,QQ6,'r');

```

```

hold on
semilogy(ks,PROT6,'*');
title('Performance Analysis of PPM-6')
xlabel('Average Photon Signal Ks')
ylabel('Average Probability of Symbol error P(SE)')

%.....PPM=7-rotation.....
C7=(6/7)*exp(-ks);
CC7=C7';
Q7=(6/49)*(sqrt(1+6*exp(-ks))-sqrt(1-exp(-ks))).^2;
QQ7=Q7';
p71=1-
[(1/7)*[cos(c).^2*([cos(M61).^2*([cos(M51).^2*[cos(M41)^2*[(cos(M21)^2*(cos(M31)^2+cos(M31opt)^2)
+cos(M21opt)^2])+cos(M41opt)^2])+cos(M51opt).^2))+cos(M61opt).^2]+cos(c1).^2];
p72=1-
[(1/7)*[cos(d).^2*([cos(M62).^2*([cos(M52).^2*[cos(M42)^2*[(cos(M22)^2*(cos(M32)^2+cos(M32opt)^2)
+cos(M22opt)^2])+cos(M42opt)^2])+cos(M52opt).^2))+cos(M62opt).^2]+cos(d1).^2];
p73=1-
[(1/7)*[cos(e).^2*([cos(M63).^2*([cos(M53).^2*[cos(M43)^2*[(cos(M23)^2*(cos(M33)^2+cos(M33opt)^2)
+cos(M23opt)^2])+cos(M43opt)^2])+cos(M53opt).^2))+cos(M63opt).^2]+cos(e1).^2];
p74=1-
[(1/7)*[cos(f).^2*([cos(M64).^2*([cos(M54).^2*[cos(M44)^2*[(cos(M24)^2*(cos(M34)^2+cos(M34opt)^2)
+cos(M24opt)^2])+cos(M44opt)^2])+cos(M54opt).^2))+cos(M64opt).^2]+cos(f1).^2];
p75=1-
[(1/7)*[cos(g).^2*([cos(M65).^2*([cos(M55).^2*[cos(M45)^2*[(cos(M25)^2*(cos(M35)^2+cos(M35opt)^2)
+cos(M25opt)^2])+cos(M45opt)^2])+cos(M55opt).^2))+cos(M65opt).^2]+cos(g1).^2];
p76=1-
[(1/7)*[cos(h).^2*([cos(M66).^2*([cos(M56).^2*[cos(M46)^2*[(cos(M26)^2*(cos(M36)^2+cos(M36opt)^2)
+cos(M26opt)^2])+cos(M46opt)^2])+cos(M56opt).^2))+cos(M66opt).^2]+cos(h1).^2];

%.....Minimal Symbol Error.....
p71opt=min(p71);
p72opt=min(p72);
p73opt=min(p73);
p74opt=min(p74);
p75opt=min(p75);
p76opt=min(p76);

%..... Minimum error angular location.....
M_71=find(p71==p71opt);
M71=c(M_71);
M71opt=b(1)-M71;
M_72=find(p72==p72opt);
M72=d(M_72);
M72opt=b(2)-M72;
M_73=find(p73==p73opt);
M73=e(M_73);
M73opt=b(3)-M73;
M_74=find(p74==p74opt);
M74=f(M_74);
M74opt=b(4)-M74;
M_75=find(p75==p75opt);
M75=g(M_75);
M75opt=b(5)-M75;
M_76=find(p76==p76opt);
M76=h(M_76);
M76opt=b(6)-M76;
PROT7=[p71opt p72opt p73opt p74opt p75opt p76opt ];
semilogy(ks,CC7,'g');
hold on
semilogy(ks,QQ7,'r');
hold on
semilogy(ks,PROT7,'*');
title('Performance Analysis of PPM-7')
xlabel('Average Photon Signal Ks')
ylabel('Average Probability of Symbol error P(SE)')

%.....PPM=8-rotation.....
C8=(7/8)*exp(-ks);

```

```

CC8=C8';
Q8=(7/64)*(sqrt(1+7*exp(-ks))-sqrt(1-exp(-ks))).^2;
QQ8=Q8';
p81=1-
[(1/8)*[cos(c).^2*( [cos(M71).^2*( [cos(M61).^2*( [cos(M51).^2*[cos(M41)^2*[cos(M21)^2*(cos(M31)^2+
cos(M31opt)^2)+cos(M21opt)^2)]+cos(M41opt)^2]]+cos(M51opt).^2)))+cos(M61opt).^2]+cos(M71opt).^2)]+c
os(c1).^2];
p82=1-
[(1/8)*[cos(d).^2*( [cos(M72).^2*( [cos(M62).^2*( [cos(M52).^2*[cos(M42)^2.*[(cos(M22)^2*(cos(M32)^2
+cos(M32opt)^2)+cos(M22opt)^2)]+cos(M42opt)^2]]+cos(M52opt).^2)))+cos(M62opt).^2]+cos(M72opt).^2)]+
cos(d1).^2];
p83=1-
[(1/8)*[cos(e).^2*( [cos(M73).^2*( [cos(M63).^2*( [cos(M53).^2*[cos(M43)^2.*[(cos(M23)^2*(cos(M33)^2
+cos(M33opt)^2)+cos(M23opt)^2)]+cos(M43opt)^2]]+cos(M53opt).^2)))+cos(M63opt).^2]+cos(M73opt).^2)]+
cos(e1).^2];
p84=1-
[(1/8)*[cos(f).^2*( [cos(M74).^2*( [cos(M64).^2*( [cos(M54).^2*[cos(M44)^2.*[(cos(M24)^2*(cos(M34)^2
+cos(M34opt)^2)+cos(M24opt)^2)]+cos(M44opt)^2]]+cos(M54opt).^2)))+cos(M64opt).^2]+cos(M74opt).^2)]+
cos(f1).^2];
p85=1-
[(1/8)*[cos(g).^2*( [cos(M75).^2*( [cos(M65).^2*( [cos(M55).^2*[cos(M45)^2.*[(cos(M25)^2*(cos(M35)^2
+cos(M35opt)^2)+cos(M25opt)^2)]+cos(M45opt)^2]]+cos(M55opt).^2)))+cos(M65opt).^2]+cos(M75opt).^2)]+
cos(g1).^2];
p86=1-
[(1/8)*[cos(h).^2*( [cos(M76).^2*( [cos(M66).^2*( [cos(M56).^2*[cos(M46)^2.*[(cos(M26)^2*(cos(M36)^2
+cos(M36opt)^2)+cos(M26opt)^2)]+cos(M46opt)^2]]+cos(M56opt).^2)))+cos(M66opt).^2]+cos(M76opt).^2)]+
cos(h1).^2];
%.....Minimal Symbol Error.....

p81opt=min(p81);
p82opt=min(p82);
p83opt=min(p83);
p84opt=min(p84);
p85opt=min(p85);
p86opt=min(p86);

%..... Minimum error angular location.....

M_81=find(p81==p81opt);
M81=c(M_81);
M81opt=b(1)-M81;
M_82=find(p82==p82opt);
M82=d(M_82);
M82opt=b(2)-M82;
M_83=find(p83==p83opt);
M83=e(M_83);
M83opt=b(3)-M83;
M_84=find(p84==p84opt);
M84=f(M_84);
M84opt=b(4)-M84;
M_85=find(p85==p85opt);
M85=g(M_85);
M85opt=b(5)-M85;
M_86=find(p86==p86opt);
M86=h(M_86);
M86opt=b(6)-M86;
PROT8=[p81opt p82opt p83opt p84opt p85opt p86opt];
semilogy(ks,CC8,'g');
hold on
semilogy(ks,QQ8,'r');
hold on
semilogy(ks,PROT8,'*');
title('Performance Analysis of PPM-8')
xlabel('Average Photon Signal Ks')
ylabel('Average Probability of Symbol error P(SE)')

```

Appendix-F

This Matlab programme computes the performance of Sub-optimal and optimal quantum receiver for 3-psk optical modulation formats.

```
ks=0:1:10;
P_c=1/3*(exp(-ks/2));
P_Q=1/3*exp(-ks)
semilogy(P_c, '--')
hold on
semilogy(P_Q, 'g')
title('Top Right Plot')
title('Performance Analysis')
legend('Sub-Optimal quantum 3-PSK', 'Optimal Quantum 3-PSKquantum')
xlabel('Average number of signal photn Ks')
ylabel(' Average probability of symbol error P(E)')
text(2, (exp(-k(2)/2)), '\leftarrow(exp(ks/2)=Classical')
text(3, 1/3*exp(-k(3))), '\rightarrow=quantum')
axis tight
```